

NBER WORKING PAPER SERIES

THE MACROECONOMIC IMPACT OF CLIMATE CHANGE:
GLOBAL VS. LOCAL TEMPERATURE

Adrien Bilal
Diego R. Känzig

Working Paper 32450
<http://www.nber.org/papers/w32450>

NATIONAL BUREAU OF ECONOMIC RESEARCH
1050 Massachusetts Avenue
Cambridge, MA 02138
May 2024, revised August 2024

We thank Marios Angeletos, Marshall Burke, Gabriel Chodorow-Reich, Simon Dietz, Stephane Hallegatte, Jim Hamilton, Xavier Jaravel, Ben Jones, Eben Lazarus, Pooya Molavi, Ishan Nath, Ben Olken, Esteban Rossi-Hansberg, Jon Steinsson, Jeffrey Shrader, Jim Stock and Chris Wolf for helpful comments and suggestions. We thank Ramya Raghavan, Lilian Hartmann and Cathy Wang for outstanding research assistance. Adrien Bilal gratefully acknowledges support from the Chae Family Economics Research Fund at Harvard University. The views expressed herein are those of the authors and do not necessarily reflect the views of the National Bureau of Economic Research.

NBER working papers are circulated for discussion and comment purposes. They have not been peer-reviewed or been subject to the review by the NBER Board of Directors that accompanies official NBER publications.

© 2024 by Adrien Bilal and Diego R. Känzig. All rights reserved. Short sections of text, not to exceed two paragraphs, may be quoted without explicit permission provided that full credit, including © notice, is given to the source.

The Macroeconomic Impact of Climate Change: Global vs. Local Temperature

Adrien Bilal and Diego R. Känzig

NBER Working Paper No. 32450

May 2024

JEL No. E01,E23,F18,O44,Q54,Q56

ABSTRACT

This paper estimates that the macroeconomic damages from climate change are six times larger than previously thought. Exploiting natural global temperature variability, we find that 1°C warming reduces world GDP by 12%. Global temperature correlates strongly with extreme climatic events unlike country-level temperature used in previous work, explaining our larger estimate. We use this evidence to estimate damage functions in a neoclassical growth model. Business-as-usual warming implies a 29% present welfare loss and a Social Cost of Carbon of \$1,065 per ton. These impacts suggest that unilateral decarbonization policy is cost-effective for large countries such as the United States.

Adrien Bilal

Department of Economics

Harvard University

1805 Cambridge Street

Cambridge, MA 02138

and NBER

adrienbilal@fas.harvard.edu

Diego R. Känzig

Department of Economics

Northwestern University

Kellogg Global Hub

2211 Campus Drive

Evanston, IL 60208

and NBER

dkaenzig@northwestern.edu

1 Introduction

Climate change is frequently described as an existential threat. This view, however, stands in stark contrast to empirical estimates of the impact of climate change on economic activity: they imply that a 1°C rise in temperature reduces world output at most by 1-3%. Under any conventional discounting, such effects seem hardly catastrophic. Why are perceptions of climate change misaligned with empirical estimates? Do existing estimates not account for the full impact of climate change, or are its costs truly small?

In this paper, we demonstrate that the macroeconomic impacts of climate change are six times larger than previously documented. We rely on a time-series local projection approach to estimate the impact of global temperature shocks on Gross Domestic Product (GDP). This approach exploits natural variability in global mean temperature—the source of variation closest to climate change—which we show to predict damaging extreme climatic events much more strongly than country-level temperature. We find that a 1°C rise in global temperature lowers world GDP by 12% at peak. We then use our reduced-form results to estimate structural damage functions in a simple neoclassical growth model. Climate change leads to a present-value welfare loss of 29% and a Social Cost of Carbon (SCC) of \$1,065 per ton of carbon dioxide.

In the first part of the paper, we develop our time-series approach. We assemble a new climate-economy dataset spanning the last 120 years from sources that are regularly updated up to recent years. We construct global and country-level measures from high-resolution gridded land and ocean surface air temperature data from Berkeley Earth. We define physical granular reanalysis measures of extreme temperature, droughts, wind speed and precipitation from the Inter-Sectoral Impact Model Intercomparison Project (ISIMIP). We obtain economic data on GDP, population, consumption, investment and productivity from the Penn World Tables spanning 173 countries from 1960 onwards, and from the Jordà-Schularick-Taylor Macrohistory database for select countries since 1900.

Identification of the impact of temperature on GDP is complicated by their jointly trending behavior. We thus construct global and local (country-level) *temperature shocks*: innovations to the temperature process that are orthogonal to their long-run trends and persist for two years using the approach in Hamilton (2018). Our choice of period is motivated by the geoscience literature. Natural climate variability is driven by multiple phenomena. External causes such as solar cycles and volcanic eruptions lead to medium- and short-run fluctuations in the Earth’s mean temperature. Internal climate variability—

interactions within the climatic system itself—lead to irregular fluctuations in temperature and weather extremes. For instance, the El Niño cycle varies unpredictably between 2 to 7 years.

We map out the dynamic causal effects of our global temperature shocks on world GDP using local projections from 1960 onwards. A 1°C global temperature shock leads to a gradual decline in world GDP that peaks at 12% after 6 years and does not fully mean-revert even after 10 years. This impact partly reflects the accumulated effects of persistently elevated global temperature itself, that remains above 0.5°C for multiple years after the shock. These results remain unchanged for alternative de-trending approaches, such as one-step ahead forecast errors or a one-sided Hodrick-Prescott filter.

Four identification concerns may challenge the causal interpretation of our headline results. We address each of them in a series of robustness exercises. First, we account for omitted variable bias: global temperature shocks may coincide with the global economic and financial cycle. We control for rich measures of world economic performance: indicators for global economic recessions and global macro-financial variables (past world real GDP, commodity prices and interest rates). Our results remain unaffected by the specific set of controls and are not driven by any particularly influential years, indicating that temperature shocks are largely unrelated to economic shocks.

Second, we account for reverse causality: as output declines after a temperature shock, energy consumption and greenhouse gas emissions fall, lowering temperatures and increasing output going forward. Qualitatively, reverse causality thus leads us to underestimate the true impact of a global temperature shock. Quantitatively, it is likely negligible because short-run fluctuations in emissions imply small temperature variations. We confirm these arguments by explicitly adjusting for the impact of past greenhouse gas and aerosol emissions with a climate model and find virtually identical results.

Third, we verify that our estimates are likely externally valid and are stable across time periods and causes of temperature variation. We find remarkably similar estimates in three time periods (1900-2019, 1960-2019—our main sample—and 1985-2019) as well as when we exclude El Niño and volcanic eruptions from our identifying variation.

Fourth, we account for regional omitted variable bias: global temperature may be particularly driven by some countries while they also experience unrelated GDP growth. We obtain virtually identical results when we project country-level GDP—rather than global GDP—on global temperature, controlling for country fixed effects and region-specific

time trends. Collectively, our robustness exercises suggest that our specification captures the causal effect of global temperature on economic activity.

Our estimated effect of temperature shocks on world GDP stands in stark contrast to existing estimates of the cost of climate change. Nordhaus (1992), Dell et al. (2012), Burke et al. (2015) and Nath et al. (2023) find that a 1°C temperature shock reduces GDP by at most 1-3% in the medium run. Why do we find effects that are six times larger?

We focus on a different source of variation: changes in *global* mean temperature capture the comprehensive impact of climate change. By contrast, previous work exploits changes in *country-level*, *local* temperature. When we estimate the impact of *local* temperature on country-level GDP with the same empirical specification, we find similarly small effects to previous studies: 1.5% per 1°C. Econometrically, panel analyses using *local* temperature net out common impacts of *global* temperature through time fixed effects. Instead, we focus on these common impacts.

Why, then, does global temperature depress economic activity so much more than local temperature? We show that global temperature is fundamentally different from local temperature. Global temperature shocks predict a large and persistent rise in the frequency of extreme climatic events that cause economic damage: extreme temperature, droughts, extreme wind, and extreme precipitation. By contrast, local temperature shocks predict a much weaker rise in these extremes. These conclusions are consistent with the geoscience literature: extreme wind and precipitation are outcomes of the global climate that depend on ocean temperatures and atmospheric humidity throughout the globe, rather than outcomes of local temperature realizations (Seneviratne et al., 2016; Wartenburger et al., 2017; Seneviratne et al., 2021; Domeisen et al., 2023).

Quantitatively, the four extreme events that we measure account for over two thirds of our estimated global temperature impact. We reach this conclusion by estimating the impact of extreme events on GDP, which we combine with the dynamic correlation between global temperature shocks and extreme events to construct a counterfactual impact of global temperature on GDP. Of course, this exercise is unlikely to account for the full effect of global temperature on GDP: we would need to specify and measure the universe of channels whereby global temperature affects the economy. Using global temperature directly bypasses this challenge.

Another possible explanation for the differential impacts of global and local temperature shocks is that general equilibrium linkages together with spatially correlated local

temperature lead panel analyses to underestimate the true impact of local temperature. However, we find that general equilibrium linkages account for at most one fifth of our global temperature estimates. To reach this conclusion, we construct an external temperature measure by aggregating the local temperature shocks of all trade partners of a given country, weighted by trade shares. External local temperature turns out to have a similarly small impact on economic activity to the direct effect of local temperature: given moderate levels of trade openness throughout the world, indirect effects cannot be substantially larger than direct effects of local temperature.

How and where do the worldwide GDP impacts of global temperature materialize? We document a significant fall in capital, investment and productivity after a global temperature shock. Warm and low-income countries appear to be more severely affected than cold and high-income countries, although these comparisons are noisy. Overall however, global temperature has more uniformly detrimental effects than local temperature.

In the second part of the paper, we develop a simple neoclassical growth model to translate our reduced-form estimates into welfare effects, similarly to Nordhaus (1992). We introduce productivity and capital depreciation damages from temperature. Critically, we use our novel reduced-form effects to estimate structural damage functions.

We estimate productivity and capital depreciation shocks that correspond to a global temperature shock by matching the estimated impulse response function of output and capital. This mapping has a closed-form expression that guarantees identification. In doing so, we account for the internal persistence of global mean temperature. We remain conservative and impose persistent level effects rather than growth effects. We find that a one-time transitory 1°C rise in global mean temperature leads to a 3% peak productivity decline and a 1 percentage point (p.p.) peak rise in the capital depreciation rate.

Our main counterfactual is a gradual increase in global mean temperature that starts in 2024 and reaches 3°C above pre-industrial levels by 2100, so 2°C above 2024 temperatures, with a 2% rate of time preference. Climate change implies precipitous declines in output, capital and consumption that reach 47% by 2100, leading to a 29% welfare loss in permanent consumption equivalent in 2024. These magnitudes are comparable to the economic damage caused by the 1929 Great Depression, but experienced *permanently*.

If the economic effects of climate change are so large, why were they not noticed after nearly 1°C of global warming since 1960? Because climate change occurs in small increments, its effects are hidden behind background economic variability. We show that since

1960, climate change caused a gradual reduction in the annual world growth rate that reaches one third of baseline by 2019. Because climate change is also persistent, its effects keep accumulating over time. Ultimately, world GDP per capita would be 18% higher today had no warming occurred between 1960 and 2019.

The estimated model lets us characterize the SCC using the global temperature response to a CO₂ pulse from Dietz et al. (2021) and Folini et al. (2024). We remain conservative and use the lower end of the range of temperature responses from Dietz et al. (2021), which are also consistent with historical emissions and warming data.

We obtain a SCC of \$1,065 per ton. This value is six times larger than the high end of existing estimates (\$185 per ton, Rennert et al., 2022). The 68% bootstrapped confidence interval for the SCC ranges from \$690 per ton to \$1,779 per ton. While this range is non-trivial, even its lower bound is multiple times larger than conventional SCC values. Our focus on global temperature shocks accounts for this substantial difference. When we re-estimate our model based on the impact of local temperature shocks as in previous research, the welfare cost of climate change is 4% and the SCC is \$223 per ton.

How sensitive are these results to specification choices? Any plausible discount rate and 2100 temperature results in welfare losses in excess of 20% and a SCC above \$500 per ton. Discount rates below 1% imply a SCC exceeding \$3,000 per ton. Scenarios with 2100 warming 5°C above pre-industrial levels lead to welfare losses larger than 50%. The median climate sensitivity from Dietz et al. (2021) implies a SCC above \$1,700 per ton.

We conclude by delineating the consequences of our results for decarbonization policy. Decarbonization interventions cost \$80 per ton of CO₂ abated on average (Bistline et al., 2023). A conventional SCC value based on local temperature of \$223 per ton implies that these policies are cost-effective only if governments internalize benefits to the entire world, as captured by the SCC. However, a government that only internalizes domestic benefits values decarbonization using a Domestic Cost of Carbon (DCC). The DCC is always lower than the SCC because damages to a single country are lower than at a global scale. Under conventional estimates, the DCC of the United States is \$45 per ton, making unilateral emissions reduction prohibitively expensive. Under our new estimates, the DCC of the United States becomes \$213 per ton and thus exceeds policy costs. In that case, unilateral decarbonization policy is cost-effective for the United States.

Related literature. Our paper contributes to the vast body of work that measures economic damages from climate change surveyed in Burke et al. (2023) and Moore et al.

(2024). The canonical approach estimates the effect of *local* temperature fluctuations over time within a spatial area on economic outcomes in a panel structure to achieve credible identification (Dell et al., 2012; Dell et al., 2014; Burke et al., 2015; Newell et al., 2021; Kahn et al., 2021). Nath et al. (2023) and Kotz et al. (2024) clarify the role of persistence in measuring damages. Consistently across all these studies, medium-term effects range from 1% to 3% of GDP and rely exclusively on climatic variation within countries or smaller geographic units. Our paper takes a fundamentally different approach: we directly exploit aggregate time-series variation in *global* mean temperature instead of relying on within-country climatic variation that nets out common effects of global temperature.

Perhaps surprisingly, few studies have explored time-series variation in temperature. Bansal and Ochoa (2011) find that a 1°C global temperature increase reduces GDP by 1% *contemporaneously*. We show that the *persistence* of the GDP response is crucial: the peak effect occurs six years out and is twelve times larger than this contemporaneous impact. Berg et al. (2023) analyze the effects of global and idiosyncratic temperature shocks on GDP *dispersion* across countries. We directly estimate the *aggregate impact* of global temperature, which is much more precisely estimated than individual country-level responses. In contemporary work, Neal (2023) and Zappalà (2023) suggest that correlated local temperature and spillover effects across countries may lead to underestimate the effect of local temperature. We show that spillovers cannot rationalize the gap between global and local temperature impacts, while extreme climatic events do. Relative to these papers, we also use our macroeconomic estimates in a structural model to evaluate welfare and the SCC.

As such, our paper relates to the literature studying the economic impact of climatic phenomena such as storms, heatwaves or El Niño (Barro, 2006; Deschênes and Greenstone, 2011; Hsiang et al., 2011; Deryugina, 2013; Hsiang and Jina, 2014; Bilal and Rossi-Hansberg, 2023; Phan and Schwartzman, 2023; Tran and Wilson, 2023; Callahan and Mankin, 2023; Dingel et al., 2023). We evaluate the impact of global temperature directly and provide new evidence on the relationship between global temperature and extreme climatic events.

Our paper also connects to the literature using Integrated Assessment Models surveyed in Nordhaus (2013). We take a “top-down” approach and directly estimate and match the macroeconomic impact of global temperature. Our analysis suggests that Integrated Assessment Models have historically delivered small costs of climate change not

so much because they relied on incomplete foundations, but instead because they were calibrated to economic damages that did not represent the full impact of climate change (Nordhaus, 2013; Stern et al., 2022).

More recently, “bottom-up” models featuring rich regional heterogeneity, migration (Desmet and Rossi-Hansberg, 2015; Desmet et al., 2021; Cruz and Rossi-Hansberg, 2023; Rudik et al., 2022; Conte et al., 2022) and capital investment (Krusell and Smith, 2022; Bilal and Rossi-Hansberg, 2023) match micro-level estimates and aggregate using the model. Our “top-down” approach is more holistic in that we do not need to specify and estimate all channels and general equilibrium effects mapping global temperature to damages, but remains necessarily limited in assessing distributional and adaptation effects.

In fact, both our global temperature approach and the conventional local temperature approach rely on moderate short-run temperature variation for identification. To the extent that adaptation may be more pronounced in response to large long-run temperature changes, our results represent an upper bound on realized economic damages from slowly unfolding climate change. Although assessing the role of adaptation is beyond the scope of this paper, existing evidence suggests a limited role for adaptation even for the United States (Burke and Emerick, 2016; Moscona and Sastry, 2022; Bilal and Rossi-Hansberg, 2023), in line with the stability of our estimates across time periods. Should there be an unprecedented uptake in adaptation in the future, our numbers would still represent society’s willingness to pay for such investments.

The rest of this paper is organized as follows. Section 2 describes the data and estimates the macroeconomic effects of temperature shocks using our time-series approach. Section 3 compares the effects of global and local temperature. Section 4 introduces our dynamic model and describes our structural estimation approach. Section 5 evaluates the welfare implications of climate change. Section 6 concludes.

2 Global Temperature and Economic Growth

2.1 A Novel Climate-Economy Dataset

Our starting point is to construct a dataset covering 173 countries over the last 120 years to study the effects of temperature on the economy. We use world aggregates from this dataset in this section, and country-level outcomes in Section 3 below.

We obtain temperature data from the Berkeley Earth Surface Temperature Database.

It provides temperature anomaly data at a spatial resolution of $1^\circ \times 1^\circ$ of latitude and longitude. Based on this gridded data, we construct population- and area-weighted temperature measures at the country level. We complement these local temperature measures with global mean temperature data from the National Oceanic and Atmospheric Administration (NOAA). As expected, global temperature aggregated from the Berkeley Earth data correlates virtually perfectly with the NOAA data series.

We rely on data from ISIMIP for information on extreme weather events. ISIMIP provides global, high-frequency datasets that record multiple atmospheric variables over the 20th and early 21st centuries. We use ISIMIP’s observed climate dataset. It contains daily reanalysis measures of temperature, wind speed and precipitation, spanning the period 1901-2019 at the $0.5^\circ \times 0.5^\circ$ resolution. We compute exposure indices to extreme weather by recording the fraction of days within a country and year that experience a weather realization above or below a fixed percentile of the daily weather distribution in 1950-1980. See Appendix A.1 for details.

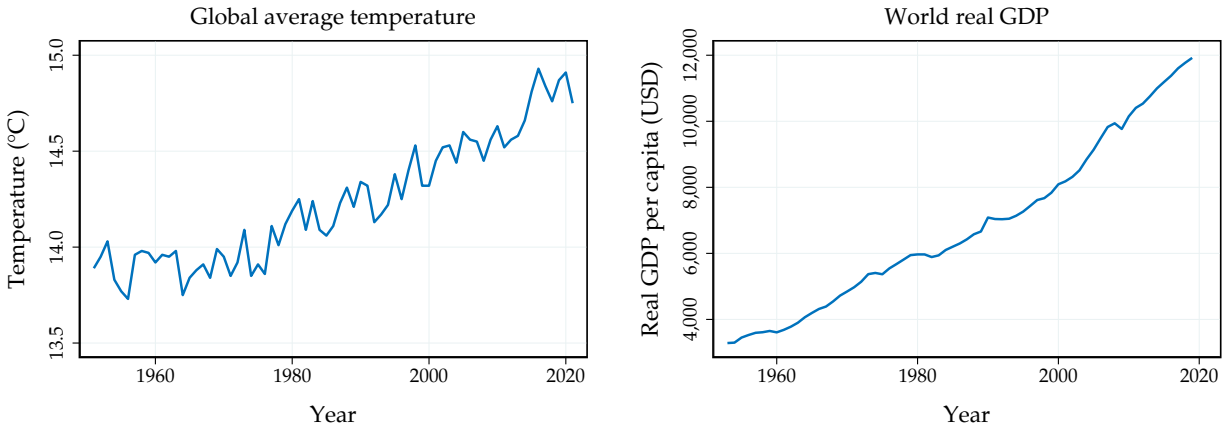
We combine our climate dataset with economic information on GDP, population, consumption, investment, and productivity. We obtain a high-quality dataset for a comprehensive selection of countries around the world from the Penn World Tables. We also rely on data from the World Bank as an alternative. Given that both datasets only go back to the 1950s or 1960s, we also include data from the Jordà-Schularick-Taylor Macrohistory database, which features high-quality economic data for a selection of high-income countries starting in the late 19th century.

2.2 Global Temperature Shocks

Figure 1 displays the evolution of global average temperature and world real GDP per capita since the post-World War II era in our dataset. In the mid-1950s to the mid-1970s, global average temperature remained relatively stable at around 14°C . However, from the late 1970s onward, global average temperature began to steadily rise again. At the same time, we observe relatively stable economic growth over the entire sample.

The trending behavior of the two series in Figure 1 complicates the identification of the economic effects of temperature increases. A simple regression of global GDP on temperature will yield a spuriously positive association between the two variables, as economic growth is associated with higher greenhouse gas emissions which eventually translate into higher temperature. Therefore, we do not focus on the level of temperature

Figure 1: Global Average Temperature and Output Since 1950



Notes: Evolution of global average temperature, computed based on global temperature anomaly data and the corresponding climatology from NOAA, in the left panel, and the evolution of world real GDP per capita (in 2017 USD) computed based on PWT data in the right panel.

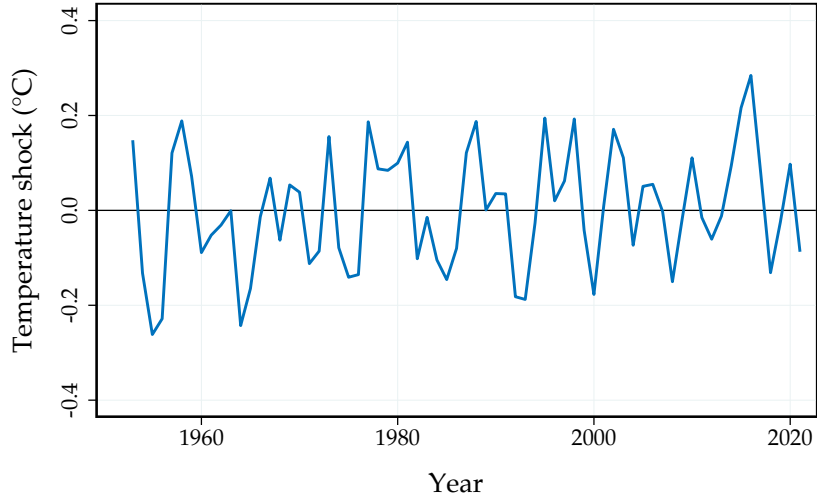
as the treatment in our projections, but instead focus on so-called *temperature shocks*. We define such shocks as possibly persistent deviations from the long-run trend in global mean temperature.

What drives these variations in temperature around the trend? The geoscience literature indicates two types of causes. First, external causes such as solar cycles and volcanic eruptions lead to short-run fluctuations in the Earth’s mean temperature. Solar cycles have a typical period of 10 years and can warm the Earth by as much as 0.1°C (National Oceanic and Atmospheric Administration, 2009). Volcanic eruptions have shorter-lived cooling effects of up to 2 years due to sulphuric aerosols that increase albedo (National Oceanic and Atmospheric Administration, 2005). Second, internal climate variability—interactions within the climatic system itself that lead to irregularly recurring events—also affects temperatures. For instance, the El Niño-La Niña cycle varies unpredictably between 2 to 7 years and substantially affects global mean temperatures and weather extremes (Kaufmann et al., 2006; National Oceanic and Atmospheric Administration, 2023).

How to isolate the trend and transient components of temperature? To estimate the effects of temperature on future economic outcomes, it is critical to preserve the causality of the data in a time-series sense: we cannot rely on future values of temperature to identify the trend in the current period. In addition, the physical properties of natural climate variability suggest to allow for somewhat persistent deviations from trend.

One approach that satisfies our needs along both these dimensions is the method pro-

Figure 2: Global Temperature Shock



Notes: Global temperature shocks, computed as in Hamilton (2018) with $(h = 2, p = 2)$, over the post-World War II era.

posed by Hamilton (2018). The idea is to regress temperature h periods out on some of its lags as of period t and construct the temperature shock as the innovation in this regression:

$$\widehat{T_{t+h}^{\text{shock}}} = T_{t+h} - (\hat{\alpha} + \hat{\beta}_1 T_t + \dots + \hat{\beta}_{p+1} T_{t-p}), \quad (1)$$

where $\hat{\beta}_i$ denotes the coefficient estimates of the regression of temperature on its lag i . This exercise amounts to isolating shocks that persist typically for h periods. Selecting the horizon h is of course an important choice. Motivated by the fact that the climatic events that we consider can last for up to several years, we select a horizon of $h = 2$ and set the number of lags to $p = 2$ in our main specification. As we show in Section 2.4 below and in Appendix A.12, varying these values leaves our results essentially unchanged. In particular, Appendix A.12.1 reproduces all our main analyses under a one-step ahead forecast error $h = 1$ as commonly used in the literature and finds virtually identical results.

Figure 2 shows the resulting global temperature shocks over our sample of interest. As expected, the temperature shocks fluctuate around zero with an almost equal number of positive and negative shocks. The largest temperature shocks in our sample are around 0.3°C. Figure A.2 in Appendix A.2 indicates that the series is also weakly autocorrelated, because we allow for relatively persistent deviations from the long-run temperature trend. In our empirical specification, we therefore control for lagged temperature

shocks as well. Otherwise, serial correlation may bias the estimated impacts when not properly accounted for (Nath et al., 2023).

2.3 The Effect of Temperature Shocks in the Time Series

The economic effects of temperature shocks may take time to materialize. Therefore, we focus on the dynamic effects of temperature shocks up to 10 years out. We evaluate directly the long-run effects of temperature without extrapolating short-term temperature impacts. Of course, we would ideally trace out even longer-run effects, but our limited sample period prevents us from doing so consistently.

We estimate the dynamic causal effects to global temperature shocks using local projections à la Jordà (2005). This approach involves estimating the following series of regressions, one for each horizon $h = 0, \dots, 10$:

$$y_{t+h} - y_{t-1} = \alpha_h + \theta_h T_t^{\text{shock}} + \mathbf{x}_t' \boldsymbol{\beta}_h + \varepsilon_{t+h}, \quad (2)$$

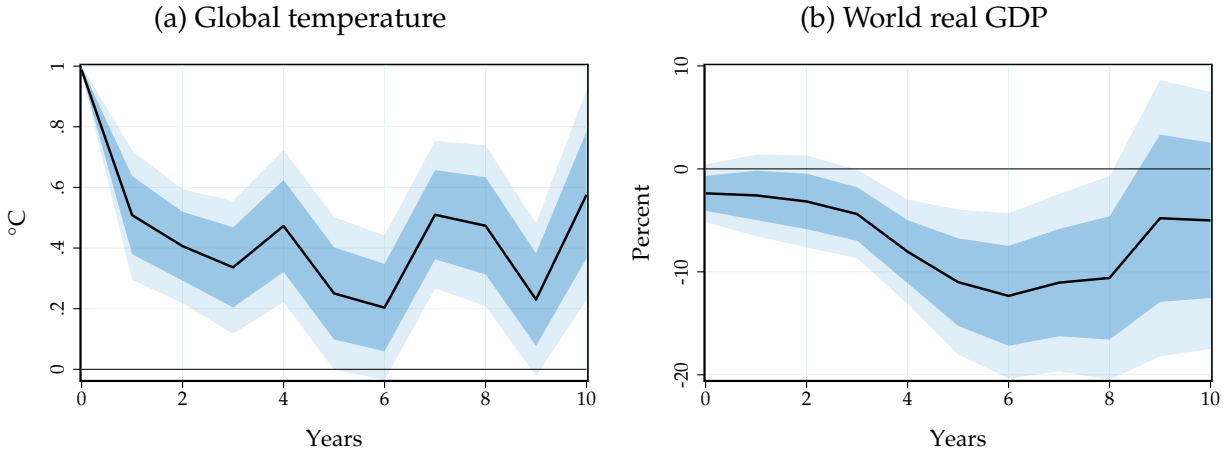
where y_t is the outcome variable of interest, T_t^{shock} is the temperature shock and θ_h is the dynamic causal effect of interest at horizon h . We refer to the dynamic causal effects up to horizon h as the Impulse Response Function (IRF). \mathbf{x}_t is a vector of controls and ε_t is a potentially serially correlated error term. Our main outcome variable of interest is (log) world real GDP per capita. Because we are using the cumulative growth rate as the dependent variable, we are estimating a level effect. The estimation sample is 1960-2019.¹

We use local projections in our main analysis because they tend to be robust at long horizons (Olea et al., 2024). Compared to Vector Autoregressions (VARs) or distributed lag models, local projections directly estimate the effects of interest rather than extrapolating from the first few autocovariances and allow for more flexible controls. Nevertheless, we obtain similar results under alternative estimation models in Appendix A.4.

To account for the serial correlation in GDP growth and temperature shocks, we include 2 lags of real GDP growth per capita and of the global temperature shock. We also include additional controls for the performance of the global economy that we discuss below in more detail. We compute the confidence bands using the lag-augmentation ap-

¹Leveraging that temperature data is available for a longer period than GDP data, we estimate the temperature shock based on this longer sample to mitigate the influence from observations at the beginning and the end of the sample.

Figure 3: The Effect of Global Temperature Shocks on World Output



Notes: Impulse responses of global mean temperature in panel (a) and world real GDP per capita in panel (b) to a global temperature shock, estimated based on (2). Solid line: point estimate. Dark and light shaded areas: 68 and 90% confidence bands.

proach (Montiel Olea and Plagborg-Møller, 2021).²

Figure 3 shows the impulse responses of global temperature and world real GDP per capita to a global temperature shock of 1°C. The solid black lines are the point estimates and the shaded areas are 68 and 90% confidence bands, respectively. As shown in the left panel, global temperature increases by 1°C on impact. The effect of a global temperature shock on global temperature turns out to be highly persistent: after 10 years global temperature is still elevated by about 0.5°C.

The persistent rise in global temperature leads to large economic effects. On impact, world GDP falls by about 2%. However, the effect builds up over time. After 6 years, world GDP falls by 12%, with effects that persist up to 10 years out. Our estimate is of the same magnitude as the growth impacts that typically occur after severe banking or financial crises (Cerra and Saxena, 2008; Reinhart and Rogoff, 2009).

The gradual decline in world GDP in panel (b) reflects not only the direct impact of the initial temperature shock, but also the subsequent effects of persistently elevated temperature from panel (a) that accumulate over time. Figure A.10 in Appendix A.10 reveals that these accumulated effects of persistently elevated temperature account for a substantial part of the peak effect and of its timing. We use the method in Sims (1986) to construct a

²As in Nath et al. (2023), we do not account for estimation uncertainty in the global temperature shock in our baseline specification. However, we alternatively conduct inference using bootstrapping techniques, and taking estimation uncertainty into account yields very similar inference. See Appendix A.3 for more details.

counterfactual path of output that would correspond to a one-time fully transitory global temperature change. We find that the peak impact is then just under 5% instead of 12%, and occurs four years after the shock instead of six. We also account for the internal persistence of temperature when we construct our counterfactuals in Section 4.

Of course, a 1°C temperature shock is a large shock that does not occur directly in our historical sample: we observe much smaller shocks in practice. Our estimate for a 1°C shock scales up the linear effect of these smaller shocks. In effect, we abstract from potential non-linearities. However, in the presence of potential tipping points, one may expect larger effects than predicted by our linear model.

2.4 Robustness

The time-series nature of our identifying variation requires care in interpreting these conclusions. We now demonstrate that our main estimate is robust to accounting for various identification concerns.

Omitted variable bias. Global temperature innovations may happen to be correlated with the global economic cycle over time. For instance, if a severe El Niño event increases global temperature at the same time that a global recession occurs for unrelated reasons, we may mistakenly attribute adverse economic impacts to climatic variations.

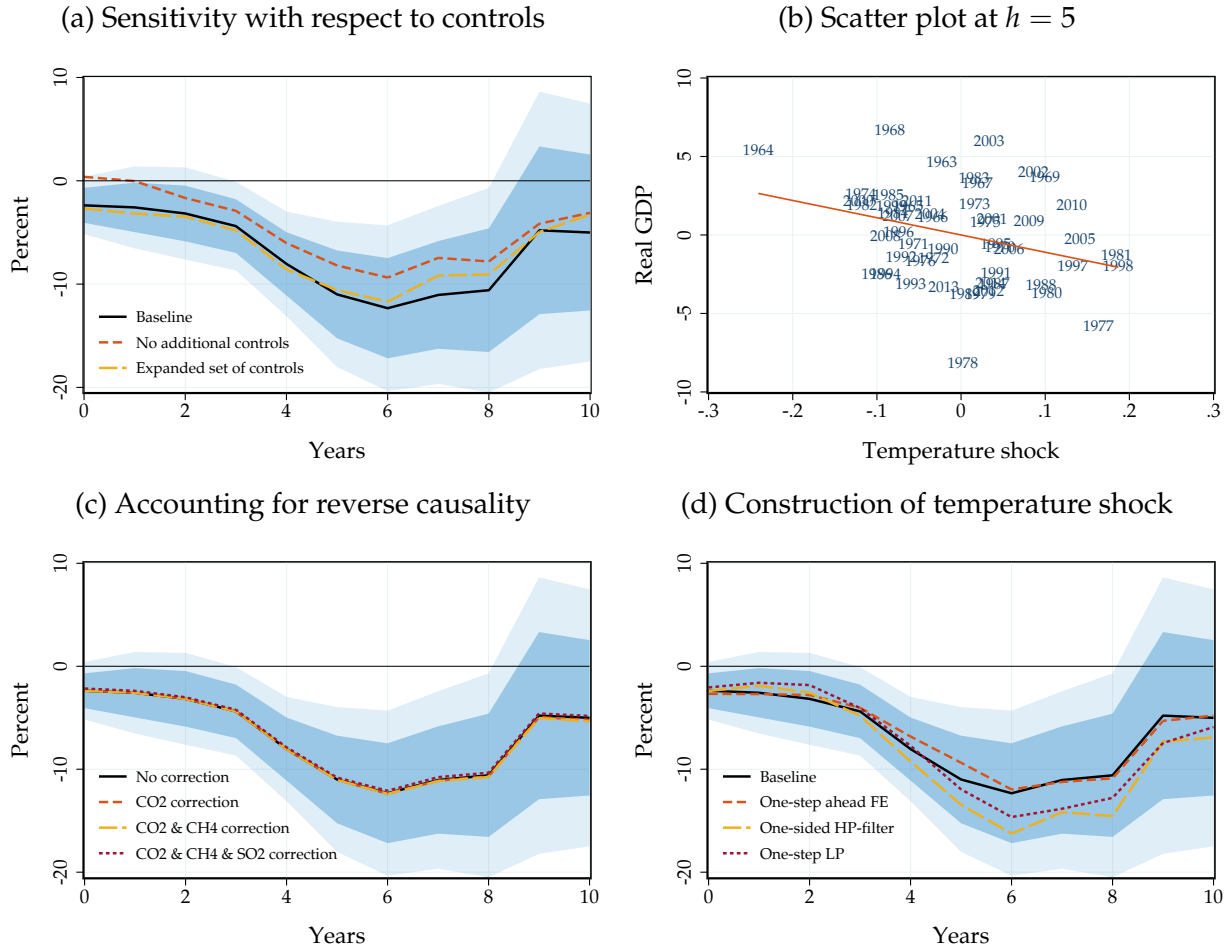
To account for this possibility, we already include rich controls of the world economic performance in our main specification in equation (2). In addition to lagged GDP, we control flexibly for global economic recessions, such as the large oil shocks in the 1970s or the Great Recession, using a set of dummy variables.³

In fact, Figure 4(a) shows that our results hold regardless of the particular set of macroeconomic controls. We compare our baseline estimates, a specification without any macro-financial controls, and a specification with an expanded set of controls that include global oil prices and the U.S. treasury yield. We obtain similar results in all specifications, suggesting that global temperature shocks and economic shocks are largely unrelated. If anything, we obtain somewhat larger effects when we control for recession periods.

We confirm that spuriously correlated economic shocks are unlikely to drive our results by examining how each year in the sample affects our estimates. For all years t ,

³Our definition of global recession dates follows the World Bank (Kose et al., 2020). Specifically, we focus on the following episodes: 1973-1975, 1979-1983, 1990-1992, and 2007-2009. To allow for potential persistent effects of recessions, we also include 2 lags of the global recession indicator variable.

Figure 4: Sensitivity of the Effect of Global Temperature Shocks in the Time Series



Notes: Impulse responses of world GDP per capita to a global temperature shock, estimated from (2). Panel (a): sensitivity with respect to controls included: baseline; specification that also controls for two lags of oil prices and the one-year US treasury yield; specification which only controls for two lags of the temperature shock and GDP growth. Panel (b): scatter plot of temperature shocks against the cumulative change in real GDP 5 years out, both after residualizing our set of controls. Panel (c): GDP response after adjusting for reverse causality. Panel (d): sensitivity with respect to the construction of the temperature shock: baseline with $h = 2$; one-step ahead forecast error $h = 1$; one-sided HP filter; one-step LP estimation with 4 lags of global temperature changes. Solid lines: point estimate. Dark and light shaded areas: 68 and 90% confidence bands, respectively in the baseline specification.

Figure 4(b) plots the change in GDP 5 years later at $t + 5$ against the temperature shocks at time t after residualizing both from our set of controls. The negative relationship turns out to be a robust one and is not driven by a specific set of outliers. Figure A.6 in Appendix A.5 displays a systematic jackknife exercise in which we censor one year at a time and find that our estimates are not driven by specific years. Overall, these results indicate that our estimates are unlikely to be driven by economic shocks spuriously correlated to

temperature shocks.

Reverse causality. Changes in economic activity may affect short-run variations in temperature: a decline in economic activity lowers emissions and temperature, and hence increases output going forward.

There are two reasons why reverse causality due to greenhouse gases is unlikely to substantially affect our interpretation. First, such reverse causality concerns typically lead us to underestimate the effect of temperature on economic output. As temperature rises and economic activity initially declines, the resulting fall in greenhouse gas emissions implies lower future temperatures and thus higher future output. Thus, true damages would be even larger than our estimates.

Second, annual fluctuations in emissions imply negligible temperature variations relative to the typical temperature shocks that we exploit. For instance, typical year-to-year fluctuations in CO₂ *emissions* are of the order of 2 gigatons. After accounting for oceanic and biosphere absorption, these annual fluctuations translate into 1 gigaton of *atmospheric* CO₂. This magnitude corresponds to 0.15 part per million (ppm) in atmospheric CO₂ *concentration*. Current CO₂ atmospheric concentration is just above 400 ppm. Given a climate sensitivity between 2 and 4, year-to-year fluctuations in emissions thus imply year-to-year fluctuations in temperature of about 0.0005°C. This is an order of magnitude lower than natural climate variability which is of the order of 0.1°C.

Aerosol emissions can also lead to reverse causality, for instance due to sulfur dioxide (SO₂). Aerosols have the opposite effect of greenhouse gases and reduce global temperature by reflecting incoming sunlight. Aerosols are shorter-lived than greenhouse gases in the atmosphere, which may amplify or dampen reverse causality concerns relative to greenhouse gases depending on the horizon of interest.

Two exercises verify that reverse causality is unlikely to affect our results. First, we test whether our temperature shocks are forecastable by past macro-financial variables with a series of Granger-causality tests in Appendix A.2. We find no evidence that global temperature shocks are forecastable, consistently with the substantial lag and small sensitivity between emissions and temperature changes.

Second, we explicitly account for the feedback between output and temperature through emissions. We consider the two most important greenhouse gases: carbon dioxide (CO₂) and methane (CH₄). We also include the main source of aerosol emissions: sulfur dioxide (SO₂). We use standard estimates of the emissions-to-GDP elasticity and leading esti-

mates of the dynamic sensitivity of temperature to an emissions impulse to construct our adjustment. We provide more details in Appendix A.6. Figure 4(c) confirms that explicitly controlling for reverse causality has no meaningful effect on our results.

External validity and temperature variability. Different ways of constructing our temperature shocks or excluding specific sources of global temperature variation may lead to different results. We address this concern with two exercises.

We show that our results hold across a variety of definitions of temperature shocks. In our baseline specification, we measure temperature shocks using the Hamilton (2018) filter with a horizon $h = 2$. In Figure 4(d), we show that constructing temperature shocks as one-step ahead forecast errors $h = 1$ following previous work (see e.g. Bansal and Ochoa, 2011; Nath et al., 2023) or using a one-sided HP filter produces similar results. In addition, Appendix A.12.1 reproduces all our main analyses under a one-step ahead forecast error $h = 1$ and finds virtually identical results.

We also show that our results are virtually unchanged when we directly estimate the effects of temperature on world GDP without highlighting the identifying variation through global temperature shocks. In that case, instead of estimating temperature shocks in a first step by projecting temperature on its lags, and then projecting world real GDP on temperature shocks in a second step, we directly project world real GDP on temperature with enough lags of temperature and GDP. Both approaches are numerically equivalent when we construct the shocks as one-step ahead forecast errors with the same controls.

In addition, our results do not depend on specific sources of global temperature variation. We re-evaluate our results after netting out temperature variation generated by El Niño by controlling for ENSO indices in our main specification. The results are shown in Figure A.3 in Appendix A.2. The responses are close to our baseline estimates. Similarly, controlling for volcanic eruptions also yields virtually unchanged results. These exercises indicate that our main results capture a broad effect of global temperature on economic activity that is not specific to particular sources of temperature variation.

Together, these robustness exercises corroborate our interpretation that global temperature shocks are driven by various external causes and internal climate variability and have a large causal effect on world GDP. We expand more flexibly on these robustness checks in the next section, where we study the effects of global temperature shocks in a panel of countries.

3 Temperature Shocks in the Panel of Countries

So far we have evaluated the impact of global temperature shocks directly on world GDP. We now exploit country-level data on GDP to achieve four distinct goals. Our first goal in Section 3.1 is to exploit the additional statistical power in the panel to further corroborate our results when controlling for possibly confounding trends at the country level and varying the span of our sample period. Our second goal in Sections 3.2 and 3.3 is to contrast the impact of global temperature shocks with existing work that has focused on country-level temperature shocks. Our third and fourth goals are to explore the margins through which GDP declines and the heterogeneity in country-level responses (Section 3.4).

3.1 Global Temperature Shocks in the Panel

To estimate the dynamic causal effects of temperature shocks in the panel, we employ the panel local projections approach in Jordà et al. (2020). In this section, we still estimate the effect of global temperature shocks, now averaged across 173 countries. However, the panel approach allows us to account for unobserved, time-invariant country characteristics using country fixed effects. We can also control for past GDP growth at the country level and regional trends. Specifically, we estimate the following series of panel regressions for horizons $h = 0, \dots, 10$:

$$y_{i,t+h} - y_{i,t-1} = \alpha_{i,h} + \theta_h T_t^{\text{shock}} + \mathbf{x}_t' \boldsymbol{\beta}_h + \mathbf{x}_{i,t}' \boldsymbol{\gamma}_h + \varepsilon_{i,t+h}, \quad (3)$$

where $y_{i,t}$ is the outcome variable of interest for country i in year t , T_t^{shock} is the global temperature shock and θ_h is the dynamic causal effect of interest at horizon h . \mathbf{x}_t is a vector of global controls, $\mathbf{x}_{i,t}$ is a vector of country-specific controls and $\varepsilon_{i,t}$ is an error term. In our baseline specification, we use the same set of global controls as before, and in addition control for two lags of country-level GDP growth. We expand on these controls in further sensitivity checks below. Our main outcome variable of interest is country-level log real GDP per capita. Our sample is an unbalanced panel spanning 1960-2019.

Because the temperature shock T_t^{shock} does not vary by country, the error term is potentially serially and cross-sectionally correlated. For inference, we rely on Driscoll and

Kraay (1998) standard errors that are robust to cross-sectional and serial dependence.⁴

By design, our specification is close to the specifications commonly used in the panel literature on the economic effects of local temperature shocks (e.g. Dell et al., 2012; Burke et al., 2015; Nath et al., 2023). Crucially however, the temperature shock T_t^{shock} does not vary by country in our case. As a result, we cannot control for time fixed effects as is common when shocks are also country-specific. Instead, we include the same global control variables as in our time-series specification (1).

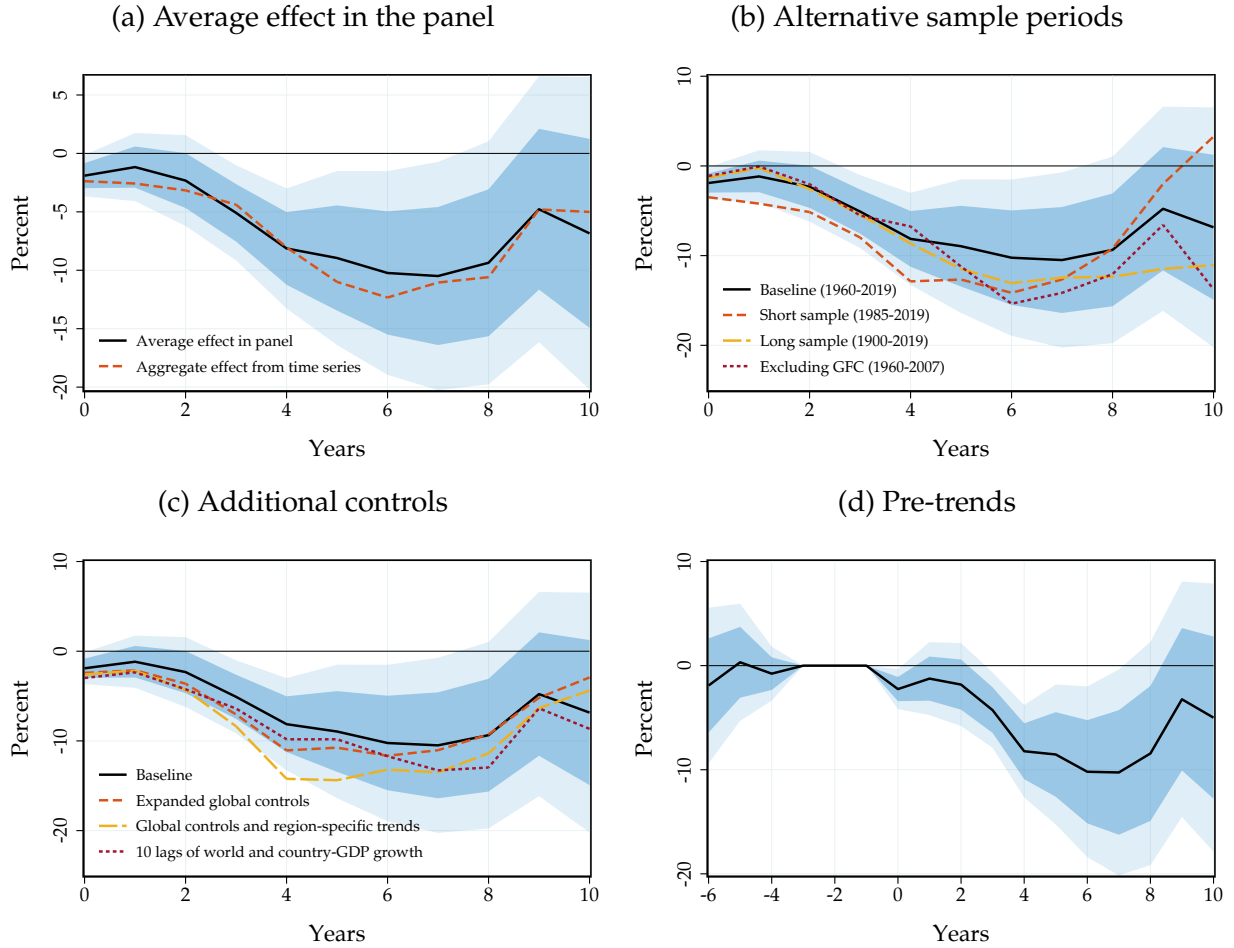
Figure 5(a) shows the impulse responses to a global temperature shock, estimated in the panel of countries. Consistently with our aggregate time-series evidence, global temperature shocks lead to a significant fall in real GDP per capita that exceeds 10% at peak and persists even 10 years out. This effect is close to our time series analysis, indicating that our results are robust to accounting for unobserved fixed country characteristics.

The increased statistical power in the panel lets us conduct a number of additional sensitivity checks. Panel (b) evaluates whether our results depend on the sample period. We obtain similar results on a sample that starts in 1985 after the large oil shocks of the 1970s or on a sample ending before the 2008 Great Recession. We also consider a much longer sample starting in 1900. For this analysis, we rely on the 18 advanced economies in the Jordà-Schularick-Taylor Macrohistory Database for which we have consistent real GDP data. The results are again very similar. The stability of our estimates across time periods suggests a lack of adaptation to temperature shocks, at least historically.

Our second sensitivity check includes more flexible controls for potential confounding effects. The main concern is that adverse global and regional economic shocks may coincide with global and regional temperature shocks. We add global oil prices, the U.S. treasury yield and, crucially, region-specific time trends. We also consider a specification in which we control for 10 lags of world and country-GDP growth to capture as much economic variability as possible. Figure 5(c) shows that our estimates turn out to be virtually invariant to the set of controls. In Appendix A.7, we further establish that unobserved global shocks are not driving our results by exploiting an intermediate level of spatial aggregation of temperature shocks. The results from this specification that allows us to include time fixed effects turn out again to be close to our baseline case.

⁴Our results are robust to using two-way clustered standard errors by country and year, or using bootstrapping techniques for inference. In fact, to construct the confidence bands for our estimated structural damage functions in Section 4.3, we rely on the distribution estimated using a Wild bootstrap. See Appendix A.3 for more details.

Figure 5: The Average Effect of Global Temperature Shocks and Sensitivity

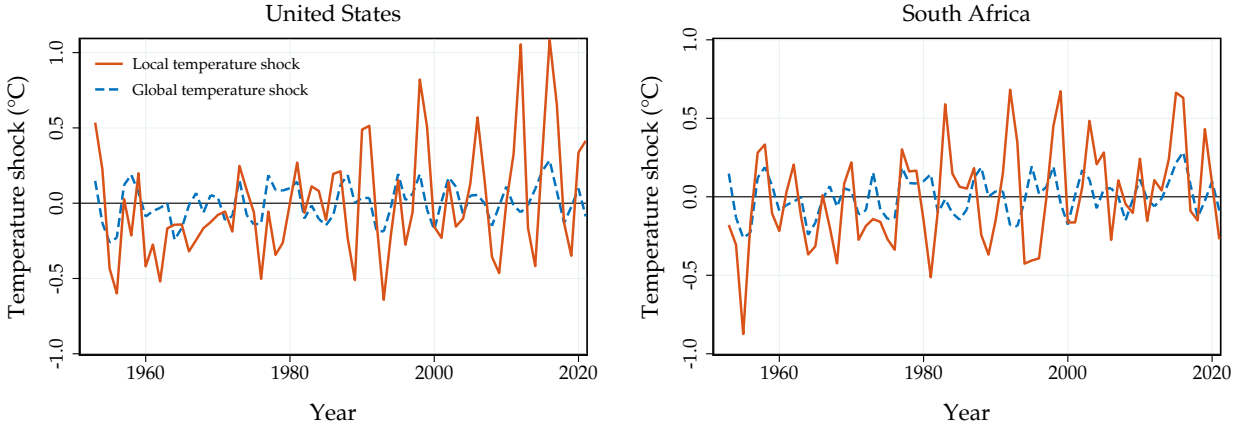


Notes: Impulse responses of real GDP per capita to a global temperature shock estimated in the panel using (3). Panel (a): baseline panel specification together with time-series response. Panel (b): results under shorter (1985-2019), excluding the Great Recession (1960-2007), and longer (1900-2019, with restricted set of countries) samples. Panel (c): sensitivity with respect to controls: baseline; specification with expanded set of global controls (adding two lags of oil price and one-year US treasury yield); specification with expanded set of global controls (four lags) and subregion-specific time trends; specification that controls for 10 lags of world and country-GDP growth. Panel (d): baseline response with pre-trends. Solid line: point estimate. Dark and light shaded areas: 68 and 90% confidence bands.

Our last sensitivity check investigates whether our results may be due to pre-trends. Although Table A.2 already suggests that Granger causality is unlikely to be a concern, Figure 5(d) plots our main estimate together with estimates 6 years prior to the global temperature shock. The effect in the three years before the shock is zero by construction since we control for two lags of GDP growth. We do not detect any statistically significant nor economically meaningful effect up to 6 years prior to the shock.

Finally, we show in Appendix A.12 that our results are robust with respect to the

Figure 6: Local and Global Temperature Shocks



Notes: Local temperature shocks for the United States (left panel) and South Africa (right panel) in red together with the global temperature shocks as the blue dashed line. All the shocks are computed based on the Hamilton (2018) approach with ($h = 2$, $p = 2$). Local shocks computed based on population-weighted country-level temperature data.

temperature and GDP data used as well as the number of lags included in our local projections. Overall, these results confirm the substantial and persistent negative effect of global temperature shocks on real GDP.

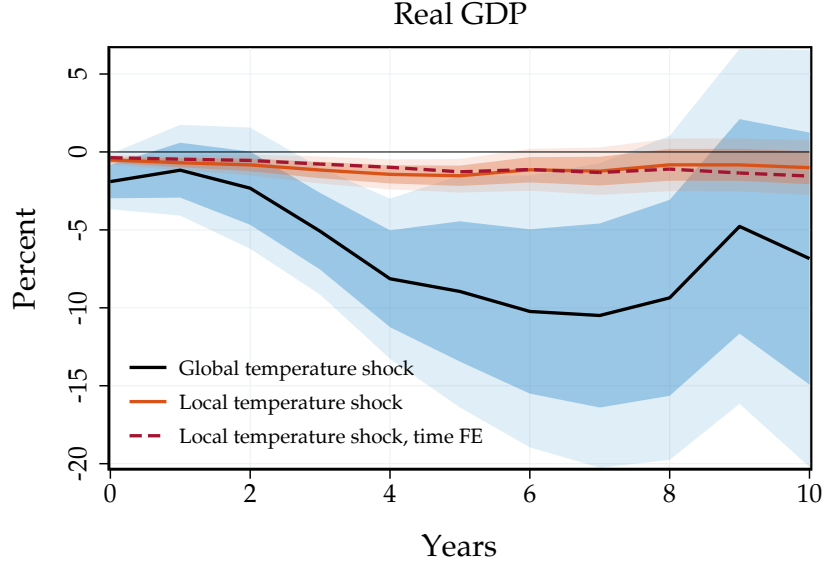
3.2 Global vs. Local Temperature

How do these effects compare to local temperature shocks? Conventional estimates imply that a 1°C rise in local temperature reduces GDP at most by 1-3% in the medium run (Dell et al., 2012; Burke et al., 2015; Nath et al., 2023). To ensure that our findings are not driven by differences in econometric specifications or data choices, we reproduce the effects of local temperature shocks in our empirical framework. We measure local temperature shocks using the Hamilton (2018) filter, as we do in Section 2.2 for global temperature, but now based on population-weighted country-level temperature data.

Figure 6 shows local temperature shocks for the United States and South Africa over our sample from 1960, as two illustrative examples. The standard deviation of local temperature shocks is about three times larger than that of global temperature shocks. While local and global shocks have a correlation of 0.33, they frequently move in different directions. Thus, local shocks do not always correspond to global shocks and vice-versa.

To estimate the responses to local shocks, we rely on our panel specification (3), with

Figure 7: The Average Effect of Local Temperature Shocks



Notes: Impulse responses of GDP per capita to a temperature shock in the panel using (3). Solid red: local temperature, no time fixed effect. Dashed brown: local temperature, time fixed effect. Solid black: global temperature. Lines: point estimates. Dark and light shaded areas: 68 and 90% confidence bands.

the critical difference that the temperature shock is a *country-specific* temperature shock $T_{i,t}^{\text{shock}}$. In this first specification, we do not include time fixed effects to maximize comparability with (3), but include global controls. Alternatively, we also use a specification that includes time fixed effects:

$$y_{i,t+h} - y_{i,t-1} = \alpha_{i,h} + \delta_{t,h} + \theta_h T_{i,t}^{\text{shock}} + \mathbf{x}_{i,t}' \gamma_h + \varepsilon_{i,t+h}, \quad (4)$$

which allows us to flexibly control for unobserved common shocks. In this case, the global controls are absorbed by the time fixed effects.

Figure 7 shows the estimated impulse responses to a local temperature shock of 1°C as the solid red line (global controls and no time fixed effect) and the dashed brown line (with time fixed effects). For comparison, we also include the impulse responses to a global temperature shock (in black). With or without time fixed effects, local temperature shocks lead to a similar and significant fall in real GDP per capita. On impact, the effect stands at -0.5% and reaches -1.5% after 5 years. These estimates are close to previous findings in Dell et al. (2012), Burke et al. (2015), and Nath et al. (2023).

Simple *statistical* explanations cannot account for the smaller impact of local tempera-

ture. Figure A.8 in Appendix A.8 evaluates a specification in which we jointly estimate the impacts of local and global temperature in the same local projections model. The effects of each temperature shock turn out to be similar to their univariate estimates, reflecting that different variation identifies the impact of global and local temperature shocks. The difference between the two coefficients is statistically significant at the 90% level.

Both global and local shocks lead to a similarly persistent increase in local temperature. Thus, the persistence of temperature following each shock cannot account for the differential impacts of global and local temperature shocks on GDP. Figure A.11 in Appendix A.10 shows that imposing the same internal persistence in response to global and local temperature shocks using the Sims (1986) method produces results that are as different as in our baseline analysis.

These comparisons reveal that *global* temperature has much more pronounced impacts on economic activity than *local* temperature. The estimated effects of global temperature shocks are six to seven times larger than for local temperature shocks, based on the same empirical model and the same sample period. Our analysis indicates that the key difference lies in the *nature* of the shock itself rather than in the set of global controls or time fixed effects: changing the set of controls or fixed effects does not affect the local temperature results meaningfully. Climatic variation within country or even smaller geographic units may help alleviate identification concerns, but misses any global effects of climate change—itsself a global phenomenon. By contrast, our approach purposefully studies these common effects by focusing on climatic variation at the global level.

3.3 Reconciling the Impacts of Global and Local Temperature

Why, then, does global temperature cause more economic harm than local temperature? We consider two possible *economic* explanations. The first explanation is that global temperature shocks are inherently different from local temperature shocks and capture potentially damaging climatic implications that local temperature does not. The second explanation is that local temperature is the true determinant of damages but compounds through economic spillovers that are however netted out in the panel specification.

Extreme Climatic Events. We start by investigating whether global temperature predicts meaningful shifts in climatic phenomena. We ask how temperature shocks correlate with the likelihood of extreme weather events: extreme temperature, drought, extreme precipitation, and extreme wind speed. As detailed in Section 2.1, we define an exposure

index for each of these events by counting the fraction of cell-days within each year and country that exceed a given threshold. This exposure index can thus be interpreted as a probability. We use the panel local projection specification (3) and denote by θ_h^X the impact of a 1°C temperature shock on the exposure index of event X at horizon h . Figure 8 displays our results.

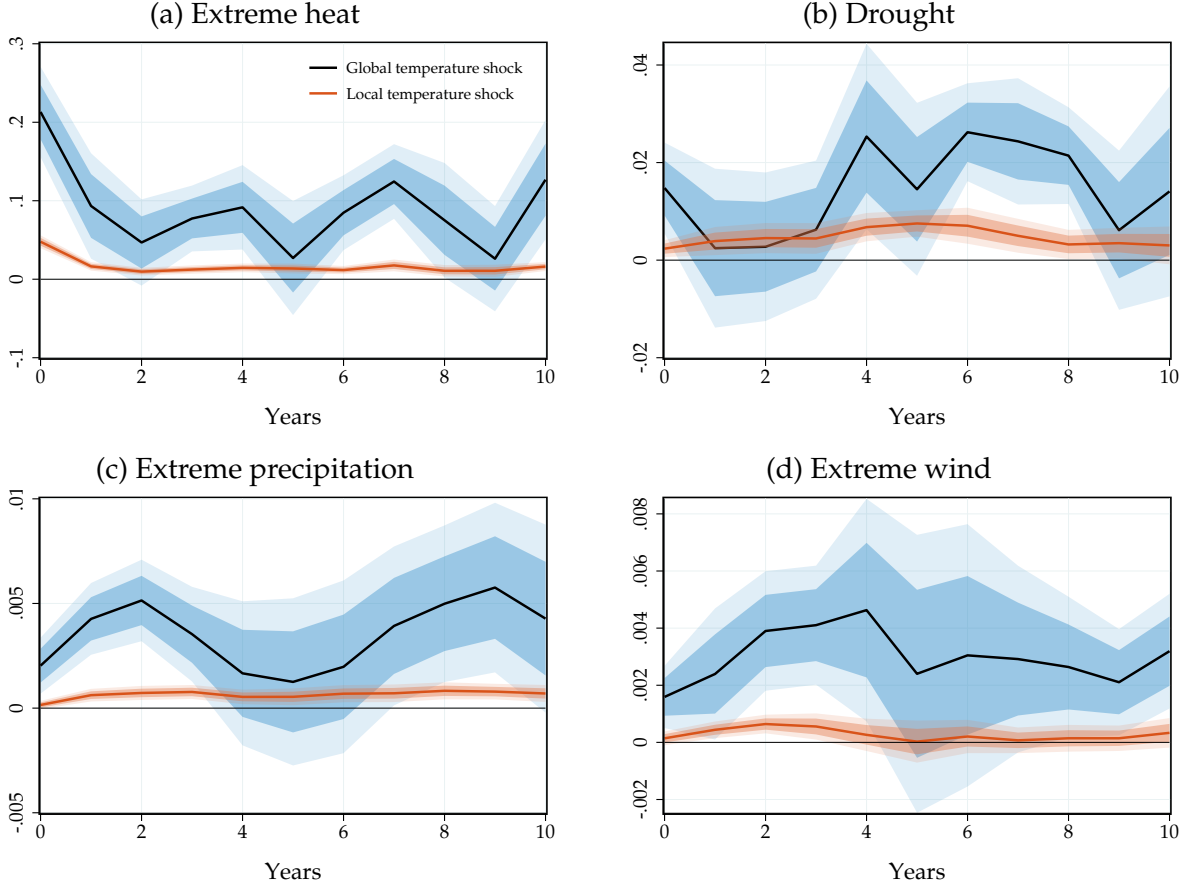
Local temperature shocks lead to an increase in the share of extreme heat and drought days. However, global temperature shocks lead to a substantially larger increase in these extremes. Our extreme heat and drought indices have a baseline probability of 0.05 and 0.25 in 1950-1980, respectively. Thus, a 1°C global temperature shock correlates with a doubling of the frequency of extreme heat and a 20% increase of the frequency of drought. The contrast is even starker for extreme precipitation and extreme wind speed: global temperature shocks predict a large increase in their frequency, while local temperature shocks barely do. We construct the extreme precipitation and wind index to have a baseline probability of 0.01 in 1950-1980. Thus, a 1°C global temperature shock correlates with an increase of the frequency of extreme precipitation and wind of around 50%.

These findings are consistent with the geoscience literature: wind speed and precipitation are outcomes of the global climate—through oceanic warming and atmospheric humidity—rather than outcomes of local temperature distributions (Seneviratne et al., 2016; Wartenburger et al., 2017; Seneviratne et al., 2021; Domeisen et al., 2023). Given that extreme climatic events are known to cause economic damage (Deschênes and Greenstone, 2011; Hsiang and Jina, 2014; Bilal and Rossi-Hansberg, 2023), the differential correlation of global versus local temperature shocks on extreme climatic events may rationalize the larger economic effects of global temperature shocks.

To gauge the quantitative importance of this channel, we start by estimating the impact of extreme events in a panel local projection specification similar to (3). We denote by ϕ_h^X the impact of extreme event X 's exposure index on GDP at horizon h . Figure A.12 in Appendix A.11 reveals that these events are associated with substantial economic damages. Doubling extreme heat exposure at the country level lowers GDP by 2% at peak. A 20% rise in drought exposure lowers GDP by 1%. A 50% increase in extreme precipitation or wind exposure lowers GDP by 0.5%.

Next, we aggregate the local impacts of extreme events. We interact the increase in extreme event exposure following a global temperature shock θ_h^X from Figure 8 with the GDP loss associated with these extreme events from Figure A.12 in Appendix A.11. To do

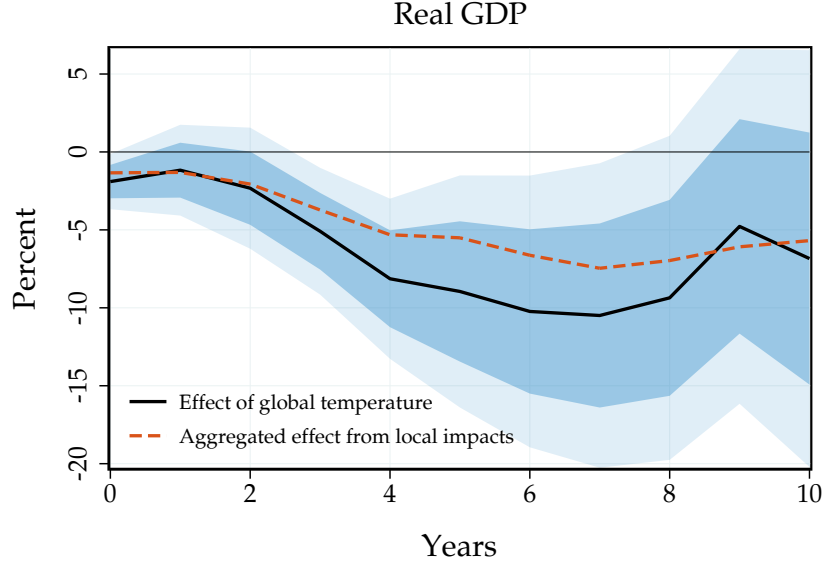
Figure 8: Extreme Weather Events and Temperature



Notes: Impulse responses θ_h^X of extreme temperature, drought, extreme precipitation, and extreme wind exposures to global and local temperature shocks, estimated based on (3). Extreme weather exposure indices record the share of cell-days in a given year and country where temperature, precipitation, or wind speed are above/below a threshold. We define thresholds using the daily weather distribution in 1950-1980. Temperature: above 95th percentile. Drought: below the 25th percentile. Precipitation: above 99th. Wind: above 99th percentile. Though not necessary for our results, we smooth the precipitation and wind measures with a backward-looking (current and previous two years) moving average to remove their inherent noise. Solid lines: point estimate. Dark and light shaded areas: 68 and 90% confidence bands.

so, we adjust the estimates ϕ_h^X to correspond to a one-time fully transitory rise in exposure using again the Sims (1986) method. This persistence adjustment transforms the initial estimates ϕ_h^X into new estimates ψ_h^X . In practice, this adjustment has minor consequences as ϕ_h^X, ψ_h^X are close because extreme events have low internal persistence on their own. We then aggregate these impacts according to $\Theta_h = \sum_X \sum_{t=0}^h \theta_t^X \psi_{h-t}^X$, where the sum over X includes the four extreme events and local temperature. Thus, the aggregate impact Θ_h now factors in the highly persistent response of extreme events to a global temperature

Figure 9: The Impact of Extreme Events on GDP Through Global Temperature



Notes: Aggregated effect on GDP based on local temperature and extreme events impacts Θ_h (dashed red) together with the impulse responses to a global temperature shock based on our baseline empirical model (3). Dark and light shaded areas: 68 and 90% confidence bands.

shock $\{\theta_h^X\}_h$.

Figure 9 displays our results. The rise in the frequency of extreme events associated with a global temperature shock implies a peak GDP impact of 7.5%, up from 1.5% under local temperature alone. The additional impact of extreme events alone represents two thirds of the direct effect of global temperature on GDP. This result indicates that global temperature has a larger impact on economic activity than local temperature because the *physical nature* of the shock is different.

Our aggregation exercise highlights that it is critical to consider climatic outcomes beyond local temperature in panel approaches (Kotz et al., 2024), but also illustrates the challenges associated with such “bottom-up” exercises. Capturing all relevant local impacts individually is challenging: researchers need to know ex-ante which variables to consider, be able to measure them consistently throughout the world, and accurately estimate their degree of internal persistence. As shown in Figure 8, persistence can vary greatly depending on global or local temperature shocks. Even then, Figure 9 suggests that this “bottom-up” approach underestimates the true impact of global temperature, perhaps because it fails to capture the changing intensity of extreme events. A key advantage of our time-series approach is its ability to encompass all relevant local impacts

that are predictable by global temperature.

Economic spillovers. Our analysis of extreme events suggests that there is little room left for economic spillovers to rationalize the large gap between global and local temperature impacts. We now confirm this argument quantitatively.

When the trading partners of a given country are hit by adverse local temperature realizations, some of the resulting economic consequences may also be felt domestically as hypothesized by Neal (2023) and shown in Dingel et al. (2023) and Zappalà (2023). In that case, these indirect effects would not appear in baseline local temperature estimates, underestimating true damages. However, they may appear in global temperature estimates if local temperature is spatially correlated.

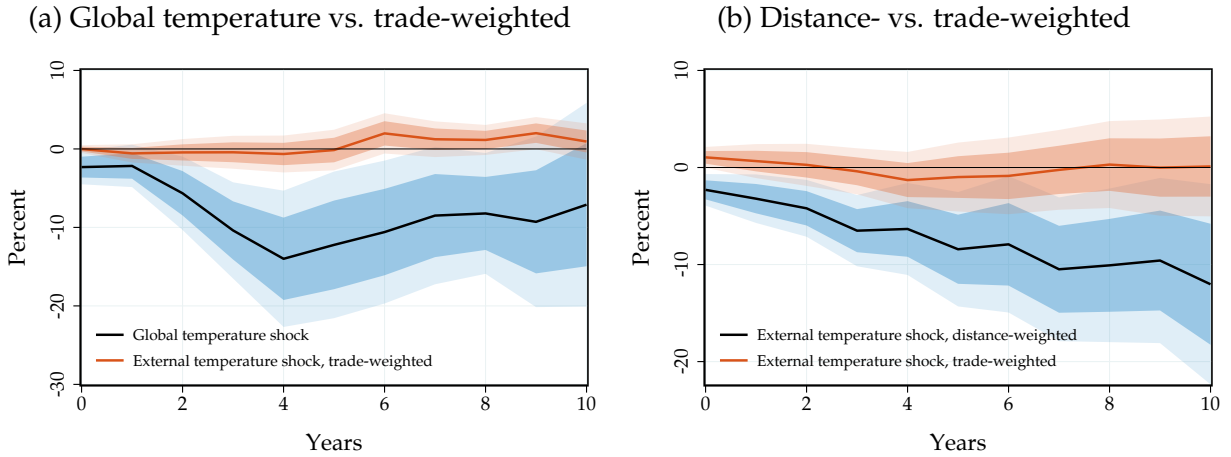
To gauge the relevance of economic spillovers, we exploit intermediate levels of spatial aggregation of local temperature shocks. We construct an external temperature shock for each country that averages local temperature shocks of surrounding countries, weighted by their respective trade share or distance at the beginning of the sample:

$$T_{i,t}^{\text{trade, ex}} = \sum_{j \neq i} \pi_{ij} T_{i,t}^{\text{shock}} \quad T_{i,t}^{\text{dist, ex}} = \sum_{j \neq i} d_{ij} T_{i,t}^{\text{shock}}, \quad (5)$$

where π_{ij} denote trade shares based on imports plus exports between countries i and j in 1960. d_{ij} is proportional to the inverse geodesic distance between the centroids of countries i and j and sums to one for each country i . We expect the trade-weighted external temperature shock $T_{i,t}^{\text{trade, ex}}$ in equation (5) to have a substantial impact on GDP if economic spillovers explain the difference between local and global temperature impacts.

To conduct a fair comparison to our physical explanation about the nature of the temperature shock and extreme events, we construct an external temperature shock that weights the shocks in the surrounding countries by their physical distance. This distance-weighted external temperature shock $T_{i,t}^{\text{dist, ex}}$ in equation (5) captures similar physical variation to global temperature shocks but with a structure comparable to our trade-weighted measure. Of course, it is well-known that trade and distance are correlated, but only imperfectly due to border and languages effects, allowing us to separately identify the impact of each measure. We expect distance-weighted external temperature to have a larger impact on GDP than trade-weighted external temperature if physical differences between global and local temperature explain the larger impact of global temperature rather than economic spillovers.

Figure 10: The Role of Economic Spillovers



Notes: Impulse responses of world real GDP per capita to external temperature shocks. Left panel: response to a global and trade-weighted shock, estimated jointly in the same local projection specification with expanded set of global controls and subregion-specific time trends. Right panel: responses to a distance-weighted and a trade-weighted shock, estimated jointly in the same local projection specification with time fixed effects. Solid lines: point estimates. Dark and light shaded areas: 68 and 90% confidence bands. Sample of countries differs from main analysis due to availability of trade data at the beginning of the sample.

We then estimate the impact of trade-weighted external temperature, jointly with either global temperature or distance-weighted external temperature. We use the specification in (3) but with both series as explanatory variables. When we use both distance- and trade-weighted temperature, we can control for time fixed effects as we exploit variation at the country level (see Appendix A.7 for more details).

Figure 10 presents the results. Panel (a) shows the response of a trade-weighted temperature shock and a global temperature shock, jointly estimated in the same local projection model. Even when controlling for the trade-weighted temperature shock, global temperature continues to have a substantial adverse impact on GDP. The shape of the response to the global temperature shock is slightly different from Figure 5 because we cannot obtain trade information for all countries at the beginning of our sample and must thus rely on a different set of countries. By contrast, trade-weighted external temperature itself has no significant effect on output. This suggests that economic spillovers cannot account for the difference between global and local temperature.

We confirm this result in Panel (b), which shows the responses to a trade- and distance-weighted temperature shock, jointly estimated in the same local projection model including time fixed effects. Distance-weighted external temperature has a substantial impact on GDP comparable to the impact of a global temperature shock while trade-weighted ex-

ternal temperature has a null impact.⁵ These results indicate that extreme climatic events provide a more plausible rationale than economic spillovers for the gap between global and local temperature impacts on GDP.

3.4 Margins of GDP and Regional Impacts

We have documented that global temperature shocks lower world GDP, but how and where does GDP respond most?

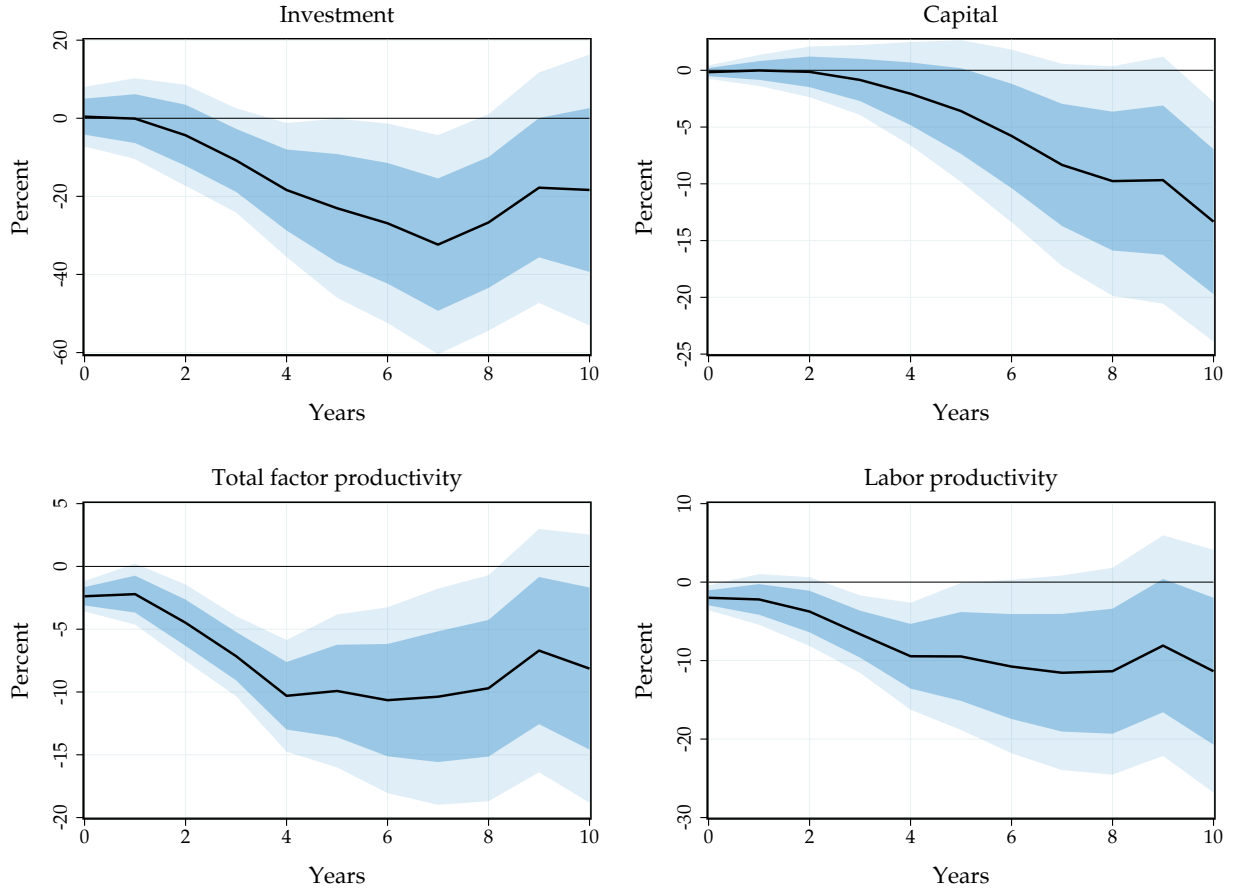
We evaluate the effects of global temperature shocks on capital, investment and productivity in our panel of countries in Figure 11. Global temperature shocks lead to a substantial and significant fall in investment and in the capital stock. The slow decline in the capital stock is consistent with the adverse impact of extreme weather events such as storms that materialize as capital depreciation shocks. Consistently with Hsiang and Jina (2014), we find that disasters associated with global warming do not stimulate growth. Instead, national income, productive capital and investment all dwindle.

Productivity also falls significantly after global temperature shocks. This is true for Total Factor Productivity (TFP) as estimated in the Penn World Tables and for labor productivity. The impact effect, which stands at -2%, is consistent with experimental studies on the impact of temperature on productivity (Seppanen et al., 2003). However, these effects build up over time, reaching -10% after four years.

In addition to unpacking the margins of world GDP, we analyze how the impact of global temperature varies across different regions. Are warmer or lower-income countries more affected? Figure 12 displays the impact of global temperature shocks on twelve regions of the world. All regions but one experience significantly negative effects. We estimate the strongest negative effects—close to 20% at peak—in hot regions such as South-east Asia and Sub-Saharan Africa. Contrary to local temperature shocks, global temperature shocks lead to adverse economic effects even in higher-income, colder regions. The peak effect in North America is around 10%, and in Europe around 7%. The only region that gains from global temperature shocks is Central and East Asia, possibly because of the relatively large number of cold countries in this region that may benefit from warmer temperatures.

⁵Appendix A.9 shows that when we do not control for distance-weighted temperature or global temperature, trade-weighted temperature shocks do have a significantly negative effect on GDP, but similarly small to the direct impact of local temperature.

Figure 11: Transmission of Global Temperature Shocks

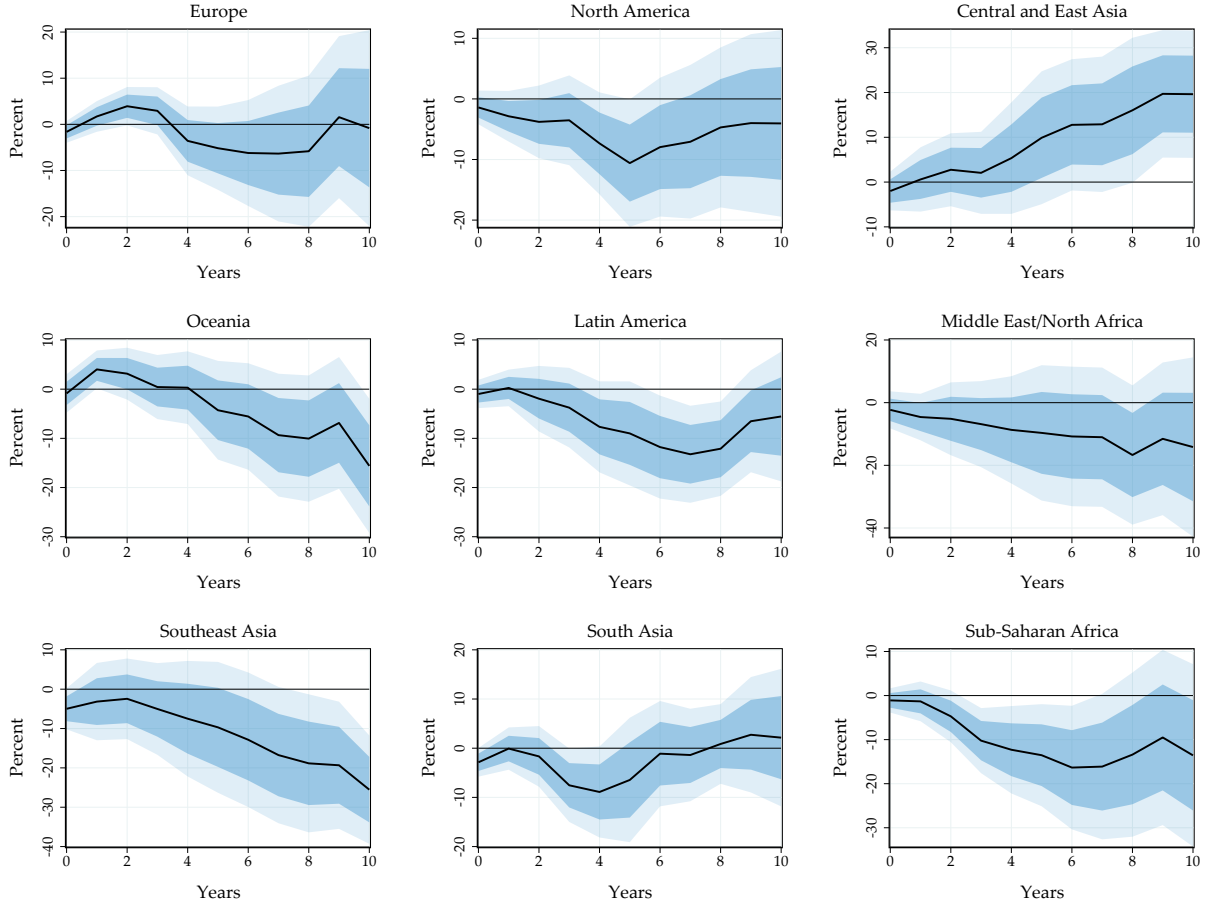


Notes: Impulse responses of investment per capita, the capital stock per capita, total factor productivity and labor productivity to a global temperature shock, estimated based on panel local projections (3). Labor productivity: output over employment. Total factor productivity: Penn World Tables. Solid line: point estimate. Dark and light shaded areas: 68 and 90% confidence bands.

We evaluate whether the impact of global temperature shocks varies by country baseline temperature and income level in Figure A.21, Appendix A.13. Although somewhat imprecisely estimated, we find suggestive evidence that warm and low-income countries display the strongest adverse effects of global temperature shocks, while cold and high-income countries are less sensitive to global temperature shocks. This result is qualitatively consistent with previous evidence on local temperature (Dell et al., 2012; Burke et al., 2015; Nath, 2022). Quantitatively, global temperature shocks have larger effects across all countries. Overall, the effects of global temperature are larger and more uniformly detrimental than those of local temperature (Burke et al., 2015).

So far we established the reduced-form impact of global temperature shocks on eco-

Figure 12: Regional Impacts of Global Temperature Shocks



Notes: Impulse responses of GDP per capita to global temperature shocks for different regions across the world based on (3), conditioning on the different regions and controlling for subregion-specific time trends. Solid lines: point estimate. Dark and light shaded areas: 68 and 90% confidence bands.

conomic activity at the world and country level. We now turn to our structural model to convert these estimates into welfare losses and a value of the Social Cost of Carbon.

4 A Model of Climate Change Across the World

Our framework closely follows the standard neoclassical growth model. As such, it mirrors the backbone of the Dynamic Integrated Climate Economy (DICE) model introduced by Nordhaus (1992). Our key innovations are to introduce capital depreciation damages and to use our new reduced-form estimates of the impact of global temperature shocks to structurally estimate the damage functions in the model.

4.1 Model Description

Setup. Time is continuous and runs forever. There is a unit continuum of infinitely-lived identical households who populate the world economy. Households have Constant Relative Risk Aversion flow preferences: $U(C) = \frac{C^{1-\gamma}-1}{1-\gamma}$. Labor supply is exogenous and set to $L_t = 1$. The pure rate of time preference of households is ρ .

Firms produce according to a Cobb-Douglas production function in capital K_t and labor L_t with time-dependent TFP Z_t : $Y_t = Z_t K_t^\alpha L_t^{1-\alpha}$. They hire labor and rent capital from households in competitive factor markets. Capital depreciates at rate Δ_t , which is covered by firms. The paths of Z_t , Δ_t are perfectly foreseen.

Households earn wages w_t , hold capital K_t and rent it out to firms for production. The net interest rate is r_t . Firms make zero profits given constant returns to scale, so we omit profits in the budget constraint of the household, which writes: $C_t + \dot{K}_t = w_t + r_t K_t$. Households are endowed with an initial capital stock K_0 .

A competitive equilibrium of our economy is a collection of sequences $\{C_t, K_t, r_t, w_t\}_{t=0}^\infty$ such that households optimize given prices $\{r_t, w_t\}_{t=0}^\infty$:

$$\max_{\{C_t, K_t\}_t} \int_0^\infty e^{-\rho t} U(C_t) dt \quad \text{subject to} \quad C_t + \dot{K}_t = w_t + r_t K_t \quad \text{given } K_0;$$

firms optimize given prices $\{r_t, w_t\}_t$: $\max_{K_t^D, L_t^D} Z_t (K_t^D)^\alpha (L_t^D)^{1-\alpha} - (r_t + \Delta_t) K_t^D - w_t L_t^D$; and factor markets clear: $K_t = K_t^D$ and $1 = L_t^D$.

Climate change. We model climate change as changes in TFP Z_t and capital depreciation Δ_t over time, relative to their baseline values Z_0, Δ_0 . We take the path of global mean temperature T_t relative to a reference level T_0 as given, and denote by $\hat{T}_t \equiv T_t - T_0$ the path of excess temperature. Global mean temperature affects TFP and capital depreciation through structural damage functions $\{\zeta_s, \delta_s\}_{s \geq 0}$:

$$Z_t = Z_0 \exp \left(\int_0^t \zeta_s \hat{T}_{t-s} ds \right) \quad \Delta_t = \Delta_0 \exp \left(\int_0^t \delta_s \hat{T}_{t-s} ds \right). \quad (6)$$

The structural damage functions ζ_s and δ_s govern the persistence of the effect of transitory global temperature shocks on TFP and capital depreciation. When ζ_s, δ_s are Dirac mass points at $s = 0$, global temperature shocks have purely transitory level effects. When ζ_s, δ_s are positive functions that asymptote to zero, global temperature shocks have persistent level effects. When ζ_s, δ_s are positive functions that asymptote to a positive value,

global temperature shocks have growth effects.

When temperature $T_t \equiv \bar{T}$ is constant, the economy converges to its steady-state with the corresponding values of TFP $\bar{Z} = Z_0 \exp((\bar{T} - T_0) \int_0^\infty \zeta_s ds)$ and capital depreciation rate $\bar{\Delta} = \Delta_0 \exp((\bar{T} - T_0) \int_0^\infty \delta_s ds)$. These expressions highlight that the cumulative damage functions $\int_0^\infty \zeta_s ds$ and $\int_0^\infty \delta_s ds$ determine the long-run impact of global temperature changes. In that case, ζ_s, δ_s need to be integrable to obtain a well-defined steady-state. This requirement rules out growth effects which would imply an economy that asymptotes to zero. In any case, we do not find any evidence supporting growth effects.

We do not model the feedback between the economy and emissions, and associated externalities, because we focus on climate damages. Thus, the competitive equilibrium is efficient as is standard in the neoclassical growth model.

Social Cost of Carbon. In our framework, we define the Social Cost of Carbon as the one-time dollar amount \mathcal{C} that households would pay at time 0 that would make them indifferent between a world with an additional ton of CO2 emitted at time 0, and a world starting in steady-state, without emissions, but having paid \mathcal{C} .

Given that we do not model emissions directly, we must map a one-time CO2 pulse into a temperature path in order to calculate the SCC. We follow Folini et al. (2024) and use the temperature response of global mean temperature to a CO2 pulse from Dietz et al. (2021), itself based on Joos et al. (2013). Dietz et al. (2021) report the temperature response in multiple state-of-the-art atmospheric circulation and radiative forcing models.

We denote by $\{\hat{T}_t^{\text{SCC}}\}_{t \geq 0}$ the path of excess warming implied by a one-time pulse of one ton of CO2 emitted at time 0. The average response in Dietz et al. (2021) indicates that temperature rises steadily and eventually stabilizes at +0.002°C after 15 years. We remain conservative and use the lower end of available temperature responses: we define $\{\hat{T}_t^{\text{SCC}}\}_{t \geq 0}$ as half of the the multi-model mean in Dietz et al. (2021). Doing so ensures that historical emissions are consistent with historical warming data. When we use the multi-model mean, our SCC numbers nearly double. Our welfare numbers would remain unchanged as they do not depend on the temperature response to a CO2 pulse, but instead on a particular warming scenario.

We then construct productivity and capital depreciation paths $\{Z_t^{\text{SCC}}, \Delta_t^{\text{SCC}}\}_{t \geq 0}$ according to equation (6) in which we use the temperature path $\{\hat{T}_t^{\text{SCC}}\}_{t \geq 0}$ rather than a global warming scenario. The model delivers a path of value functions $\{V_t^{\text{SCC}}(K)\}_{t \geq 0}$, equilibrium capital stocks $\{K_t^{\text{SCC}}\}_{t \geq 0}$ with initial condition $K_0^{\text{SCC}} = K^{\text{ss}}$, leading to a path

of realized values $\{V_t^{\text{SCC}}(K_t^{\text{SCC}})\}_{t \geq 0}$, in response to this CO2 pulse-induced warming. Our definition requires that the SCC \mathcal{C} is given implicitly by:

$$V^{ss}(K^{ss} - \mathcal{C}) = V_0^{\text{SCC}}(K^{ss}), \quad (7)$$

where ss superscripts denote initial steady-state quantities.

To gain intuition, consider the case when the SCC is not too large. Then, a first order perturbation implies that the SCC satisfies $\mathcal{C} = \int_0^\infty e^{-\rho t} u'(C^{ss})(C^{ss} - C_t^{\text{SCC}}) dt = \frac{1}{\rho} \frac{C^{ss} - \bar{C}^{\text{SCC}}}{C^{ss}}$, where $\frac{C^{ss} - \bar{C}^{\text{SCC}}}{C^{ss}}$ is the consumption-equivalent welfare loss from the warming implied by the CO2 pulse. These identities indicate that the SCC is equal to the present *stock* valuation of *flow* consumption-equivalent welfare losses from the warming induced by the CO2 pulse. While these conditions are useful to gain intuition, in our quantification we always use the nonlinear definition (7) that accounts for a time-varying marginal rate of substitution.

4.2 Estimation Strategy

Our next step is to estimate the structural damage functions ζ_s, δ_s . To do so, we match the reduced-form impulse response functions of output and capital to global temperature shocks from Figures 7 and 11. We proceed in two steps.

In the first step, we calibrate our model based on standard values from the literature, with the exception of our damage functions. We set risk-aversion to $\gamma = 2$. The capital share is $\alpha = 0.33$. The baseline annual capital depreciation rate is $\Delta_0 = 0.08$. Our choice of annual pure rate of time preference $\rho = 0.02$ follows Rennert et al. (2022) and is consistent with a 2% annual interest rate in steady-state.⁶ Of course, the equilibrium path of consumption in the model determines the effective consumption-based discount rate. We assess the robustness of our results with respect to the rate of time preference in Section 5.4 below.

In the second step, we invert our model to estimate the sequence of TFP and depreciation shocks that correspond to a temperature shock. We leverage that the actual temperature shocks that arise during our sample are small as in Figure 6 and therefore imply

⁶This framework immediately accommodates balanced productivity growth. Provided we adjust the rate of time preference and the baseline capital depreciation rate, standard rescaling arguments ensure that allocations and welfare would be identical in counterfactuals when the baseline economy is in steady-state or on a balanced growth path.

output and capital fluctuations of the order of 1%. Therefore, we can use a first-order perturbation of the model around the initial steady-state. For any sequence of temperature shocks \hat{T}_t , we denote by \hat{z}_t the resulting log deviation in TFP and by $\hat{\Delta}_t$ the resulting level deviation capital depreciation rates. We denote by \hat{y}_t , \hat{k}_t the log deviations in output and capital along the transition. We emphasize that we use log-linearization for *estimation* only, *not* for *counterfactuals*.

Proposition 1. (*Model inversion*)

There exists $\mathcal{K}_t(\hat{z})$, $\mathcal{J}_{t,s}$ given in Appendix B.3 such that, to a first order in $\{\hat{T}_t\}_{t \geq 0}$:

$$\hat{y}_t = \hat{z}_t + \alpha \hat{k}_t \quad \hat{k}_t = \mathcal{K}_t(\hat{z}) + \int_0^\infty \mathcal{J}_{t,s} \hat{\Delta}_s ds$$

Proof. See Appendix B.3. □

Proposition 1 delivers an identification result. Given observed output and capital responses \hat{y}_t , \hat{k}_t , we can recover the underlying sequence of productivity shocks \hat{z}_t and capital depreciation shocks $\hat{\Delta}_t$. The first equation of Proposition 1 lets us recover the sequence of productivity shocks directly from the observed output and capital responses—this relationship is immediate from the production function.

The main content of Proposition 1 lies in the second equation. By log-linearizing the equilibrium conditions of the model and solving explicitly for the equilibrium sequence of capital, we relate capital deviations to the sequence of capital depreciation rates through the sequence-space Jacobian $\mathcal{J}_{t,s}$ (Auclert et al., 2021; Bilal and Goyal, 2023) given productivity shocks embedded in $\mathcal{K}_t(\hat{z})$. In the context of the neoclassical growth model, this Jacobian admits a closed-form expression as a function of parameters and steady-state objects. When $\mathcal{J}_{t,s}$ is invertible, the capital depreciation shocks are identified. We use Proposition 1 to obtain the sequence of TFP and depreciation rates \hat{z}_t , $\hat{\Delta}_t$ that correspond to any sequence of temperature shocks \hat{T}_t .

We use these observations to estimate ζ_s , δ_s . We consider the path of output and capital in response to an *observed* temperature shock, that corresponds to the underlying temperature path \hat{T}_t in Figure 3. Proposition 1 delivers the corresponding sequence of productivity and capital depreciation shocks \hat{z}_t , $\hat{\Delta}_t$. We then identify ζ_t and δ_t as the innovations to these sequences as per equation (6).

This approach is consistent with households having rational expectations about future temperature shocks: after a temperature shock, households expect temperature to

remain persistently elevated as in Figure 3. One advantage of this approach is that we identify damage functions off of empirical impulse responses to a shock that is itself persistent. Thus, counterfactuals that focus on a permanent increase in temperature build on moments identified from responses to a persistent shock—though not a fully permanent shock—rather than a purely transitory shock.

In practice, we face two additional challenges. We address both of them by imposing a smooth functional form for our structural damage function. We constrain ζ_s, δ_s to be of the form $A(e^{-Bs} - e^{-Cs})$.

The first challenge that our constrained estimation addresses is that we can only estimate the impulse response functions \hat{y}_t, \hat{k}_t up to a finite horizon. By contrast, Proposition 1 requires the entire impulse response function. We cannot simply set the capital impulse response to 0 from year 11 onwards, as this would imply a large underlying capital wind-fall gain for the economy. By constraining the shape of the structural damage functions, we use our 10 data points to estimate 3 parameters per damage function.

The second challenge is to discipline the long-run effects of temperature shocks. By constraining the structural damage functions, we ensure that the effects of transitory temperature changes vanish in the very long run. If we estimated the structural damage functions entirely unconstrained and with a longer horizon, temperature shocks could potentially have longer-ranging but extremely imprecisely estimated effects. Therefore, our approach is conservative in that it limits the long-run impact of a one-time transitory temperature shock.

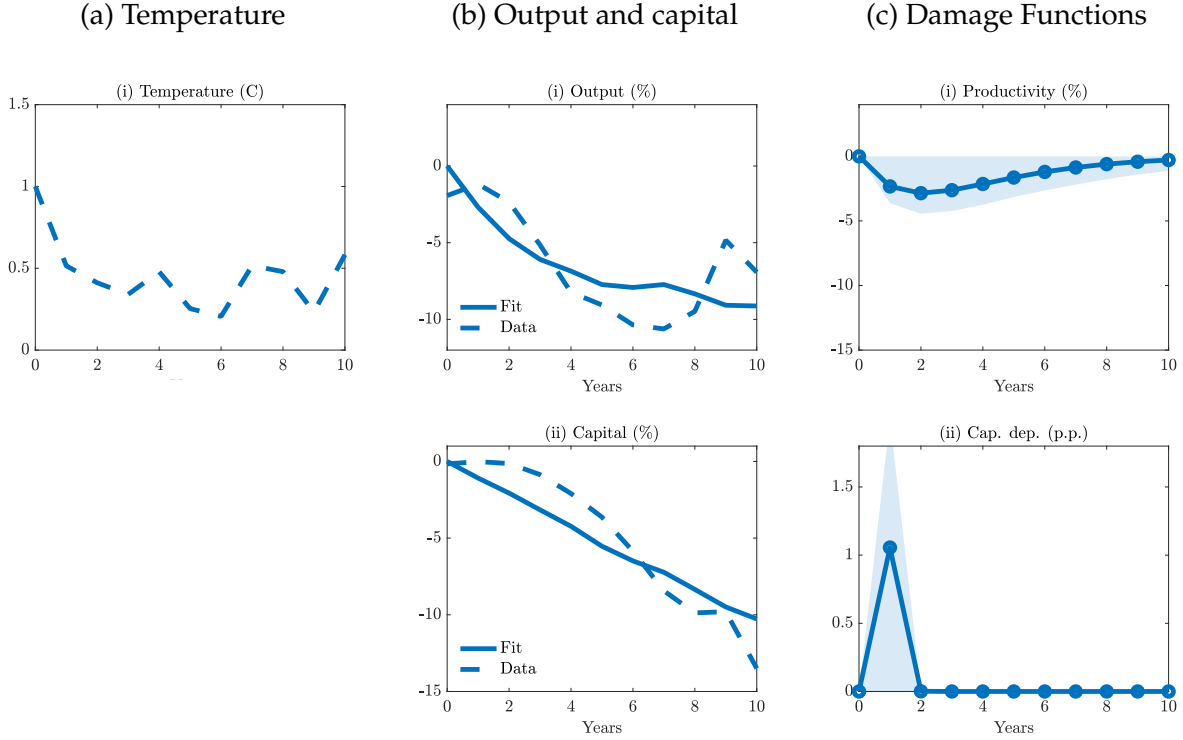
Hence, instead of exactly inverting the model, we estimate A, B and C for ζ_s, δ_s separately using Non-Linear Least Squares to minimize the squared deviations from the equations in Proposition 1 for the first 10 years only.

4.3 Estimation Results

Figure 13 shows our estimation results. Column (a) displays the underlying temperature path from Figure 3. Column (b) reveals that the estimated model closely fits the empirical responses given its limited degrees of freedom. Of course, the model fit relies on our constrained functional form: if we did not constrain the damage function, the fit would be one-to-one.

Column (c) depicts the estimated structural damage functions, ζ_s and δ_s . They coincide with the productivity and capital depreciation responses to a one-time transitory

Figure 13: Productivity and Capital Depreciation after Global Temperature Shocks



Notes: Estimation results from matching the model impulse responses to the empirical responses to global temperature shocks. Column (a): underlying temperature path. Column (b): output and capital responses to this internally persistent temperature path. Dashed lines: data. Solid lines: model fit. Column (c): implied productivity and capital depreciation shocks, together with 68% confidence intervals (shaded area) based on 1,000 bootstrap draws from the empirical output, capital and temperature IRFs. We estimate structural damage functions and solve for counterfactuals for each draw.

global temperature shock of 1°C . It implies a short-run productivity loss of 3% and an increase in the capital depreciation rate of 1 p.p. Despite the corresponding temperature shock being transitory, the impact on productivity decays only slowly and persists for up to 10 years. The capital depreciation response, however, is short-lived. The bootstrapped confidence bands reflect the confidence intervals around our empirical output and capital responses.

How do the productivity and capital depreciation effects of global temperature shocks compare to those associated with local temperature shocks? Given that the empirical responses are substantially smaller for local temperature shocks as shown in Figure 7, such shocks likely also imply smaller damages. To answer this question quantitatively, we repeat our estimation but targeting the impulse response functions following local

temperature shocks.

Figure B.1 in Appendix B.4 displays the productivity and capital depreciation effects of local temperature shocks. The productivity effect of local temperature shocks is five to six times smaller than under global temperature shocks. The impact response of capital depreciation is about half of its value under global temperature shocks. We conclude that global temperature shocks have much larger effects on economic fundamentals.

5 The Welfare Impact of Climate Change

5.1 Representing Climate Change

To evaluate the consequences of climate change, we specify a path for global mean temperature. The baseline year $t = 0$ corresponds to 2024. The world subsequently warms by 3°C above pre-industrial levels by 2100, after which temperature asymptotes to 3.3°C. This scenario is broadly consistent with IPCC business-as-usual scenarios that imply 3 to 4°C of warming by 2100 (Lee et al., 2023). Given that the world has warmed by approximately 1°C since pre-industrial times, this scenario implies 2°C of additional warming since $t = 0$ (2024) by year $t = 76$ (2100).

We construct two counterfactuals to highlight the role of global temperature. In the first counterfactual, we use the structural damage functions estimated under *global* temperature shocks $\zeta_s^{\text{global}}, \delta_s^{\text{global}}$ in Figure 13(c) to construct productivity and capital depreciation changes using equation (6) together with excess temperature \hat{T}_t . In the second counterfactual, we instead use the structural damage functions estimated under *local* temperature shocks $\zeta_s^{\text{local}}, \delta_s^{\text{local}}$ in Figure B.3(c), Appendix B.4, using again equation (6) together with the same excess temperature path \hat{T}_t .

Our counterfactuals compare allocations and welfare in an economy that warms according to \hat{T}_t , to allocations and welfare in an economy that remains in steady-state under $\hat{T}_t \equiv 0$. Welfare losses from climate change are defined as an equivalent percent decline in steady-state consumption. The SCC is defined in equation (7) and is independent from the global warming scenario because it relies on the temperature response to a given CO2 pulse $\{\hat{T}_t^{\text{SCC}}\}_{t \geq 0}$. Conversely, the welfare calculations are independent from $\{\hat{T}_t^{\text{SCC}}\}_{t \geq 0}$. To solve for counterfactuals, we use standard global numerical methods to obtain the global solution—we only use log-linearization for estimation.

5.2 Welfare and the Social Cost of Carbon

Figure 14 presents our main results. Panel (a) depicts the path of global mean temperature. Panel (b) reveals that output drops rapidly as global temperature rises, relative to a world that is not warming. In 2050, output declines by 19%. In 2100, output is 47% below what it would have been without climate change. This substantial decline reflects accumulated productivity losses that eventually reach 34% and a 2.3 p.p. rise in the capital depreciation rate, representing a 29% increase.

Panel (c) highlights the combined adverse impact of lower productivity and higher depreciation rates on capital accumulation. Initially, investment rises as households anticipate lower income going forward and therefore save, following standard permanent income logic. Capital starts decumulating rapidly thereafter under the combined pressure of lower output and higher depreciation. By 2100, capital is 50% below what it would have been without climate change.

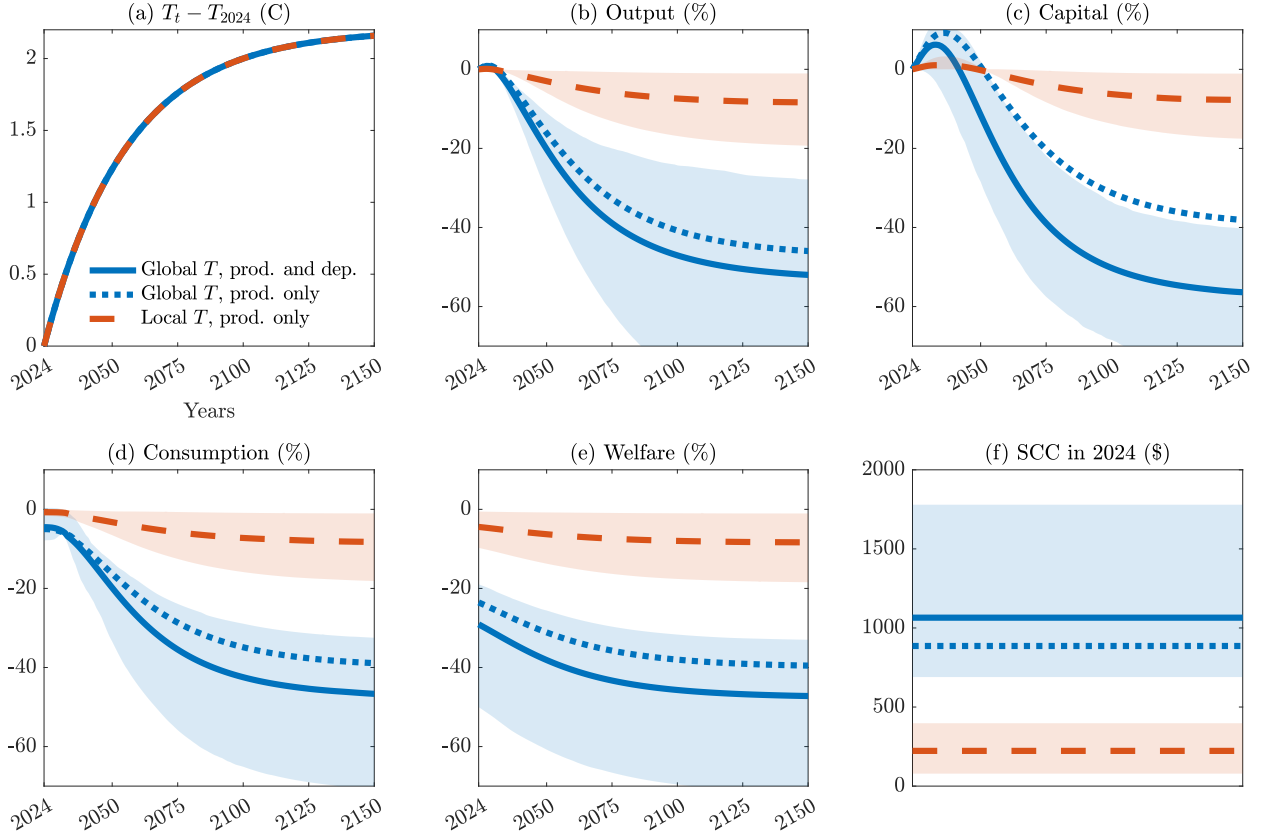
Panel (d) reveals that consumption declines as much as output, eventually reaching a 47% loss in the long run. This substantial decline in consumption translates into large welfare losses. Panel (e) shows that the 2024 welfare impact of climate change amounts to a 29% loss in consumption equivalent percent. This welfare loss exceeds the consumption impact as households discount but value future declines in consumption as well. As temperature keeps rising, welfare continues to decline and reaches a 47% loss.

Our results indicate that the impact of climate change is substantial. The welfare cost of climate change is 640 times the cost of business cycles, or 10 times the cost of moving from current trade relations to complete autarky. Perhaps most strikingly, in terms of output, capital, consumption, and thus welfare, climate change is comparable in magnitude to the effect of the 1929 Great Depression in the United States. However, climate change is *permanent*. Thus, the losses from living in a world with climate change relative to a world without it are comparable to living in the 1929 Great Depression, *forever*.

Panel (f) uses our structural damage function to construct the SCC. We obtain a SCC of \$1,065 per ton. This value is more than six times larger than the \$185 per ton value in Rennert et al. (2022). There are two possible reasons why we obtain a large SCC and substantial welfare costs of climate change. The first possible reason is our focus on global temperature shocks. The second possible reason is that we include damages to productivity and capital depreciation, rather than productivity alone as in most previous work.

We demonstrate that our focus on global temperature shocks is the main driver of our

Figure 14: Transitional Dynamics Under Climate Change



Notes: Transitional dynamics of the estimated model under the scenario in panel (a). Solid blue lines: model estimated under global temperature, with productivity and capital depreciation damages. Shaded blue areas: 68% confidence intervals. Dotted blue lines: model estimated under global temperature, with productivity damages only. Dashed red lines: model estimated under local temperature, with productivity damages only. Shaded red: 68% confidence intervals. Confidence intervals based on 1,000 bootstrap draws from output, capital and temperature IRFs.

conclusions. We do so by re-estimating our model based on the impact of local temperature shocks on productivity only, consistently with previous research. In that case, Figure 14 shows that climate change then implies a long-run output decline of 7%, a present value welfare cost of 4% and a SCC of \$223 per ton. These values are consistent with results in Nordhaus (1992), Dell et al. (2012), Burke et al. (2015), Nath et al. (2023), and Rennert et al. (2022). When we estimate our model based on the impact of global temperature shocks on productivity only, we obtain a welfare loss of 24% and a SCC of \$886 per ton, four times larger than with local shocks. Including damages to capital depreciation further increases these values to our main results. Our bootstrapped confidence intervals

highlight the uncertainty around these point estimates. The 68% confidence interval for the SCC based on global temperature ranges from \$690 per ton to \$1,779 per ton. Despite non-trivial uncertainty, even the lower bound of that confidence interval is several times larger than conventional SCC estimates.

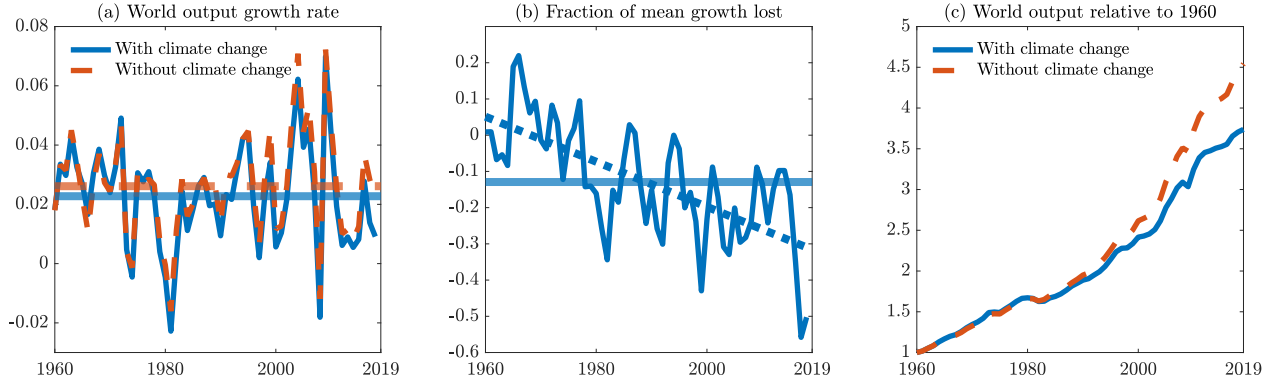
5.3 Growth Accounting

If the economic effects of climate change are so large, why were they not noticed after nearly 1°C of global warming since 1960? We answer this question by analyzing the historical impact of climate change. We start the economy in 1960 and feed in the realized path of warming until 2019, after which we impose constant temperature. We construct counterfactual changes in output relative to a baseline economy that remains in steady-state. We then add these changes directly to the data.

Figure 15 displays the results. Panel (a) reveals that climate change is responsible for moderate but persistent reductions in the world’s annual growth rate. In the 1960s, there is little warming and so few effects on economic growth. By 2019, potential growth without climate change deviates more systematically from realized growth with climate change. Panel (a) highlights that historical warming shocks have moderate economic year-to-year effects in comparison to other economic shocks. The analysis in Section 2 detects these effects that are otherwise hidden behind background economic variation.

Panels (b) and (c) show that the annual growth effects of climate change eventually accumulate because climate change is a permanent shock, despite having an initially moderate effect on growth. Panel (b) indicates that climate change reduces the world growth rate by as much as a third of baseline growth in the 21st century. Panel (c) shows that this growth slowdown implies that world GDP per capita would be 18% higher today had no warming occurred between 1960 and 2019. Even though in this counterfactual we hold temperature constant at its 2019 level in all subsequent years, economic losses continue to accumulate after 2019. These delayed impacts are due to the lagged productivity effects embedded in our estimated damage functions $\{\zeta_s\}_s$ and to the internal transitional dynamics of the neoclassical growth model. By 2040, output is 25% below its potential due to climate change: more than one quarter of the economic losses caused by past warming are yet to materialize.

Figure 15: Growth Accounting With Climate Change



Notes: Impact of past climate change on world GDP. Panel (a): world output growth rate with (solid blue) and without (dashed red) climate change. Horizontal lines: sample averages. Panel (b): fraction of growth rate lost to climate change (annual growth loss out of 1960-2019 mean). Horizontal line: sample average. Dashed line: linear regression fit. Panel (c): world output with (solid blue) and without (dashed orange) climate change, normalized to one in 1960.

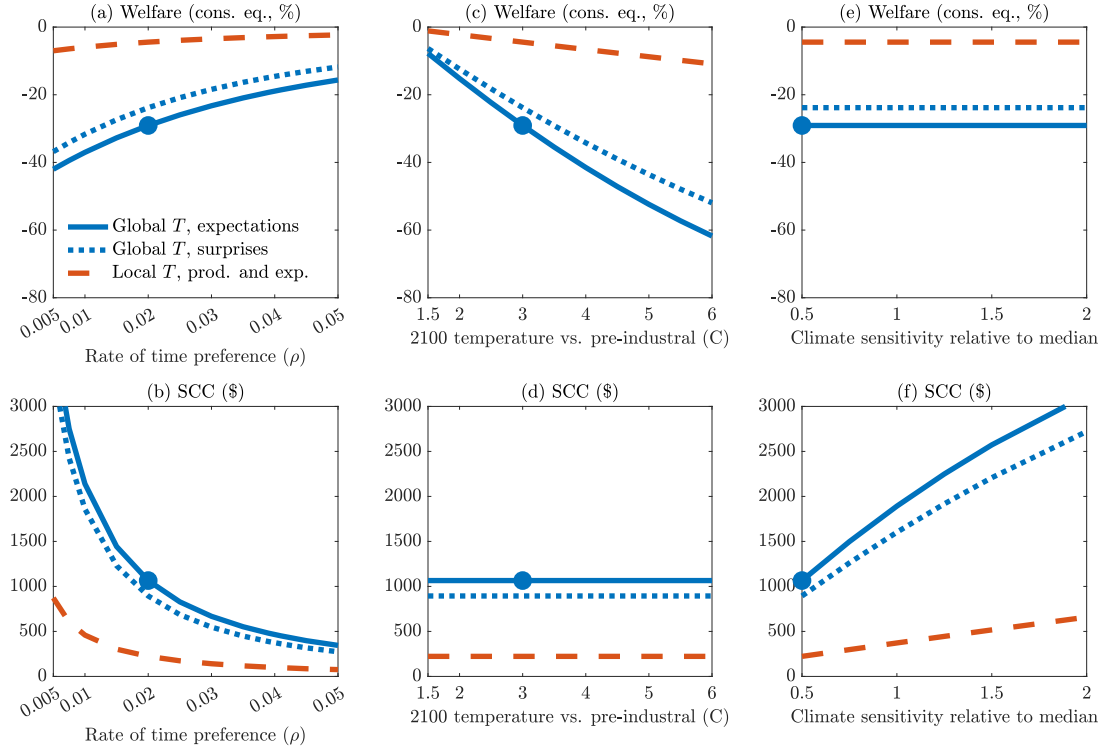
5.4 Sensitivity

Given the sizeable magnitude of our results, we investigate which parameters may be driving them. Figure 16 displays how our results depend on four key choices: the rate of time preference ρ , our treatment of expectations, 2100 global mean temperature, and the climate sensitivity.

Panel (a) shows 2024 welfare losses as a function of the rate of time preference ρ , and panel (b) shows the corresponding SCC. As expected, a higher rate of time preference lowers welfare losses and the SCC: households then discount more damages that are far in the future. Our baseline rate of time preference $\rho = 0.02$ is consistent with Rennert et al. (2022) and with the secular decline in interest rates. However, even at much higher discount rates—up to 0.04 or 0.05—we still obtain sizable losses in excess of 20% in consumption equivalent. The corresponding SCC remains two to three times as large as the high end of previous estimates. By contrast, as we approach very low discount rates consistent with Stern (2006), welfare losses exceed 40% and the SCC rises above \$3,000 per ton. Welfare losses are less sensitive to the discount rate than the SCC because welfare losses represent an annualized flow of losses, while the SCC is a discounted stock valuation.

Figure 16 also shows how our conclusions change when we treat household expectations differently. In our main estimation, we assume that households have rational

Figure 16: Welfare and the Social Cost of Carbon under Alternative Choices



Notes: Sensitivity of welfare costs and Social Cost of Carbon in 2024 with respect to the rate of time preference (ρ), 2100 global mean temperature, the climate sensitivity and treatment of expectations. Solid blue lines: model estimated using global temperature shocks under baseline expectations. Dotted blue lines: model estimated using global temperature shocks with temperature shock surprises. Dashed red lines: model estimated using local temperature shocks under baseline expectations with productivity shocks only.

expectations about the temperature path following a temperature shock. An alternative is to assume that households are surprised every period by persistently elevated temperatures following a temperature shock. Under this assumption, we linearly combine our estimated impulse response functions to obtain the output and capital responses to a one-time transitory temperature shock. We then target these responses to a transitory shock to estimate structural damage functions, instead of estimating damage functions first as in our baseline. We provide more details in Appendix B.4.

The dotted lines in Figure 16 displays our results under this alternative treatment of expectations. The results are similar to our baseline, although slightly smaller. Both specifications are close because productivity losses drive most of climate damages in our estimated framework as shown in Figure 14. Proposition 1 highlights that productivity damages are a direct function of the data that is independent from household expecta-

tions. Thus, expectations only affect the estimation of the capital depreciation shocks and thus a small fraction of economic losses. Figure B.2 in Appendix B.4 shows that capital depreciation shocks are smaller when we assume that households are surprised: they do not foresee future capital depreciation shocks that increase the marginal product of capital, and hence invest less than under rational expectations. The model then requires smaller capital depreciation shocks to rationalize the same decline in capital in the data.

Panels (c) and (d) show welfare losses and the SCC when we vary 2100 temperature relative to pre-industrial levels. Welfare losses under 20% materialize only at very low warming scenarios of 1.5°C since pre-industrial levels by 2100. The IPCC evaluates that the world is on track for 3°C to 4°C above pre-industrial levels under business as usual: global mean temperatures already largely exceed 1°C since pre-industrial levels, and some estimates indicate that 2023 reached 1.48°C since pre-industrial levels. By contrast, pessimistic scenarios under which global mean temperatures reach 6°C since pre-industrial levels in 2100 lead to present value welfare losses of 60%. Of course, in Panel (d), the 2024 SCC is independent from the warming scenario because it only depends on the temperature response to a CO₂ pulse.

Panels (e) and (f) display how the climate sensitivity affect our conclusions. The climate sensitivity governs how carbon emissions map into current and future warming. Consequently, welfare losses to a given warming scenario in as in panel (e) are independent from the climate sensitivity. However, as shown in panel (f), the SCC is not. Our main analysis uses a strongly conservative climate sensitivity: half of the median climate sensitivity in Dietz et al. (2021). This choice allows our analysis to remain more closely consistent with the historical link between emissions and warming, but is below what climate models tend to predict. When we use the median climate sensitivity, the SCC exceeds \$1,700 per ton. With a larger climate sensitivity, the SCC exceeds \$3,000 per ton.

This analysis indicates that substantial climate damages occur over a wide range of specification choices. We conclude that climate change poses a substantial threat to the world economy.

6 Conclusion

In this paper, we demonstrate that the impact of climate change on economic activity is substantial. We leverage natural climate variability in global mean temperature to obtain

time-series estimates that are representative of the overall impact of global warming. We find that a 1°C rise in global temperature causes global GDP to persistently decline, with a peak loss at 12%. This large effect is due to an associated surge in extreme climatic events. By contrast, local temperature shocks used in the traditional panel literature lead to a minimal rise in extreme events and to much smaller economic effects. Together, our results imply a SCC of \$1,065 per ton and a 29% welfare loss from a moderate warming scenario. These effects are comparable to experiencing the 1929 Great Depression, forever.

Not only do our results indicate that climate change represents a major threat to the world economy, they also have salient consequences for decarbonization policy. Most decarbonization interventions cost \$80 per ton of CO₂ abated (Bistline et al., 2023). A conventional SCC value of \$223 per ton implies that these policies are cost-effective only if governments internalize benefits to the entire world, as captured by the SCC. However, a government that only internalizes domestic benefits values mitigation benefits using a Domestic Cost of Carbon. The DCC is always lower than the SCC because damages to a single country are less than to the entire world. For instance, under conventional estimates based on local shocks, the DCC of the United States is \$45 per ton, making unilateral emissions reduction prohibitively expensive. Under our new estimates however, the DCC of the United States becomes \$213 per ton and thus largely exceeds policy costs. In that case, unilateral decarbonization policy is cost-effective for the United States.

References

- Auclert, Adrien, Bence Bardóczy, Matthew Rognlie, and Ludwig Straub** (2021). “Using the Sequence-Space Jacobian to Solve and Estimate Heterogeneous-Agent Models”. *Econometrica* 89.5, pp. 2375–2408.
- Bansal, Ravi and Marcelo Ochoa** (2011). “Temperature, Aggregate Risk, and Expected Returns”. *NBER Working Paper Series* 17575.
- Barro, Robert J.** (Aug. 2006). “Rare Disasters and Asset Markets in the Twentieth Century”. *The Quarterly Journal of Economics* 121.3, pp. 823–866.
- Berg, Kimberly A., Chadwick C. Curtis, and Nelson Mark** (2023). “GDP and temperature: Evidence on cross-country response heterogeneity”. *National Bureau of Economic Research Working Paper Series* 31327.
- Bilal, Adrien and Shlok Goyal** (2023). “Some Pleasant Sequence-Space Arithmetic in Continuous Time”. *SSRN Working Paper* 4634993.
- Bilal, Adrien and Esteban Rossi-Hansberg** (2023). “Anticipating Climate Change Across the United States”. *National Bureau of Economic Research Working Paper* 31323.
- Bistline, John, Neil R. Mehrotra, and Catherine Wolfram** (2023). “Economic Implications of the Climate Provisions of the Inflation Reduction Act”. *Brookings Papers on Economic Activity*.
- Burke, Marshall and Kyle Emerick** (2016). “Adaptation to Climate Change: Evidence from US Agriculture”. *American Economic Journal: Economic Policy* 8.3, 106–40.
- Burke, Marshall, Solomon M. Hsiang, and Edward Miguel** (2015). “Global non-linear effect of temperature on economic production”. *Nature* 527.7577, pp. 235–239.
- Burke, Marshall, Mustafa Zahid, Noah Diffenbaugh, and Solomon M Hsiang** (2023). “Quantifying Climate Change Loss and Damage Consistent with a Social Cost of Greenhouse Gases”. *National Bureau of Economic Research Working Paper Series* 31658.
- Callahan, Christopher W. and Justin S. Mankin** (2023). “Persistent effect of El Niño on global economic growth”. *Science* 380.6649, pp. 1064–1069.
- Cerra, Valerie and Sweta Chaman Saxena** (2008). “Growth Dynamics: The Myth of Economic Recovery”. *American Economic Review* 98.1, pp. 439–57.
- Conte, Bruno, Klaus Desmet, and Esteban Rossi-Hansberg** (2022). *On the Geographic Implications of Carbon Taxes*. Working Paper 30678. National Bureau of Economic Research.
- Cruz, José-Luis and Esteban Rossi-Hansberg** (2023). “The Economic Geography of Global Warming”. *The Review of Economic Studies* 91.2, pp. 899–939.

- Dell, Melissa, Benjamin F. Jones, and Benjamin A. Olken** (2012). "Temperature shocks and economic growth: Evidence from the last half century". *American Economic Journal: Macroeconomics* 4.3, pp. 66–95.
- (2014). "What Do We Learn from the Weather? The New Climate–Economy Literature". *Journal of Economic Literature* 52.3, pp. 740–798.
- Deryugina, Tatyana** (2013). "The role of transfer payments in mitigating shocks: Evidence from the impact of hurricanes". Available at SSRN 2314663.
- Deschênes, Olivier and Michael Greenstone** (2011). "Climate Change, Mortality, and Adaptation: Evidence from Annual Fluctuations in Weather in the US". *American Economic Journal: Applied Economics* 3.4, pp. 152–85.
- Desmet, Klaus, Robert E. Kopp, Scott A. Kulp, Dávid Krisztián Nagy, Michael Oppenheimer, Esteban Rossi-Hansberg, and Benjamin H. Strauss** (2021). "Evaluating the Economic Cost of Coastal Flooding". *American Economic Journal: Macroeconomics* 13.2, pp. 444–86.
- Desmet, Klaus and Esteban Rossi-Hansberg** (2015). "On the Spatial Economic Impact of Global Warming". *Journal of Urban Economics* 88, pp. 16–37.
- Dietz, Simon, Frederick van der Ploeg, Armon Rezai, and Frank Venmans** (2021). "Are Economists Getting Climate Dynamics Right and Does It Matter?" *Journal of the Association of Environmental and Resource Economists* 8.5, pp. 895–921.
- Dingel, Jonathan I., Kyle C. Meng, and Solomon M. Hsiang** (2023). "Spatial correlation, trade, and inequality: Evidence from the global climate". *National Bureau of Economic Research Working Paper*.
- Domeisen, Daniela I. V., Elfatih A. B. Eltahir, Erich M. Fischer, Reto Knutti, Sarah E. Perkins-Kirkpatrick, Christoph Schär, Sonia I. Seneviratne, Weisheimer Antje, and Heini Wernli** (2023). "Prediction and Projection of Heatwaves". *Nature Reviews Earth and Environment* 4, 36–50.
- Driscoll, John C. and Aart C. Kraay** (1998). "Consistent covariance matrix estimation with spatially dependent panel data". *Review of Economics and Statistics* 80.4, pp. 549–560.
- Folini, Doris, Aleksandra Friedl, Felix Kübler, and Simon Scheidegger** (Jan. 2024). "The Climate in Climate Economics". *The Review of Economic Studies*.
- Hamilton, James D.** (2018). "Why you should never use the Hodrick-Prescott filter". *Review of Economics and Statistics* 100.5, pp. 831–843.
- Hsiang, Solomon M. and Amir S. Jina** (2014). "The Causal Effect of Environmental Catastrophe on Long-Run Economic Growth: Evidence From 6,700 Cyclones". *National Bureau of Economic Research Working Paper* 20352.

- Hsiang, Solomon M., Kyle C. Meng, and Mark A. Cane** (2011). “Civil conflicts are associated with the global climate”. *Nature* 476, 438–441.
- Joos, F., R. Roth, J. S. Fuglestedt, G. P. Peters, I. G. Enting, W. von Bloh, V. Brovkin, E. J. Burke, M. Eby, N. R. Edwards, T. Friedrich, T. L. Frölicher, P. R. Halloran, P. B. Holden, C. Jones, T. Kleinen, F. T. Mackenzie, K. Matsumoto, M. Meinshausen, G.-K. Plattner, A. Reisinger, J. Segschneider, G. Shaffer, M. Steinacher, K. Strassmann, K. Tanaka, A. Timmermann, and A. J. Weaver** (2013). “Carbon dioxide and climate impulse response functions for the computation of greenhouse gas metrics: a multi-model analysis”. *Atmospheric Chemistry and Physics* 13.5, pp. 2793–2825.
- Jordà, Òscar** (2005). “Estimation and inference of impulse responses by local projections”. *American Economic Review* 95.1, pp. 161–182.
- Jordà, Òscar, Moritz Schularick, and Alan M. Taylor** (2020). “The effects of quasi-random monetary experiments”. *Journal of Monetary Economics* 112, pp. 22–40.
- Kahn, Matthew E., Kamiar Mohaddes, Ryan N.C. Ng, M. Hashem Pesaran, Mehdi Raissi, and Jui-Chung Yang** (2021). “Long-term macroeconomic effects of climate change: A cross-country analysis”. *Energy Economics* 104, p. 105624.
- Kaufmann, Robert K., Heikki Kauppi, and James H. Stock** (2006). “Emissions, concentrations, & temperature: a time series analysis”. *Climatic Change* 77, pp. 249–278.
- Kose, M. Ayhan, Naotaka Sugawara, and Marco E. Terrones** (2020). “Global recessions”.
- Kotz, Maximilian, Anders Levermann, and Leonie Wenz** (2024). “The Economic Commitment of Climate Change”. *Nature* 628, 551–557.
- Krusell, Per and Anthony A. Smith** (2022). *Climate change around the world*. Tech. rep. National Bureau of Economic Research.
- Lee, Hoesung, Katherine Calvin, Dipak Dasgupta, Gerhard Krinner, Aditi Mukherji, Peter Thorne, Christopher Trisos, José Romero, Paulina Aldunce, Ko Barrett, et al.** (2023). “IPCC, 2023: Climate Change 2023: Synthesis Report, Summary for Policymakers. Contribution of Working Groups I, II and III to the Sixth Assessment Report of the Intergovernmental Panel on Climate Change [Core Writing Team, H. Lee and J. Romero (eds.)]. IPCC, Geneva, Switzerland.”
- Montiel Olea, José Luis and Mikkel Plagborg-Møller** (2021). “Local projection inference is simpler and more robust than you think”. *Econometrica* 89.4, pp. 1789–1823.
- Moore, Frances C., Moritz A. Drupp, James Rising, Simon Dietz, Ivan Rudik, and Gernot Wagner** (2024). “Synthesis of Evidence Yields High Social Cost of Carbon Due to Structural Model Variation and Uncertainties”. *National Bureau of Economic Research Working Paper Series* 32544.

- Moscona, Jacob and Karthik A. Sastry** (Oct. 2022). “Does Directed Innovation Mitigate Climate Damage? Evidence from U.S. Agriculture*”. *The Quarterly Journal of Economics* 138.2, pp. 637–701.
- Nath, Ishan** (2022). “Climate Change, The Food Problem, and the Challenge of Adaptation through Sectoral Reallocation”. *Working Paper*.
- Nath, Ishan B., Valerie A. Ramey, and Peter J. Klenow** (2023). “How Much Will Global Warming Cool Global Growth?” *Mimeo*.
- National Oceanic and Atmospheric Administration** (2005). *Volcanos and Climate*. [Online Resource](#).
- (2009). *Climate Change: Incoming Sunlight*. [Online Resource](#).
- (2023). *What are El Niño and La Niña?* [Online Resource](#).
- Neal, Timothy** (2023). “The Importance of External Weather Effects in Projecting the Macroeconomic Impacts of Climate Change”. *UNSW Economics Working Paper 2023-09*.
- Newell, Richard G., Brian C. Prest, and Steven E. Sexton** (2021). “The GDP-temperature relationship: implications for climate change damages”. *Journal of Environmental Economics and Management* 108, p. 102445.
- Nordhaus, William D.** (1992). “An optimal transition path for controlling greenhouse gases”. *Science* 258.5086, pp. 1315–1319.
- (2013). “Integrated economic and climate modeling”. *Handbook of Computable General Equilibrium Modeling*. Vol. 1. Elsevier, pp. 1069–1131.
- Olea, José Luis Montiel, Mikkel Plagborg-Møller, Eric Qian, and Christian K. Wolf** (2024). “Double Robustness of Local Projections and Some Unpleasant VARithmetic”. *National Bureau of Economic Research Working Paper*.
- Phan, Toan and Felipe F. Schwartzman** (2023). “Climate defaults and financial adaptation”.
- Reinhart, Carmen M. and Kenneth S. Rogoff** (2009). “The aftermath of financial crises”. *American Economic Review* 99.2, pp. 466–472.
- Rennert, Kevin, Frank Errickson, Brian C. Prest, Lisa Rennels, Richard G. Newell, William Pizer, Cora Kingdon, Jordan Wingenroth, Roger Cooke, Bryan Parthum, et al.** (2022). “Comprehensive evidence implies a higher social cost of CO₂”. *Nature* 610.7933, pp. 687–692.
- Rudik, Ivan, Gary Lyn, Weiliang Tan, and Ariel Ortiz-Bobea** (2022). “The Economic Effects of Climate Change in Dynamic Spatial Equilibrium”.
- Seneviratne, S. I., X. Zhang, M. Adnan, W. Badi, C. Derczynski, A. Di Luca, S. Ghosh, I. Iskandar, J. Kossin, S. Lewis, F. Otto, I. Pinto, M. Satoh, S.M. Vicente-Serrano, M.**

- Wehner, and B. Zhou** (2021). “Chapter 11: Weather and Climate Extreme Events in a Changing Climate”. In *Climate Change 2021: The Physical Science Basis. Contribution of Working Group I to the Sixth Assessment Report of the Intergovernmental Panel on Climate Change*; Masson-Delmotte, V., P. Zhai, A. Pirani, S.L. Connors, C. Péan, S. Berger, N. Caud, Y. Chen, L. Goldfarb, M.I. Gomis, M. Huang, K. Leitzell, E. Lonnoy, J.B.R. Matthews, T.K. Maycock, T. Waterfield, O. Yelekçi, R. Yu, and B. Zhou (eds.). Cambridge University Press, Cambridge, United Kingdom and New York, NY, USA, 1513–1766.
- Seneviratne, Sonia I., Markus G. Donat, Andy J. Pitman, Reto Knutti, and Robert L. Wilby** (2016). “Allowable CO₂ Emissions Based on Regional and Impact-Related Climate Targets”. *Nature* 529, 477–483.
- Seppanen, Olli, William J. Fisk, and David Faulkner** (2003). “Cost benefit analysis of the night-time ventilative cooling in office building”.
- Sims, Christopher A.** (1986). “Are forecasting models usable for policy analysis?” *Quarterly Review* 10.Win, pp. 2–16.
- Stern, N.** (2006). *Stern Review: The Economics of Climate Change*.
- Stern, Nicholas, Joseph Stiglitz, and Charlotte Taylor** (2022). “The economics of immense risk, urgent action and radical change: towards new approaches to the economics of climate change”. *Journal of Economic Methodology* 29.3, pp. 181–216.
- Tran, Brigitte Roth and Daniel J. Wilson** (2023). “The local economic impact of natural disasters”. Federal Reserve Bank of San Francisco.
- Wartenburger, R., M. Hirschi, M. G. Donat, P. Greve, A. J. Pitman, and S. I. Seneviratne** (2017). “Changes in Regional Climate Extremes as a Function of Global Mean Temperature: an Interactive Plotting Framework”. *Geoscientific Model Development* 10, 3609–3634.
- Zappalà, Guglielmo** (2023). “Estimating Sectoral Climate Impacts in a Global Production Network”. *IMF Working Paper* 2023/053.

Online Appendix

The Macroeconomic Impact of Climate Change

Adrien Bilal[†]

Diego R. Känzig[‡]

Contents

A. Empirics	51
A.1. Data	51
A.1.1. Economic Data	51
A.1.2. Climate Data	51
A.2. Statistical Properties of Global Temperature Shocks	56
A.3. Accounting for Estimation Uncertainty in Temperature Shocks	58
A.4. Alternative Estimation Models	59
A.5. Searching for Influential Observations	61
A.6. Reverse Causality	62
A.7. Time Fixed Effects and Correlated Temperature Shocks	68
A.8. Global vs. Local Temperature Shocks	69
A.9. External Temperature Shocks	70
A.10. Accounting for the Persistence of Temperature Shocks	71
A.11. Impacts of Extreme Events	73
A.12. Additional Robustness Checks	75
A.12.1. Results Based on One-step Forecast Error Temperature Shocks	78
A.13. Regional Impacts	84
B. Model	86
B.1. Equilibrium	86
B.2. Linearization	86
B.3. Model Inversion: Proof of Proposition 1	88
B.4. Estimation	90

[†]Harvard University, CEPR and NBER. E-mail: adrienbilal@fas.harvard.edu.

[‡]Northwestern University, CEPR and NBER. E-mail: dkaenzig@northwestern.edu.

A Empirics

A.1 Data

A.1.1 Economic Data

We obtain economic information on GDP, population, consumption, investment and productivity for a comprehensive selection of countries around the world from the Penn World Tables (PWT; Feenstra et al., 2015). Our main output measure is real GDP per capita from the national accounts (rgdpna/pop). For our country comparisons by income, we use (expenditure-side) real GDP per capita at chained PPPs (rgdpe/pop). For capital, we use the capital stock from national accounts (rnna). Investment, we compute using data on capital and capital depreciation (δ) based on the capital accumulation equation $I_t = K_t - (1 - \delta_t)K_{t-1}$. For total factor productivity, we also use the measure based on national accounts (rtfpna). We compute a measure of labor productivity based on output and employment data (rgdpna/emp).¹

The PWT data set is commonly used in the literature and of high quality. However, as an alternative, we also use data from the World Bank. One limitation of both of these data sets is that they only go back to the 1950s or 1960s. To extend our analysis to a longer historical sample period, we therefore also include data from the Macro-history Database (Jordà et al., 2017), which features high-quality economic data for 18 developed countries starting in the late 19th century.

A.1.2 Climate Data

Gridded temperature datasets. Our primary gridded temperature dataset is Berkeley Earth, due to its geographic coverage, temporal coverage, and update frequency.

We obtain gridded temperature anomalies (using air temperatures at sea ice) at a daily and monthly frequency between 1850 and 2022 from Berkeley Earth (2023), at a resolution of $1^\circ \times 1^\circ$ latitude-longitude grid. Temperature anomalies are deviations from the climatology, which is measured as the 1951-1980 mean temperature (Rohde and Hausfather, 2020). Grid-level temperature levels are constructed by adding the grid-level climatology to the grid-level anomaly series.

¹We use employment as a proxy for the labor input because the data on average hours is not very well populated.

We also obtain gridded estimates of temperature, wind, and precipitation at a daily frequency between 1901 and 2019 from the Inter-Sectoral Impact Model Intercomparison Project (ISIMIP), at a 0.5° spatial resolution (Lange et al., 2023).

To assess the sensitivity of the results to the gridded temperature data used, we obtain alternate, prominent datasets used in the literature. We obtain gridded temperature levels (surface air temperature) at a monthly frequency between 1948 and 2014 from the Princeton Global Forcing Dataset (version 2) constructed by Sheffield et al. (2006), a later version of which was used, for instance, by Nath et al. (2023). Additionally, we obtain the gridded temperature levels (surface air temperatures) at a monthly frequency between 1900 and 2014 from the Willmott and Matsuura, University of Delaware Dataset (version 4.01) (Matsuura and National Center for Atmospheric Research Staff, 2023), earlier versions of which were used, for instance, by Dell et al. (2012) and Burke et al. (2015).

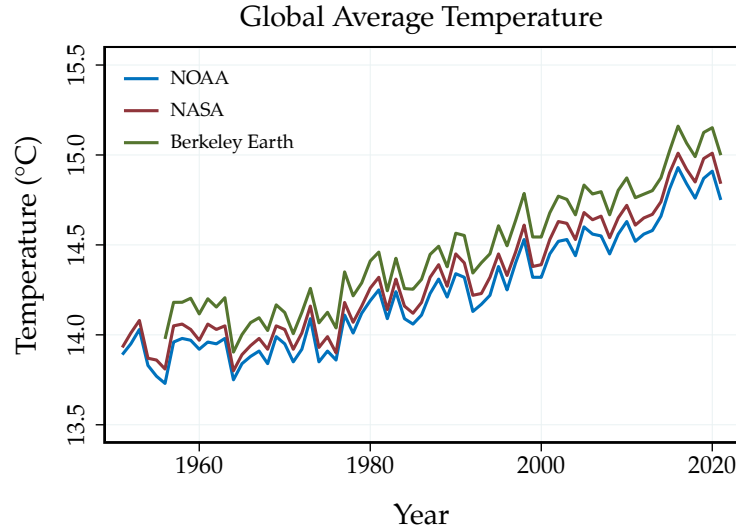
Aggregation of gridded temperature datasets. To aggregate the gridded temperature datasets to the global or country level we consider two different type of weights. One approach is to use area weights. Specifically, we use the area of the grid, calculated using the latitude and longitude. Alternatively, we use population weights. In that case, we use the grid-level population count in 2000 as weights, obtained from the Center for International Earth Science Information Network (CIESIN), Columbia University (2018).

Global temperatures. We obtain land and ocean surface temperature anomalies (in degrees Celsius) at an annual frequency between 1850 and 2022 from NOAA National Centers for Environmental Information (2023a). Temperature anomalies are deviations from the climatology, which is measured as the 1901-2000 mean temperature, 13.9 degree Celsius (NOAA National Centers for Environmental Information, 2023b). Temperature levels are constructed by adding the climatology to the anomaly series.

We also obtain the combined land-surface air and sea-surface water temperature anomalies (in degrees Celsius) at an annual frequency between 1880 and 2022 from Lenssen et al. (2019) and NASA Goddard Institute for Space Studies (2023). Temperature anomalies are deviations from the climatology, which is measured as the 1951-1980 mean temperature, approximately 14 degree Celsius (NASA Earth Observatory, 2020). Temperature levels are similarly constructed by adding the climatology to the anomaly series.

As a quality check of the gridded temperature data, we compute population- and area-weighted global temperature measures and compare them to the official measures from NOAA and NASA. Note that both official measures follow an area-weighted aggregation

Figure A.1: Global Average Temperature Since 1950



Notes: Evolution of global average temperature. The NOAA and NASA measures are constructed by adding the climatology to the official anomaly series. The Berkeley Earth measure is constructed by first, obtaining grid-level temperature levels by adding the grid-level climatology to the grid-level anomaly series, and second, aggregating the grid-level temperature levels using area weights. We plot the Berkeley Earth series starting 1956, following which the percentage of monthly grid-level missing observations is consistently below $\approx 2\%$.

scheme. Reassuringly, aggregating the Berkeley Earth gridded temperature data using area weights to obtain a global temperature measure produces a series that is virtually perfectly correlated with both the NOAA and NASA global temperature series: we find that the measures based on all these different data sets align very well, as shown in Figure A.1.

Country-level temperatures. We use the Berkeley Earth gridded temperature data to construct population- and area-weighted country-level mean temperatures. In our analyses, we use population-weighted temperature as the baseline, however, using area-weighted measures produces very similar results. To assess the sensitivity of the results with respect to the gridded temperature data used, we similarly compute the population- and area-weighted country-level mean temperatures using the Princeton Global Forcing Dataset and the University of Delaware Dataset. We find that the results are consistent across different temperature datasets.

Extreme climatic events. We use the ISIMIP gridded estimates of temperature, wind, and precipitation at a daily frequency between 1901 and 2019 to construct extreme events

indicators for each latitude-longitude grid. To define a threshold for extreme events, we use the percentiles of the distribution of the variables between 1950 and 1980, and define an extreme event as one where the realization of a variable was above a given percentile of its distribution. Specifically, we use the percentiles of the worldwide distribution to construct “absolute” extreme events indicators, and the percentiles of a country’s distribution for “relative” indicators. We use the relative indicators as our baseline, however, our results are robust to using the absolute indicators.

To aggregate the variables across the grids to construct country-level measures, we use two methods. First, we construct the daily average of the variable for the country, and then compute the fraction of days in the year when the variable was above the threshold percentile (i.e., “country-level” extreme events indicator). We define these threshold percentiles such that the extreme heat, drought, extreme precipitation and extreme wind indices have a baseline probability of 0.05, 0.25, 0.01 and 0.01, respectively. Alternatively, we also compute the fraction of days in the year when the variable was above the threshold percentile *at the grid-level*, and then aggregate this indicator for the country (i.e., “cell-level” extreme events indicator). Of course, the threshold percentile changes across the definitions: for the former, we use the distribution of daily country-level averages, and for the latter, the distribution of daily grid-level observations between 1950 and 1980. As a robustness exercise, we used alternative thresholds computed based on data from 1900 to 1930, yielding very similar results. Note that similar to the aggregation of gridded temperature datasets, we consider both area- and population-weights in both methods above. We use the country-level, area-weighted indicators as our baseline. However, the results are robust to using our alternative measures (cell-level and/or population-weighted).

Descriptive statistics. Our main data set spans the period from 1960 to 2019. We drop countries for which we have fewer than 20 non-missing observations of temperature and real GDP per capita. This leaves us with 173 countries. Our results are robust to restricting the selection of countries further. In Appendix A.12, we replicate our results based on the original panel datasets used in Dell et al. (2012) and Burke et al. (2015).

In Table A.1, we present some descriptive statistics on the main variables of interest. In Panel (a), we report statistics on our global time-series variables. In Panel (b), we show statistics for the country-level variables. Specifically, we report the number of non-missing observations, the mean, median, standard deviation as well as the minimum and the maximum observation.

Table A.1: Descriptive Statistics

	Obs	Mean	SD	Median	Min	Max
<i>Panel (a): Global variables</i>						
Global temperature anomaly	60	0.36	0.30	0.34	-0.15	1.03
Global temperature shock	60	0.00	0.12	-0.01	-0.24	0.28
World real GDP per capita growth	59	2.06	1.47	2.13	-1.74	6.36
Oil price change	59	8.55	30.32	1.70	-47.79	167.83
US Treasury yield	60	5.04	3.31	5.00	0.12	14.78
<i>Panel (b): Country-level variables</i>						
Local temperature anomaly	10379	0.40	0.57	0.35	-1.89	3.33
Local temperature shock	10379	0.01	0.46	0.00	-2.59	2.89
Real GDP per capita growth	9090	2.07	6.31	2.23	-67.01	94.17
Investment per capita growth	8938	6.58	23.61	4.68	-98.36	499.01
TFP growth	5716	0.33	4.90	0.47	-65.22	83.10
Labor productivity growth	8353	1.75	6.63	1.79	-67.31	142.17
Extreme heat days	10379	0.10	0.08	0.08	0.00	0.87
Drought days	10033	0.29	0.10	0.27	0.05	0.91
Extreme precipitation days	10033	0.01	0.01	0.01	0.00	0.08
Extreme wind days	10033	0.01	0.01	0.01	0.00	0.06

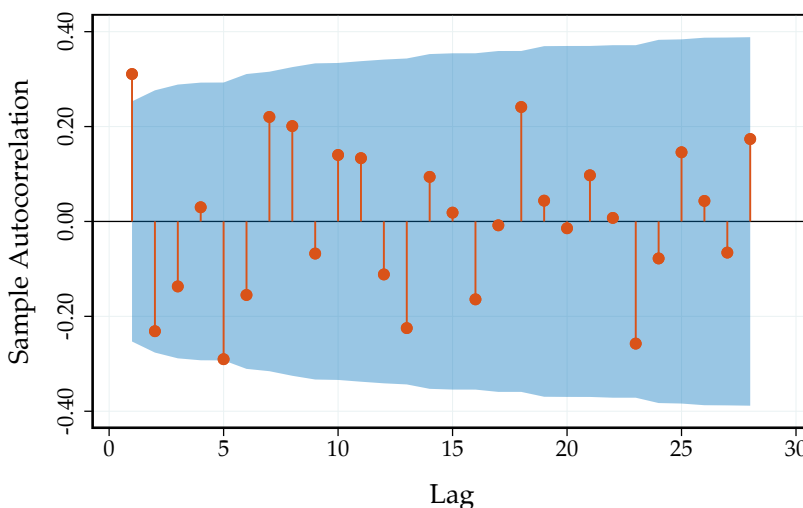
Notes: Descriptive statistics for our global and country-level variables. We report the number of non-missing observations, the mean, standard deviation, median, and min and max for the main variables used in our analysis over the period 1960-2019.

A.2 Statistical Properties of Global Temperature Shocks

In this appendix, we discuss some of the statistical properties of global temperature shocks in more detail.

Serial correlation. Figure A.2 shows the autocorrelation function of the global temperature shock. The shocks are weakly autocorrelated. This is not too surprising, given that we construct the shocks as multi-step forecast errors. To account for this serial correlation, we therefore include two lags of the global temperature shock in our local projections. However, as we show in Appendix A.12, our results are robust with respect to the number of lags for the temperature shock.

Figure A.2: Autocorrelation of Global Temperature Shock



Notes: Autocorrelation function of global temperature shocks, together with the 95% confidence bands, computed based on Bartlett’s formula for MA(q).

Forecastability. A desirable feature of “shocks” is that they should not be forecastable by past information (Ramey, 2016). In our context, if global temperature shocks were forecastable by economic variables, this could point to reverse causality or other endogeneity threats. Thus, we check whether our temperature shocks are forecastable, considering a wide set of past macroeconomic or financial variables in a series of Granger-causality tests. To account for the long and variable lags between emissions and warming, we conservatively include up to 8 years worth of lags.² Table A.2 reports the results. We find no

²We would like to ideally include 10 lags (= our impulse horizon) but unfortunately in our baseline sample we do not have enough degrees of freedom to do so.

Table A.2: Granger-causality Tests

Variable	p-value
Real GDP	0.494
Population	0.801
Brent price	0.756
Commodity price index	0.664
Treasury 1Y	0.830
Overall	0.825

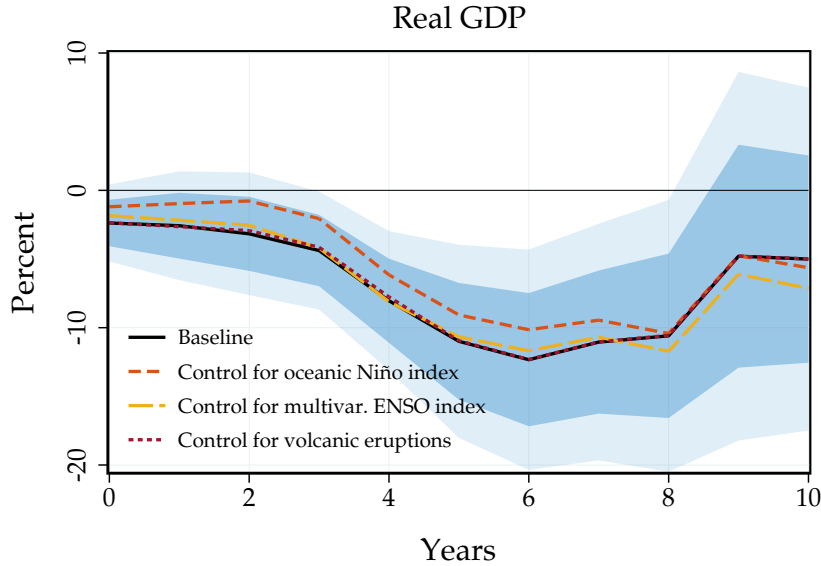
Notes: p-values of a series of Granger causality tests of the global temperature shock series using a selection of macroeconomic and financial variables. Non-stationary variables are transformed to growth rates. We allow for up to 8 lags.

evidence that macroeconomic or financial variables have any power in forecasting global temperature shocks. None of the selected variables Granger cause the series at conventional significance levels. The joint test is also insignificant.

The role of El Niño and other temperature variability. Are our results are driven by specific sources of temperature variability such as El Niño events? To answer this question, we net out variation coming from El Niño by controlling for ENSO indices in our main specification. The results are shown in Figure A.3.

The responses are similar to our baseline estimates, suggesting that our main results capture a common effect of global temperature on economic activity that does not depend heavily on being driven by El Niño or other sources of climate variability. A related concern is that major volcanic eruptions may affect world real GDP through other channels than temperature, for instance by limiting air travel. Controlling for volcanic eruptions also yields virtually unchanged results.

Figure A.3: The Role of El Niño and Other Temperature Variability



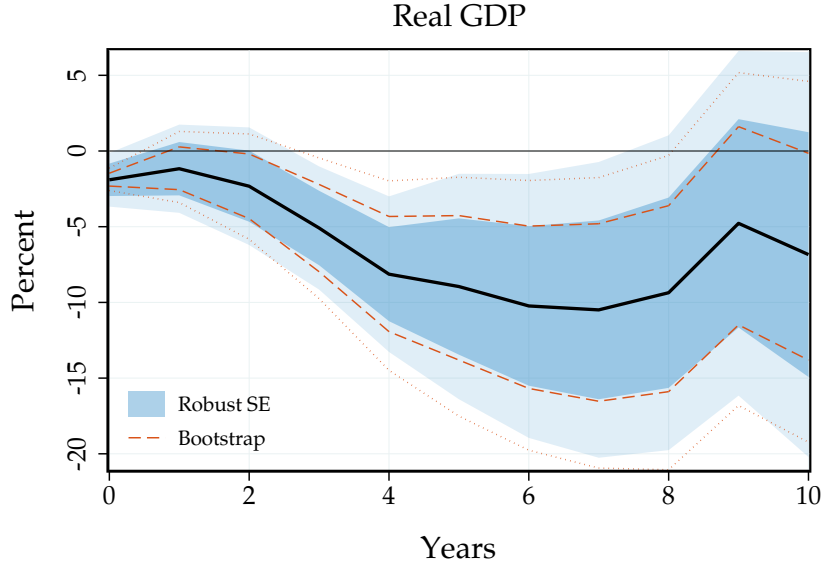
Notes: Impulse responses of real GDP per capita to a global temperature shock estimated based on the panel local projection approach, controlling for El Niño and volcanic eruptions. Dark and light shaded areas: 68 and 90% confidence bands for our baseline estimates.

A.3 Accounting for Estimation Uncertainty in Temperature Shocks

Our baseline specifications take the global temperature shock as given and do not take estimation uncertainty in the shock into account. To assess the potential role of estimation uncertainty in the shock, we alternatively construct the confidence bands using bootstrapping techniques. We resample the shock and controls using a Wild bootstrap and then compute bootstrapped series of our outcome variables based on our autoregressive model. We repeat this procedure a 1,000 times and re-estimate our local projection specification for each iteration of the bootstrap. Based on the bootstrapped distribution, we can then compute confidence bands for all our objects of interest.

Figure A.4 compares the confidence bands based on our baseline lag-augmentation approach with the bootstrapped confidence bands. The coverage is similar, suggesting that taking estimation uncertainty in the global temperature shock into account turns out to be inconsequential in the context of our application.

Figure A.4: The Role of Estimation Uncertainty in Temperature Shocks



Notes: Impulse responses of real GDP per capita to a global temperature shock, estimated based on the panel local projection approach. Solid black line: point estimate. Dark and light shaded areas are 68 and 90% confidence bands based on our simple lag-augmentation approach. Red dotted and dashed lines: 68 and 90% confidence bands based on our bootstrap, taking estimation uncertainty in the temperature shock into account.

A.4 Alternative Estimation Models

Our main empirical specification relies on local projection techniques. In this appendix, we alternatively estimate the responses based on VAR techniques. Starting point is the following structural vector moving-average representation

$$\mathbf{Y}_t = \mathbf{B}(L)\mathbf{S}\boldsymbol{\varepsilon}_t, \quad (\text{A.1})$$

where \mathbf{Y}_t is a $k \times 1$ vector of annual time series, $\boldsymbol{\varepsilon}_t$ is a vector of structural shocks driving the economy with $\mathbb{E}[\boldsymbol{\varepsilon}_t \boldsymbol{\varepsilon}_t'] = \mathbf{I}$, $\mathbf{B}(L) \equiv \mathbf{I} + \mathbf{B}_1 L + \mathbf{B}_2 L^2 + \dots$ is a matrix lag polynomial, and \mathbf{S} is the structural impact matrix.

Assuming that the vector-moving average process (A.1) is invertible, it admits the following VAR representation:

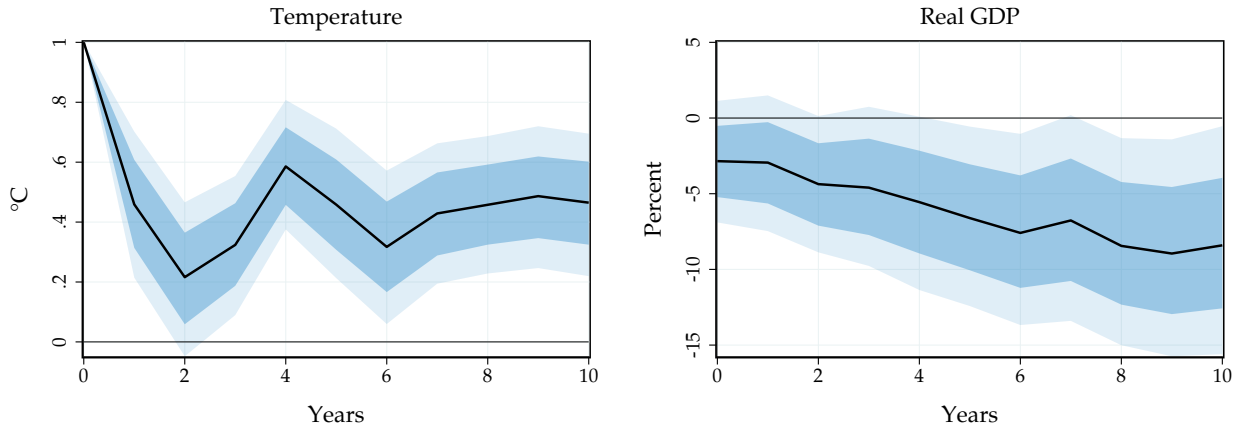
$$\mathbf{A}(L)\mathbf{Y}_t = \mathbf{S}\boldsymbol{\varepsilon}_t = \mathbf{u}_t, \quad (\text{A.2})$$

where \mathbf{u}_t is a $k \times 1$ vector of reduced-form innovations with variance-covariance matrix $\mathbb{E}[\mathbf{u}_t \mathbf{u}_t'] = \Sigma_u$ and $\mathbf{A}(L) \equiv \mathbf{I} - \mathbf{A}_1 L - \dots$ is a matrix lag polynomial. Truncating the VAR to order p , we can estimate the model using standard techniques and recover an estimate of $\mathbf{B}(L)$.

The main identification problem is then to find the structural impact matrix \mathbf{S} . From the linear relation between the structural shocks and the reduced-form innovations, we obtain the following covariance restrictions $\mathbf{S}\mathbf{S}' = \Sigma_u$. We assume that temperature shocks can impact on all variables in the VAR contemporaneously, while other shocks only affect temperature with a lag. This is motivated by the fact that emissions increases usually translate into temperature with a substantial lag. The identifying restriction can be implemented via the Cholesky decomposition of Σ_u , denoted by $\tilde{\mathbf{S}}$.

In terms of model specification, \mathbf{Y}_t includes global temperature and real GDP growth. To mitigate concerns about non-invertibility, we also include oil price growth and the U.S. treasury yield. The lag order is set to 4 and we also include our recession dummies as an exogenous variable.

Figure A.5: VAR Responses



Notes: Impulse responses of global temperature and real GDP per capita to a global temperature shock, estimated based on our VAR model (A.2). Solid lines: point estimates. Dark and light shaded areas: 68 and 90% confidence bands.

Figure A.5 shows the results. The estimated impacts turn out to be consistent with our local projection evidence. As expected, the shape of the impulse response is not exactly as in Figure 3 because the VAR extrapolates from the first four autocovariances between GDP and temperature to obtain impacts at higher horizons, while the local projection in Figure 3 directly estimates these impacts at higher horizons.

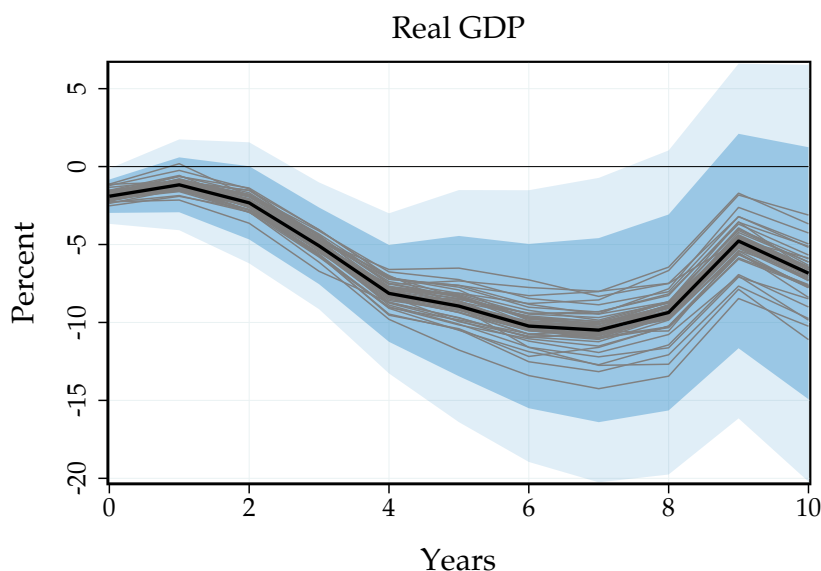
A.5 Searching for Influential Observations

Section 2.2 displays the identifying variation in a scatter plot. The negative relationship between temperature and GDP turns out to be a robust one and does not appear to be driven by a particular set of extreme observations.

Nevertheless, there were two potentially influential temperature shocks: a strong negative temperature shock in 1964 that was followed by a significant economic upswing and a large positive temperature shock in 1977. This latter observation precedes the second oil shock and the following Volker disinflation, even though we already control for these events through our set of recession dummies.

To formally assess the role of influential observations, we perform a jackknife exercise. Specifically, we censor one shock value at a time to zero, and re-run our local projection. To account for the differential impact on our controls, we also include a dummy variable for the year we censor.

Figure A.6: Sensitivity of the Response to Global Temperature Shocks



Notes: Baseline response of real GDP per capita to a global temperature shock (in black), together with the responses obtained from the jackknife, censoring one shock value at a time (in gray). Dark and light shaded areas: 68 and 90% confidence bands for our baseline response.

Figure A.6 shows our baseline response in black, together with the responses from the jackknife exercise in gray. The estimated impact of temperature on GDP is not driven any single extreme shock. When censoring certain shocks we can get even bigger impacts,

while when dropping others the effects can be somewhat attenuated. In all cases, the peak effect is always larger than 7-8% and well within the confidence bands. Excluding the 1977 shock value corresponds to one of the more attenuated responses in the jackknife. However, even in this case we still find a sizeable effect.

A.6 Reverse Causality

In this appendix, we describe how we account for reverse causality. We assume that we start from detrended, stationary variables. We specify for GDP:

$$y_t = \sum_{s=-\infty}^t T_s \theta_{t-s} + \varepsilon_t,$$

where T_s is the temperature deviation, and ε_t is a possibly autocorrelated shock. We are interested in estimating the vector θ . For temperature, we specify:

$$T_t = \sum_{s=-\infty}^t y_s \gamma_{t-s} + \tau_t,$$

where τ_t is a possibly autocorrelated shock, and we know γ . Without loss of generality, We normalize the variance of T_t and y_t to 1. The local projection estimates:

$$P_h^{YT} \equiv \text{Cov}[y_{t+h} - y_{t-1}, T_t | \mathbf{x}_{t-1}] \equiv \text{Cov}_{t-1}[y_{t+h} - y_{t-1}, T_t],$$

where \mathbf{x}_{t-1} is our vector of controls, and we denote $\text{Cov}_{t-1}[\bullet, \bullet] \equiv \text{Cov}[\bullet, \bullet | \mathbf{x}_{t-1}]$. We have:

$$\begin{aligned} P_h^{YT} &= \text{Cov}_{t-1}[y_{t+h} - y_{t-1}, T_t] \\ &= \text{Cov}_{t-1} \left[\sum_{s=-\infty}^{t+h} T_s \theta_{t+h-s} + \varepsilon_{t+h} - y_{t-1}, T_t \right] \\ &= \text{Cov}_{t-1} \left[\sum_{s=-\infty}^{t+h} T_s \theta_{t+h-s} + \varepsilon_{t+h}, T_t \right] \\ &= \text{Cov}_{t-1} \left[\sum_{s=-\infty}^{t+h} T_s \theta_{t+h-s}, T_t \right] + \text{Cov}_{t-1} [\varepsilon_{t+h}, T_t] \\ &= \text{Cov}_{t-1} \left[\sum_{s=-\infty}^{t-1} T_s \theta_{t+h-s}, T_t \right] + \text{Cov}_{t-1} \left[\sum_{s=0}^h T_{t+s} \theta_{h-s}, T_t \right] + \text{Cov}_{t-1} [\varepsilon_{t+h}, T_t] \end{aligned}$$

The third equality holds because we include lagged GDP y_{t-1} in our vector of controls \mathbf{x}_{t-1} . From the last line, as long as we include sufficiently many lags of temperature and GDP in our vector of controls to cover the moving average structure, the first term is zero. We proceed under the assumption that we include sufficiently many lags. Hence,

$$\begin{aligned} P_h^{YT} &= \text{Cov}_{t-1} \left[\sum_{s=0}^h T_{t+s} \theta_{h-s}, T_t \right] + \text{Cov}_{t-1} [\varepsilon_{t+h}, T_t] \\ &= \sum_{s=0}^h \theta_{h-s} \text{Cov}_{t-1} [T_{t+s}, T_t] + \text{Cov}_{t-1} [\varepsilon_{t+h}, T_t] \end{aligned}$$

There are two sources of reverse causality: internal persistence (first term), and residual shocks to GDP (second term). Of course, residual shocks can also affect the covariance in the first term, but one can condition this channel out with the deconvolution procedure that conditions on the realized temperature path after a shock.

We start with the second term:

$$\begin{aligned} \text{Cov}_{t-1} [\varepsilon_{t+h}, T_t] &= \text{Cov}_{t-1} \left[\varepsilon_{t+h}, \sum_{s=-\infty}^t y_s \gamma_{t-s} + \tau_t \right] \\ &= \sum_{s=-\infty}^t \gamma_{t-s} \text{Cov}_{t-1} [\varepsilon_{t+h}, y_s] + \text{Cov}_{t-1} [\varepsilon_{t+h}, \tau_t] \\ &= \gamma_0 \text{Cov}_{t-1} [\varepsilon_{t+h}, y_t] + \text{Cov}_{t-1} [\varepsilon_{t+h}, \tau_t] \\ &= \gamma_0 \text{Cov}_{t-1} [\varepsilon_{t+h}, y_t] \\ &= \gamma_0 \text{Cov}_{t-1} [\varepsilon_{t+h}, \theta_0 T_t + \varepsilon_t] \\ &= \gamma_0 \text{Cov}_{t-1} [\varepsilon_t, \varepsilon_{t+h}] + \gamma_0 \theta_0 \text{Cov}_{t-1} [\varepsilon_{t+h}, T_t] \end{aligned}$$

The third equality obtains because we again assume that control for enough lags of GDP. The fourth equality obtains because we assume that structural shocks are orthogonal. The fifth equality follows from substituting the equation for output and noting that we include enough lags of temperature as controls. Re-arranging, we obtain:

$$\text{Cov}_{t-1} [\varepsilon_{t+h}, T_t] = \frac{\gamma_0}{1 - \gamma_0 \theta_0} \text{Cov}_{t-1} [\varepsilon_t, \varepsilon_{t+h}]$$

We now denote by $P_s^{TT} = \text{Cov}_{t-1} [T_{t+s}, T_t]$ the (observed) autocovariance function of the temperature process. We also denote by $E_s = \text{Cov}_{t-1} [\varepsilon_t, \varepsilon_{t+s}]$ the (unobserved) autoco-

variance function of the GDP residuals. We have shown that our local projection estimator is:

$$P_h^{YT} = \sum_{s=0}^h \theta_{h-s} P_s^{TT} + \frac{\gamma_0}{1 - \gamma_0 \theta_0} E_h.$$

The first term represents the how internal persistence to the temperature process affects our estimator. We start our discussion by abstracting from the bias in the second term.

If we are only interested in the response to a purely transitory temperature shock—i.e. the θ 's—then we can directly correct our estimator for this internal persistence using the observed autocovariance P_s^{TT} . However, if we want to reconstruct the unbiased GDP response to a temperature shock with the same amount of persistence as in the data, i.e.

$$\tilde{\theta}_h = \sum_{s=0}^h \theta_{h-s} \text{Cov}_{t-1}[\tau_t, \tau_{t+s}],$$

we need to construct the autocovariance function of the structural temperature shocks $\mathcal{V}_s \equiv \text{Cov}_{t-1}[\tau_t, \tau_{t+s}]$. Since we assumed that we know the γ 's, we can simply residualize the temperature process using lagged GDP and the known γ 's and obtain the τ 's.

Now we turn to the second term. This term is the classic reverse causality bias. However, since we assume that we know γ_0 , we can construct E_h as a function of θ and known covariances, and then solve for θ . Indeed, we have:

$$\begin{aligned} E_h &= \text{Cov}_{t-1}[\varepsilon_t, \varepsilon_{t+h}] \\ &= \text{Cov}_{t-1} \left[y_t - \sum_{s=-\infty}^t \theta_{t-s} T_s, y_{t+h} - \sum_{s=-\infty}^{t+h} \theta_{t+h-s} T_s \right] \\ &= \text{Cov}_{t-1} \left[y_t - \theta_0 T_t, y_{t+h} - \sum_{s=0}^h \theta_{h-s} T_{t+s} \right] \\ &= \text{Cov}_{t-1}[y_t, y_{t+h}] - \theta_0 \text{Cov}_{t-1}[y_{t+h}, T_t] - \sum_{s=0}^h \theta_{h-s} \text{Cov}_{t-1}[y_t, T_{t+s}] + \theta_0 \sum_{s=0}^h \theta_{h-s} \text{Cov}_{t-1}[T_t, T_{t+s}] \\ &= P_h^{YY} - \theta_0 P_h^{YT} - \sum_{s=0}^h \theta_{h-s} P_s^{TY} + \theta_0 \sum_{s=0}^h \theta_{h-s} P_s^{TT}. \end{aligned}$$

The third equality obtains because we controls for enough lags. In the fourth equality we defined $P_h^{YY} = \text{Cov}_{t-1}[y_t, y_{t+h}]$ the known autocovariance function of output. We recog-

nized the local projection P_h^{YT} . We defined as $P_s^{TY} = \text{Cov}_{t-1}[y_t, T_{t+s}]$ the local projection of temperature on output (the “reverse” of our baseline local projection).

Hence, we obtain the collection of equations (some nonlinear) indexed by h :

$$P_h^{YT} = \sum_{s=0}^h \theta_{h-s} P_s^{TT} + \frac{\gamma_0}{1 - \gamma_0 \theta_0} \left\{ P_h^{YY} - \theta_0 P_h^{YT} - \sum_{s=0}^h \theta_{h-s} P_h^{TY} + \theta_0 \sum_{s=0}^h \theta_{h-s} P_s^{TT} \right\}$$

The θ 's are the unknowns. Everything else is known or observable. The only nonlinearity comes from θ_0 . Conditional on θ_0 , these are linear equations. Hence, we examine the equation for θ_0 separately. We obtain:

$$P_0^{YT} = \theta_0 + \frac{\gamma_0}{1 - \gamma_0 \theta_0} \left\{ 1 - \theta_0 P_0^{YT} - \theta_0 P_0^{TY} + \theta_0^2 \right\},$$

where recall that we normalized $V_0 = 1$ and $Y_0 = 1$. We also note that $P_0^{YT} = P_0^{TY}$ by definition (but not at higher lags). Multiplying by $1 - \gamma_0 \theta_0$,

$$P_0^{YT}(1 - \gamma_0 \theta_0) = \theta_0(1 - \gamma_0 \theta_0) + \gamma_0 \left\{ 1 - 2\theta_0 P_0^{YT} + \theta_0^2 \right\}.$$

Re-arranging, we observe that the quadratic terms cancel out. Hence the equation for θ_0 is actually also linear. We obtain:

$$\theta_0 = \frac{P_0^{YT} - \gamma_0}{1 - \gamma_0 P_0^{YT}}.$$

We have thus constructed an unbiased estimator of θ_0 .

Then given θ_h , we construct θ_{h+1} by induction. We have (using some changes of indices):

$$\begin{aligned} P_{h+1}^{YT} &= \theta_{h+1} + \sum_{s=0}^h \theta_s P_{h+1-s}^{TT} \\ &+ \frac{\gamma_0}{1 - \gamma_0 \theta_0} \left\{ P_{h+1}^{YY} - \theta_0 P_{h+1}^{YT} - \sum_{s=0}^h \theta_s P_{h+1-s}^{TY} - P_0^{YT} \theta_{h+1} + \theta_0 \sum_{s=0}^h \theta_s P_{h+1-s}^{TT} + \theta_0 \theta_{h+1} \right\} \end{aligned}$$

Re-arranging:

$$\left(1 + \frac{\gamma_0}{1 - \gamma_0 \theta_0} \left\{ -P_0^{YT} + \theta_0 \right\} \right) \theta_{h+1} = P_{h+1}^{YT} - \sum_{s=0}^h \theta_s P_{h+1-s}^{TT} - \frac{\gamma_0}{1 - \gamma_0 \theta_0} \left\{ P_{h+1}^{YY} - \theta_0 P_{h+1}^{YT} - \sum_{s=0}^h \theta_s P_{h+1-s}^{TY} + \theta_0 \sum_{s=0}^h \theta_s P_{h+1-s}^{TT} \right\}.$$

Further re-arranging:

$$\frac{1 - \gamma_0 P_0^{YT}}{1 - \gamma_0 \theta_0} \theta_{h+1} = \frac{1}{1 - \gamma_0 \theta_0} P_{h+1}^{YT} - \sum_{s=0}^h \theta_s P_{h+1-s}^{TT} - \frac{\gamma_0}{1 - \gamma_0 \theta_0} \left\{ P_{h+1}^{YY} - \sum_{s=0}^h \theta_s P_{h+1-s}^{TY} + \theta_0 \sum_{s=0}^h \theta_s P_{h+1-s}^{TT} \right\}.$$

Therefore:

$$\theta_{h+1} = \frac{1}{1 - \gamma_0 P_0^{YT}} P_{h+1}^{YT} - \frac{1 - \gamma_0 \theta_0}{1 - \gamma_0 P_0^{YT}} \sum_{s=0}^h \theta_s P_{h+1-s}^{TT} - \frac{\gamma_0}{1 - \gamma_0 P_0^{YT}} \left\{ P_{h+1}^{YY} - \sum_{s=0}^h \theta_s P_{h+1-s}^{TY} + \theta_0 \sum_{s=0}^h \theta_s P_{h+1-s}^{TT} \right\}.$$

This correction delivers the θ 's after adjusting for reverse causality. We observe that the "classic" reverse causality adjustment scales with γ_0 .

We can then construct $\tilde{\theta}_h$, the response to a persistent temperature shock τ_t . We start from the unbiased θ 's. Then, we construct the autocovariance function of the τ 's, i.e. \mathcal{V} . We have:

$$\begin{aligned} \mathcal{V}_h &= \text{Cov}_{t-1}[\tau_{t+h}, \tau_t] \\ &= \text{Cov}_{t-1} \left[T_{t+h} - \sum_{s=-\infty}^{t+h} y_s \gamma_{t+h-s}, T_t - \sum_{s=-\infty}^t y_s \gamma_{t-s} \right] \\ &= \text{Cov}_{t-1} \left[T_{t+h} - \sum_{s=0}^h y_{t+s} \gamma_{h-s}, T_t - y_t \gamma_0 \right] \\ &= P_h^{TT} - \gamma_0 P_h^{TY} - \sum_{s=0}^h \gamma_{h-s} (P_s^{YT} - \gamma_0 P_s^{YY}) \end{aligned}$$

The third equality follows from including enough controls. Then we construct:

$$\tilde{\theta}_h = \sum_{s=0}^h \theta_{h-s} \mathcal{V}_s.$$

Implementation. In practice, we need a sequence γ . We construct a central case, and some alternatives for robustness.

The central case uses the following parameters. We use $\eta = 1$ for CO₂, CH₄ and SO₂: emissions move one-for-one with output, which is consistent with a Cobb-Douglas production function.

Average world CO₂ emissions during our 1960-2019 sample are $\bar{E}^{\text{CO}_2} = 22.5 \text{ Gt/y}$.³ The temperature response in Celsius to a 100 Gt pulse in Dietz et al. (2021) is well-approximated by:

$$\begin{aligned} 100 \times \phi_h^{\text{CO}_2} &= a_{100}^{\text{CO}_2} \times (e^{-b^{\text{CO}_2} \times h} - e^{-c^{\text{CO}_2} \times h}) + d_{100}^{\text{CO}_2} \times (1 - e^{-f^{\text{CO}_2} \times h}) \\ a_{100}^{\text{CO}_2} &= 0.1878, b^{\text{CO}_2} = 0.083, c^{\text{CO}_2} = 0.2113, d_{100}^{\text{CO}_2} = 0.1708, f^{\text{CO}_2} = 0.2113. \end{aligned}$$

Then we define: $\gamma_h^{\text{CO}_2} = \eta \times \bar{E}^{\text{CO}_2} \times \phi_h^{\text{CO}_2}$.

We use CH₄ emissions of $\bar{E}^{\text{CH}_4} = 125 \text{ Mt/y}$.⁴ The temperature response in Celsius to a 1 Mt pulse in Azar et al. (2023) is well-approximated by:

$$\begin{aligned} \phi_h^{\text{CH}_4} &= a^{\text{CH}_4} \times (e^{-b^{\text{CH}_4} \times h} - e^{-c^{\text{CH}_4} \times h}) + d^{\text{CH}_4} \times (1 - e^{-f^{\text{CH}_4} \times h}) \\ a^{\text{CH}_4} &= 4.9970, b^{\text{CH}_4} = 0.1230, c^{\text{CH}_4} = 0.1376, d^{\text{CH}_4} = 0.0109, f^{\text{CH}_4} = 0.0019. \end{aligned}$$

Then we define: $\gamma_h^{\text{CH}_4} = \eta \times \bar{E}^{\text{CH}_4} \times \phi_h^{\text{CH}_4}$.

We use SO₂ emissions of $\bar{E}^{\text{SO}_2} = 100 \text{ Mt/y}$.⁵ The temperature response in Celsius to a 1 Mt pulse in Albright et al. (2021) is well-approximated by:

$$\begin{aligned} \phi_h^{\text{SO}_2} &= F^{\text{SO}_2} \times (A_1^{\text{SO}_2} e^{-h/\tau_1^{\text{SO}_2}} + A_2^{\text{SO}_2} e^{-h/\tau_2^{\text{SO}_2}} + A_3^{\text{SO}_2} e^{-h/\tau_3^{\text{SO}_2}}) \\ F^{\text{SO}_2} &= -0.0051 \\ A_1^{\text{SO}_2} &= 0.2537, \tau_1^{\text{SO}_2} = 0.6700, A_2^{\text{SO}_2} = 0.0269, \tau_2^{\text{SO}_2} = 12, A_3^{\text{SO}_2} = 0.0010, \tau_3^{\text{SO}_2} = 352 \end{aligned}$$

³See <https://ourworldindata.org/co2-emissions>.

⁴See <https://www.iea.org/reports/global-methane-tracker-2023/overview>.

⁵See <https://ourworldindata.org/grapher/so-emissions-by-world-region-in-million-tonnes>.

Then we define: $\gamma_h^{\text{SO}_2} = \eta \times \bar{E}^{\text{SO}_2} \times \phi_h^{\text{SO}_2}$.

Finally, we define $\gamma = \gamma^{\text{CO}_2} + \gamma^{\text{CH}_4} + \gamma^{\text{SO}_2}$. Alternative, plausible choices of emissions-to-GDP elasticities or temperature sensitivity do not affect the reverse causality correction materially because it is small to begin with.

A.7 Time Fixed Effects and Correlated Temperature Shocks

In this appendix, we shed further light on the role of time fixed effects. Figure A.7(a) compares the impulse responses of GDP to local temperature shocks with and without time fixed effects. The responses from the local temperature shock specification with time fixed effects are strikingly close to the baseline with global controls. The coverage of the confidence bands is also comparable. Overall, these results suggest that our controls successfully account for common economic shocks.

To further mitigate concerns that other unobserved global factors may confound our results, we exploit regional variation in temperature. We construct country-level temperature shocks that also incorporate external temperature. For each country, we compute a shock that is a weighted average of its own temperature shock and all other temperature shocks in the world, weighted by country distance with closer countries getting a higher weight as in equation (5). Specifically, we construct the correlated shock as

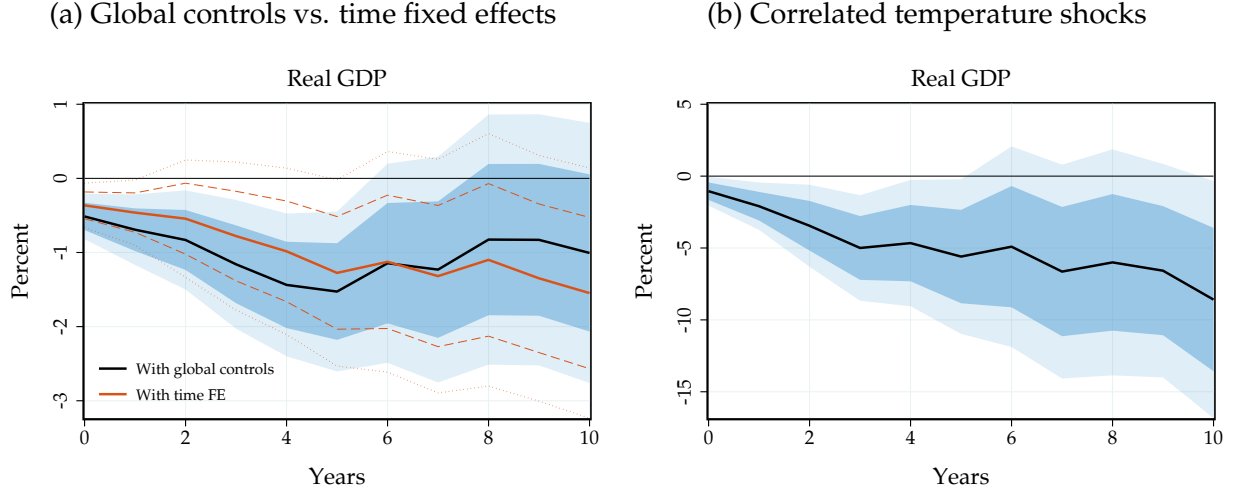
$$T_{i,t}^{\text{corr}} = \sum_j d_{ij} T_{i,t}^{\text{shock}}, \quad (\text{A.3})$$

where d_{ij} is proportional to the inverse geodesic distance between the centroids of countries i and j and sums to one for each country i .⁶ We thus obtain correlated temperature shocks that still vary by country, which allows us to control for time fixed effects—which we cannot do in the specification with global temperature shocks.

Figure A.7(b) displays the results. Real GDP per capita falls substantially after such correlated temperature shocks, approaching -9% at its peak. Thus, the effects are again substantially larger than for local temperature shocks, and close those for global temperature shocks. We conclude that global temperature shocks lead to larger economic effects than local temperature shocks.

⁶We compute these ourselves using the Python geopandas package. We use the inverse distance as the weight and include the own country with the same weight as its closest neighbor.

Figure A.7: The Role of Time Fixed Effects



Notes: Impulse responses of real GDP per capita. Panel (a): responses to a local temperature shock, with global controls (3) or with time FE (4). Black line: specification with global controls. Red line: specification with time fixed effects. Panel (b): impulse response to correlated temperature shocks from a specification controlling for time fixed effects. Solid line: point estimate. Dark and light shaded areas: 68 and 90% confidence bands.

A.8 Global vs. Local Temperature Shocks

In this appendix, we estimate the impact of global and local temperature jointly in the same local projection specification. We estimate the following local projection model:

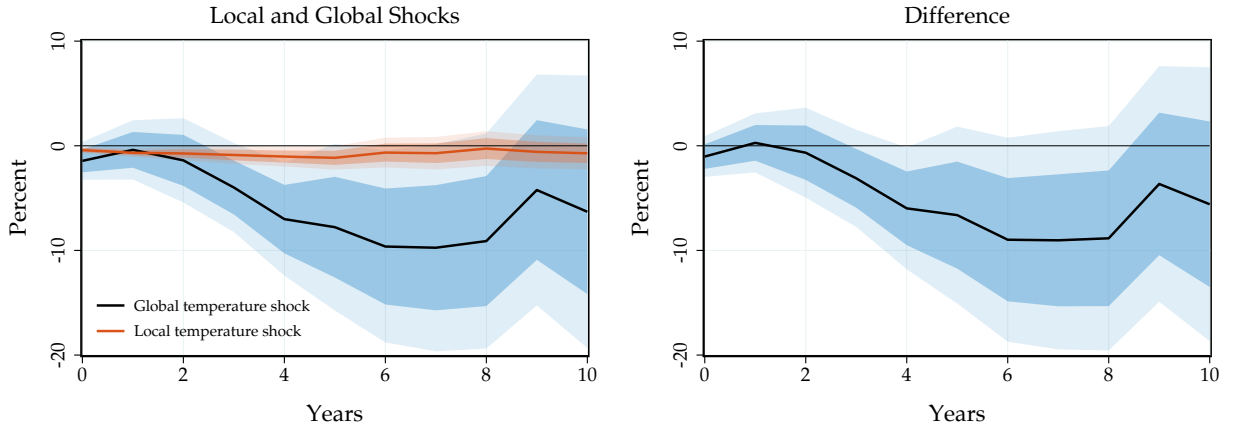
$$y_{i,t+h} - y_{i,t-1} = \alpha_{i,h} + \theta_h^{\text{global}} T_t^{\text{shock}} + \theta_h^{\text{local}} T_{i,t}^{\text{shock}} + \mathbf{x}_t' \beta_h + \mathbf{x}_{i,t}' \gamma_h + \varepsilon_{i,t+h}, \quad (\text{A.4})$$

where T_t^{shock} is our global temperature shock, $T_{i,t}^{\text{shock}}$ is a local, country-level temperature shock, and θ_h^{global} and θ_h^{local} are the associated impulse responses, respectively.

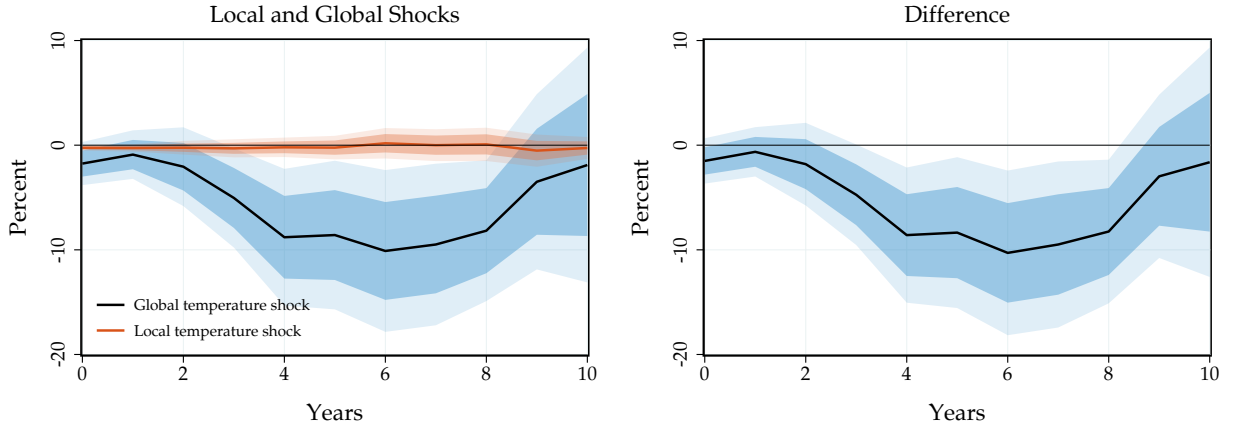
Figure A.8 displays the results. Panel (a) shows the responses based on our main specification. The jointly estimated responses are very close to our baseline responses. However, the difference between the responses turns out to be only borderline significant at the 90% level. Therefore, we also report results from the specification with our expanded set of controls (expanded global controls and subregion-specific time trends) in Panel (b). Reassuringly, the point estimates remain very similar. However, these additional controls help reduce sampling uncertainty, and the difference is now highly significant even at the 90% level.

Figure A.8: Local vs. Global Temperature Shocks

(a) Baseline specification



(b) Specification with expanded set of controls



Notes: Impulse responses of GDP per capita to global and local temperature shocks together with the difference between global and local shock impulse responses, estimated based on (A.4). Panel (a): Baseline specification. Panel (b): Specification with expanded set of controls (expanded global controls and subregion-specific time trends). Lines: point estimates. Dark and light shaded areas: 68 and 90% confidence bands.

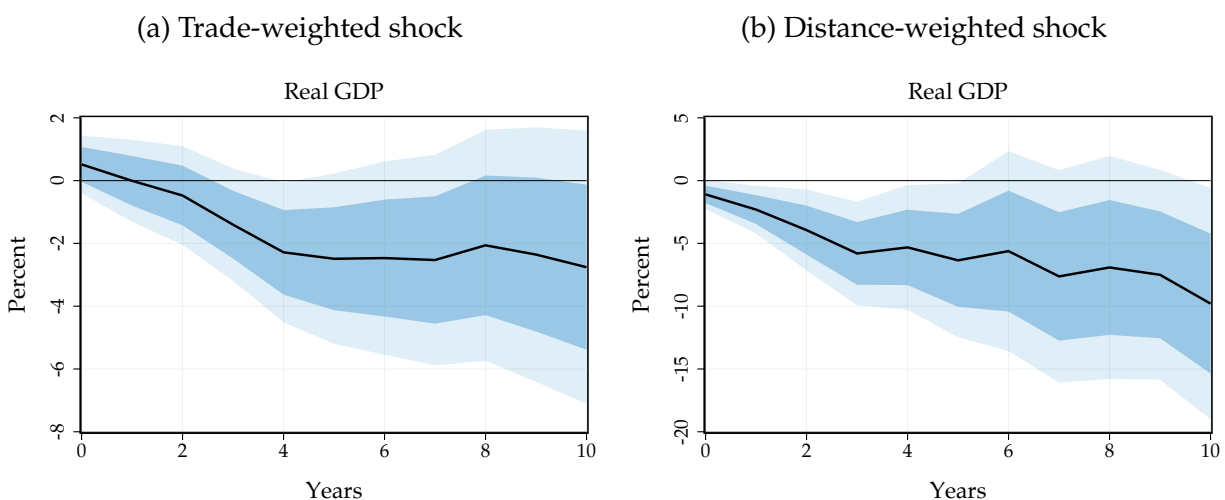
A.9 External Temperature Shocks

As discussed in Section 3.3, we also construct external temperature shocks. For each country, we define external temperature shocks as the weighted average of the local temperature shocks in all other countries. We consider both trade and distance weights. Trade weights are based on total trade flows (imports plus exports) in 1960 from [TRADHIST](#). We then normalize total trade flows such that all weights sum to one for any given country. Distance weights are based on physical distance (geodesic distance between country

centroids), which we also normalize to sum to one. Unlike when we defined correlated temperature shocks in Appendix A.7, we do not include the domestic temperature shock of country i in the weighted average of country i . We thus maximize comparability between trade- and distance-weighted external temperature shocks since they only differ by the weights.

Figure A.9 shows the impulse responses of world real GDP to the two external temperature shocks, estimated in separate specifications. Temperature shocks to a country's trading partners (trade-weighted external temperature shocks) lead to a notable fall in output, comparable to the impacts of local, idiosyncratic temperature shocks. However, Figure 10 shows that this effect vanishes when we control for global or distance-weighted temperature shocks. On the other hand, the effects of distance-weighted external temperature shocks are robust to controlling for trade-weighted external temperature.

Figure A.9: The Impact of External Temperature Shocks



Notes: Impulse responses of world real GDP per capita to external temperature shocks, estimated based on (4). Left panel: response to a trade-weighted shock. Right panel: responses to a distance-weighted shock. Solid lines: point estimates. Dark and light shaded areas: 68 and 90% confidence bands. Sample of countries differs from main analysis due to availability of trade data at the beginning of the sample.

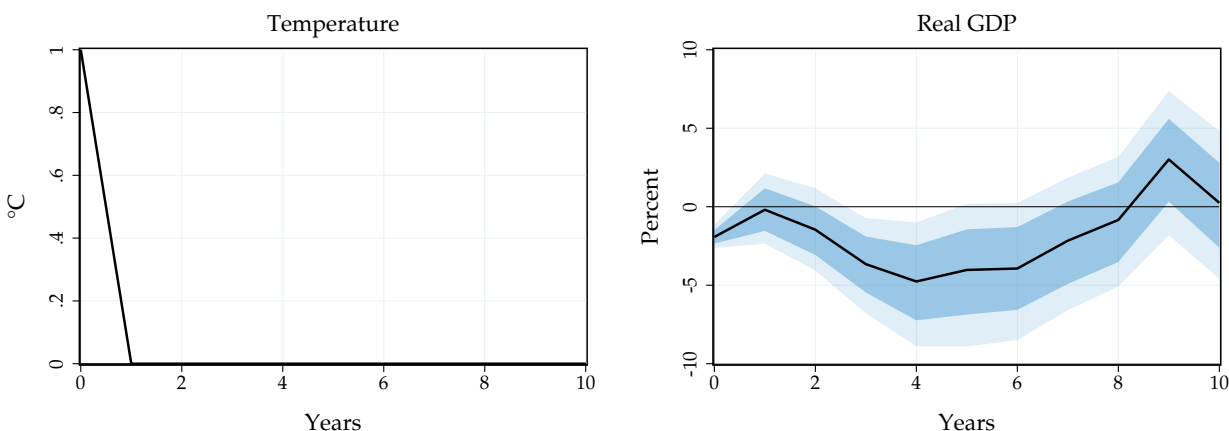
A.10 Accounting for the Persistence of Temperature Shocks

Global temperature shocks lead to a persistent increase in the level of global temperature. This increase in global temperature is much more persistent than the shock itself and persists even 10 years out as shown in Figure 3.

In this appendix, we show that this internal persistence accounts for a substantial fraction of the slow and large impact of global temperature shocks on GDP. We compute the responses to a purely transitory global temperature shock, i.e. a shock that raises temperature by 1°C in the current year but has no effect on temperature afterwards. We do using the Sims (1986) method, which amounts to construct a sequence of temperature shocks to exactly offset the internal persistence.

Figure A.10 displays our results. Two observations stand out. First, the peak impact of a transitory temperature shock is much smaller, at 5%. Second, the effects materialize more quickly and are less persistent, with a peak response after about 3-4 years. After 8 years, the effect reverts to zero. These findings highlight that a substantial share of the estimated damages and their sluggishness are driven by the internal persistence of the temperature response itself that leads to accumulating economic damages.

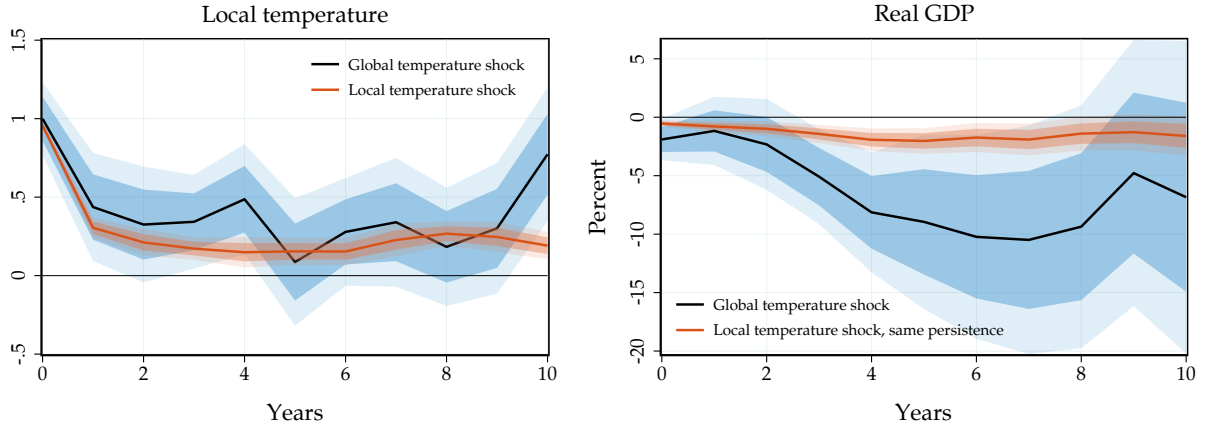
Figure A.10: The Effects of a Transitory Global Temperature Shock



Notes: Impulse responses of real GDP per capita to purely transitory global temperature shock, constructed using the Sims (1986) method based on our panel estimates. Solid lines: point estimates. Dark and light shaded areas: 68 and 90% confidence bands.

Next, we ask whether differential internal persistence between global and local temperature shocks could account for the gap in GDP impacts. The left panel in Figure A.11 shows the response of local temperature levels to global and local temperature shocks, respectively. Global and local shocks lead to a comparable increase in local temperature. The response turns out to be slightly more persistent for the global shock, however, the difference seems not stark enough to account for the vastly different GDP impacts. We confirm this intuition formally, estimating the effects of local temperature shocks on real

Figure A.11: The Effects of Local and Global Temperature Shocks



Notes: Left panel: impulse response of local temperature to a global and local temperature shock. Right panel: impulse responses of real GDP per capita to a local temperature shock, estimated in the panel using (3), against the effects of a global temperature shock. We impose that the local temperature shock has the same effect on local temperature levels as global temperature shocks using the Sims (1986) method. Solid lines: point estimates. Dark and light shaded areas: 68 and 90% confidence bands.

GDP, imposing the same persistence of the local temperature response as for global temperature shocks. We do so again using the Sims (1986) approach.

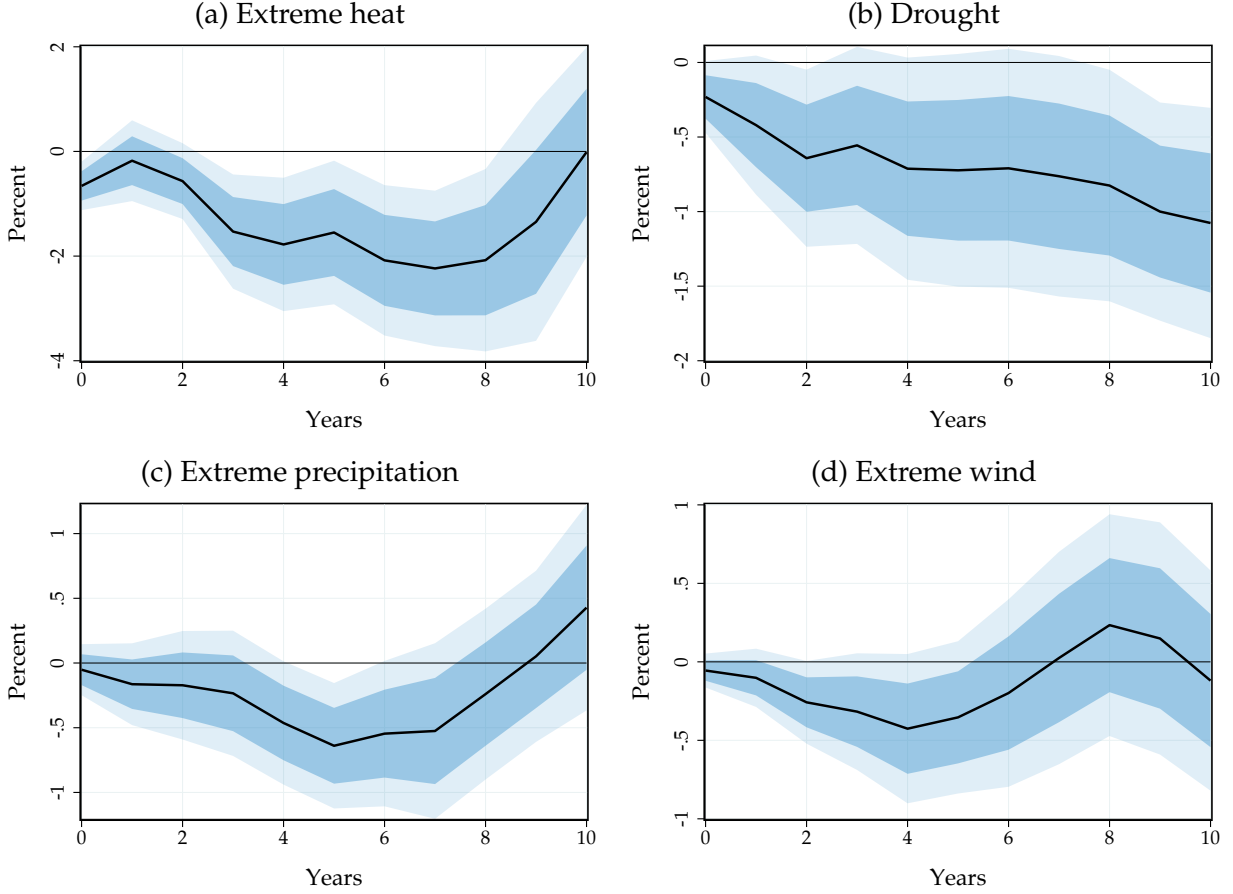
The right panel in Figure A.11 shows that the effects of local temperature shocks are in this case slightly more pronounced than in our baseline, depicted in Figure 7. Importantly, however, the effects of the global temperature shocks are still by a magnitude larger than for local temperature shocks because global and local temperature have a similar degree of internal persistence. The small difference in persistence cannot account for the differential impacts of global and local temperatures shocks.

A.11 Impacts of Extreme Events

Figure 8 shows that global temperature shocks strongly correlate with the exposure to extreme weather events: extreme temperature, drought, extreme precipitation, and extreme wind. Here we project world real GDP on extreme event exposure directly, so that we can aggregate up the impact of global temperature on GDP through extreme events. We use the panel local projection specification (3), except that we replace the global temperature shock on the right-hand-side with extreme event exposure. We denote by ψ_h^X the impact of an increase in exposure for extreme event X on country-level GDP at horizon h .

Figure A.12 displays our results. Graphically, we normalize the estimated impact nor-

Figure A.12: The Impact of Extreme Events on GDP



Notes: Impulse responses of world real GDP per capita to extreme events, estimated based on (3) with our expanded set of controls. Extreme weather variables record the share of cell-days in a given year and country where temperature, precipitation, or wind speed are above/below a threshold. We define threshold using the daily weather distribution in 1950-1980. Temperature: above 95th percentile. Drought: below 25th percentile. Extreme precipitation: above 99th percentile. Wind: above 99th percentile. Though not necessary for our results, we smooth the precipitation and wind measures with a backward-looking (current and previous two years) moving average to remove their inherent noise. Responses are normalized to the peak increase in frequency from Figure 8: graphical responses report $\psi_h^X / (\max_t \theta_t^X)$. Solid lines: point estimates. Dark and light shaded areas: 68 and 90% confidence bands.

malized by the peak frequency rise in exposure from Figure 8 to ease interpretation: we report $\frac{\phi_h^X}{\max_t \theta_t^X}$. Extreme weather events lead to a significant and persistent fall in GDP. The response is particularly pronounced for extreme heat and extreme precipitation and droughts but also extreme wind has substantial adverse effects, even though somewhat less precisely estimated.

To construct the aggregate impact of global temperature on GDP through extreme events, we further need to adjust the estimates ϕ_h^X for internal persistence. Underlying

the estimates in Figure A.12, extreme event exposures turn out to have very low internal persistence. Thus, the estimates in Figure A.12 largely represent the GDP impact of a one-time increase in extreme events. Nevertheless, we convert the estimates ϕ_h^X in response to a realized rise in extreme event frequency to estimates in response to a one-time fully transitory surge in extreme event frequency using the Sims (1986) method. We denote those adjusted estimates by ψ_h^X . In practice, the ϕ_h^X and ψ_h^X are close. We then aggregate these estimates using the definition of Θ_h in Section 3.3.

A.12 Additional Robustness Checks

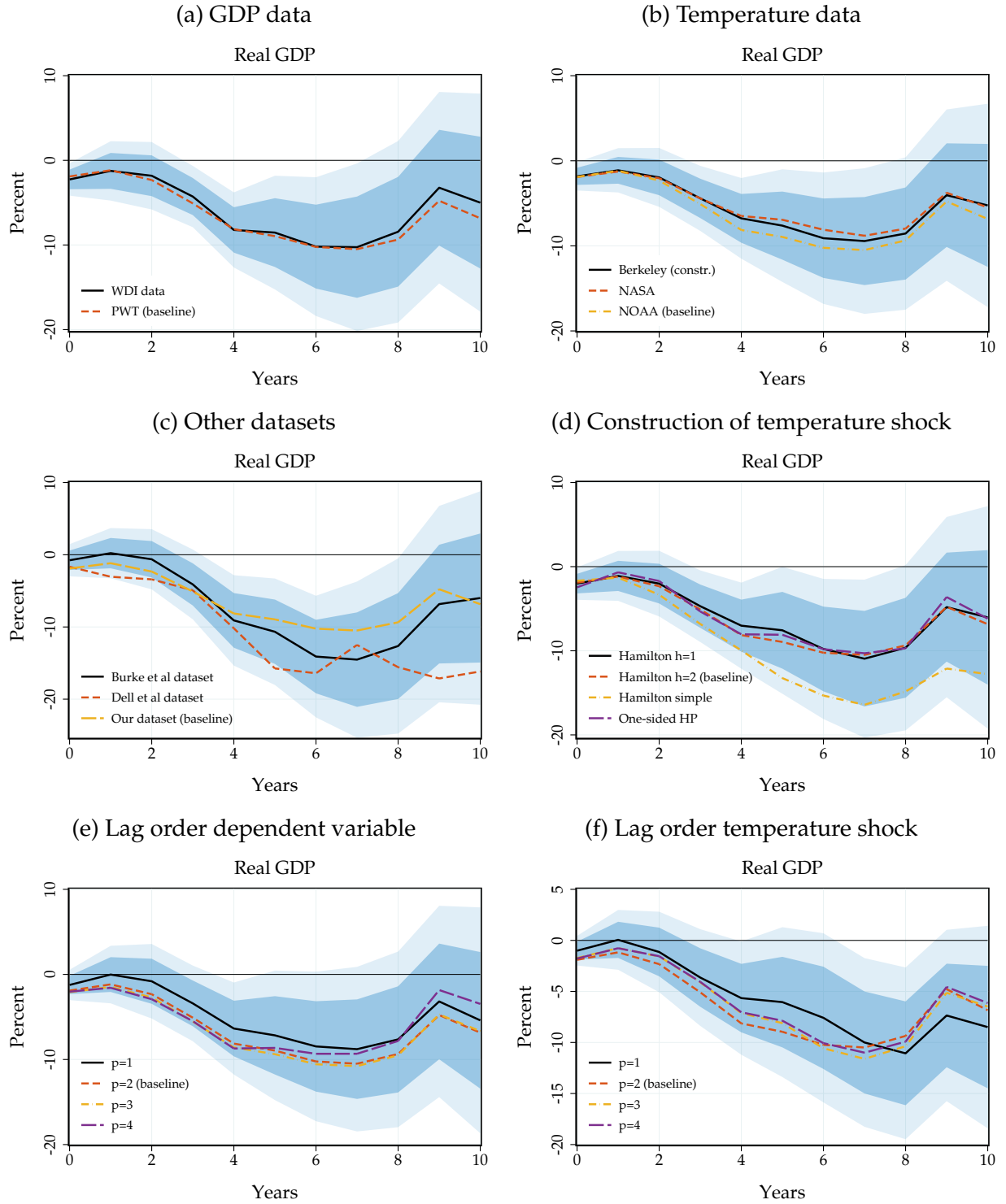
In this appendix, we perform a number of additional sensitivity checks on the effect of global temperature shocks based on our panel local projections. We start by examining the role of data choices, the construction of the temperature shock, and the number of lags included.

Figure A.13 collects the results. Panels (a)-(b) assess the sensitivity with respect to the GDP and temperature data we use. Using real GDP per capita from the PWT or from the WDI produces very similar results. Similarly, using aggregated global mean temperature data from the Berkeley Earth dataset or off-the-shelf measures from NASA or NOAA produces virtually identical results. In Panel (c), we replicate our results with the datasets from Burke et al. (2015) and Dell et al. (2012). We obtain their datasets from the respective replication packages, merge our global temperature shock, and compute the impulse responses to the shock. We obtain similar results with their datasets.

Panel (d) assesses additional ways of constructing of the temperature shocks. Using simple one-step ahead forecast errors, using the one-sided HP filter or the simple 2-year difference proposed in Hamilton (2018) produces qualitatively very similar results.

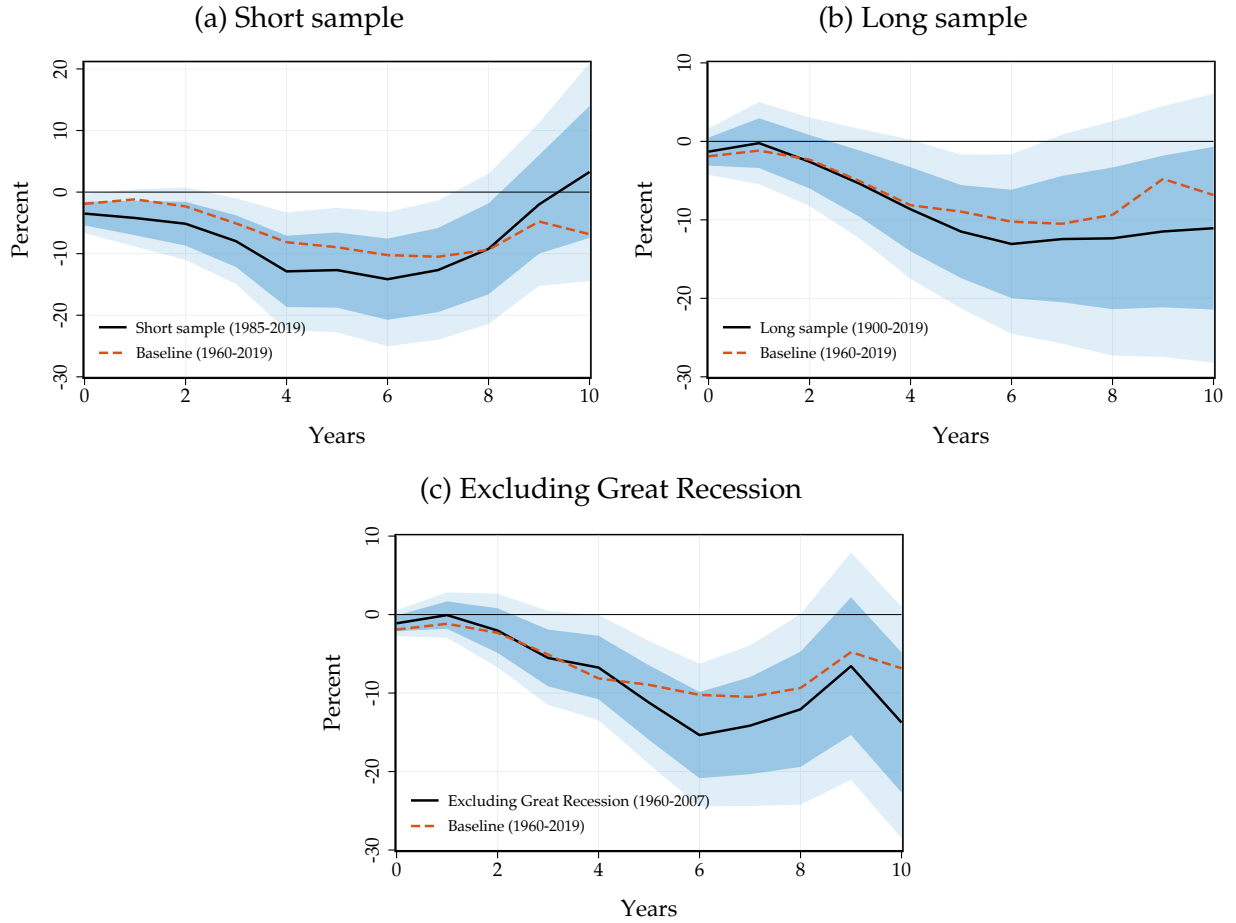
Panels (e)-(f) evaluate sensitivity with respect to the number of lags included for real GDP and temperature shocks. When varying the lag order of the dependent variable, we keep the lag order of our temperature shock at the baseline value and vice versa. Our results turn out to be robust with respect to the lag order. In fact, in the main text, we show that our results even survive when we control up to 10 lags of real GDP.

Figure A.13: Sensitivity of the Average Effect of Global Temperature Shocks



Notes: Sensitivity of the effects of global temperature shocks on real GDP per capita to a global temperature shock, with respect to data choices, the construction of the temperature shock, and the number of lags included. Solid line: point estimate. Dark and light shaded areas: 68 and 90% confidence bands, respectively.

Figure A.14: Sensitivity of the Average Effect of Global Temperature Shocks II



Notes: Sensitivity of the effects of global temperature shocks on real GDP per capita to a global temperature shock, with respect to the sample period. Solid line: point estimate. Dark and light shaded areas: 68 and 90% confidence bands, respectively.

Figure 5 in the main text shows that our point estimates are similar in a longer sample (1900-2019, based on a smaller selection of countries), a shorter sample (1985-2019), and stopping the sample prior to the Great Recession (1960-2007).⁷ However, are the responses also statistically significant? Figure A.14 shows the impulse responses on the three periods that we consider, together with the associated confidence bands. The esti-

⁷The longer sample includes 18 advanced economies, specifically Australia, Belgium, Canada, Denmark, Finland, France, Germany, Ireland, Italy, Japan, Netherlands, Norway, Portugal, Spain, Sweden, Switzerland, UK, and USA. We control for the world wars using a dummy for the years 1914-1918 and 1939-1945. We further control for the Great Depression and the Great Recession using a recession dummy (1929-1939 and 2007-2009). In the shorter sample, we add the European debt crisis to our recession dummy (2011-2012). This period was marked by low growth globally and is relatively more important in the shorter sample, which is why we control for it.

ated impact is significant in all the alternative sample periods.

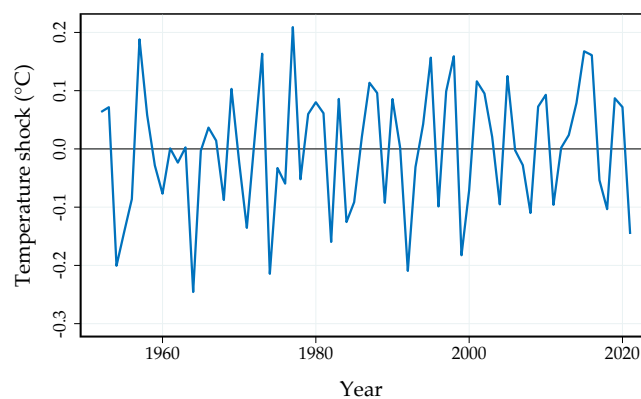
Overall, these results further illustrate the robustness of our finding that global temperature shocks lead to a sizeable, persistent and statistically significant fall in economic output that is by a magnitude larger than the estimates in the literature for local temperature shocks.

A.12.1 Results Based on One-step Forecast Error Temperature Shocks

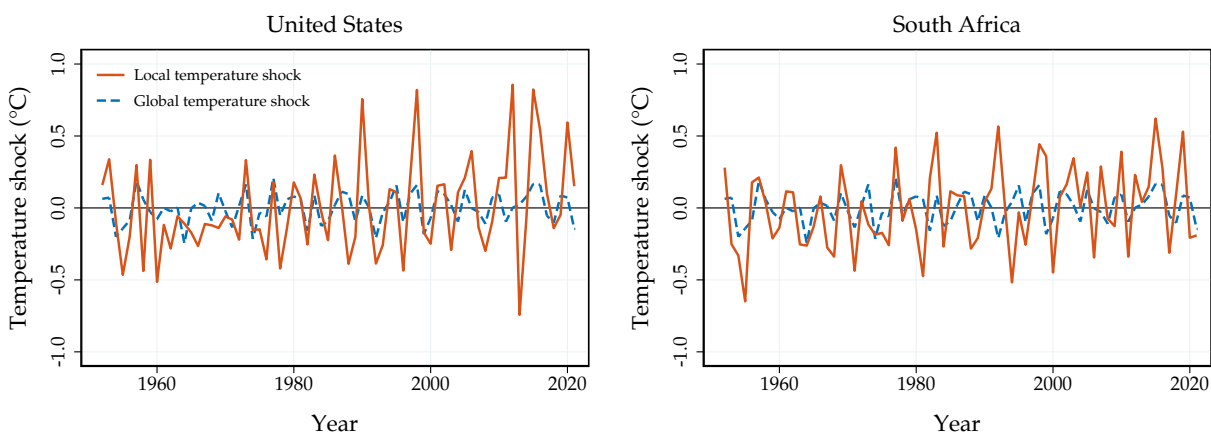
As our baseline, we measure the temperature shocks as two-step ahead forecast errors, motivated by the period of the climatic variation we aim to capture. A more common choice in the literature is to construct temperature shocks as one-step ahead forecast errors, as in Bansal and Ochoa (2011) and Nath et al. (2023). We have already showed that the GDP response is virtually identical when using the one- or two-step ahead forecast error as the relevant shock measure. For completeness, we present all our main results based on the one-step ahead temperature forecast error. The results are shown in Figures A.15-A.20. Our results turn out to be virtually identical using this alternative shock measure.

Figure A.15: Alternative Global and Local Temperature Shocks

(a) Global temperature shock

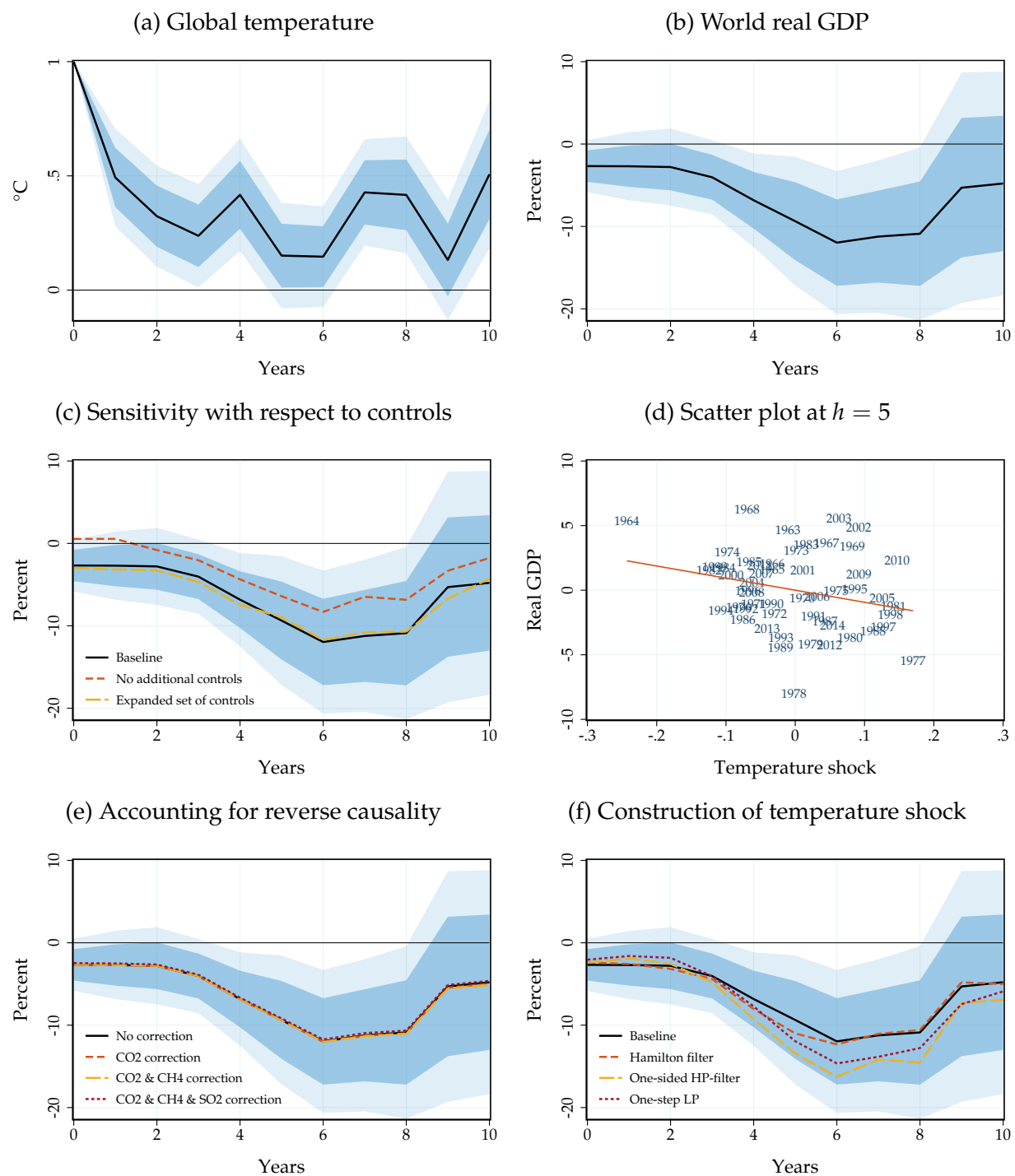


(b) Global vs. local temperature shock



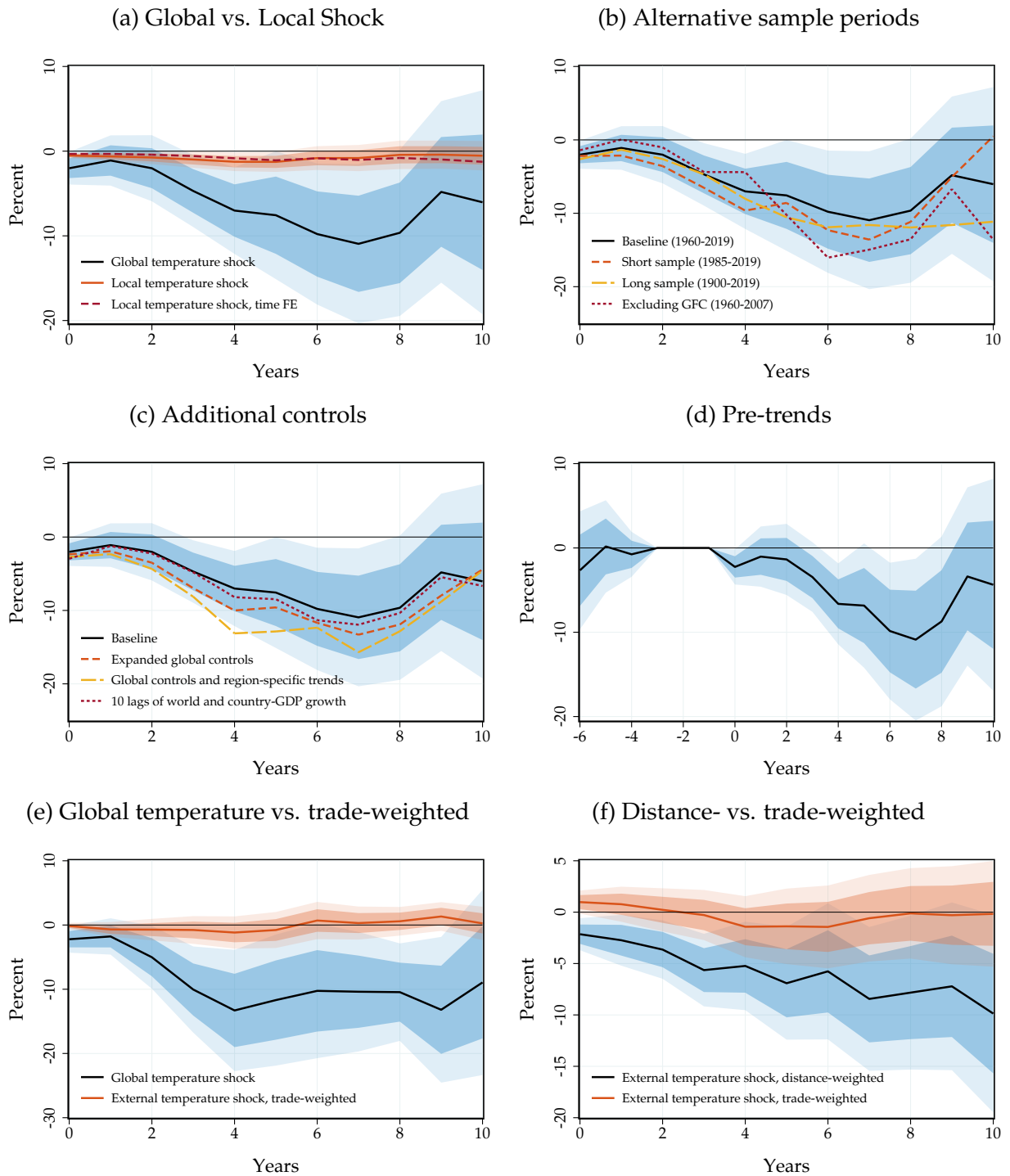
Notes: Panel (a): Global temperature shocks, computed as in Hamilton (2018) with $(h = 1, p = 2)$, over the post-World War II era. Panel (b): Local temperature shocks for the United States (left panel) and South Africa (right panel) in red together with the global temperature shocks as the blue dashed line. All shocks computed based on the Hamilton (2018) approach with $(h = 1, p = 2)$, over our sample from 1960. Local shocks computed based on population-weighted country-level temperature data.

Figure A.16: Time-series Results Based on One-Step Ahead Forecast Error



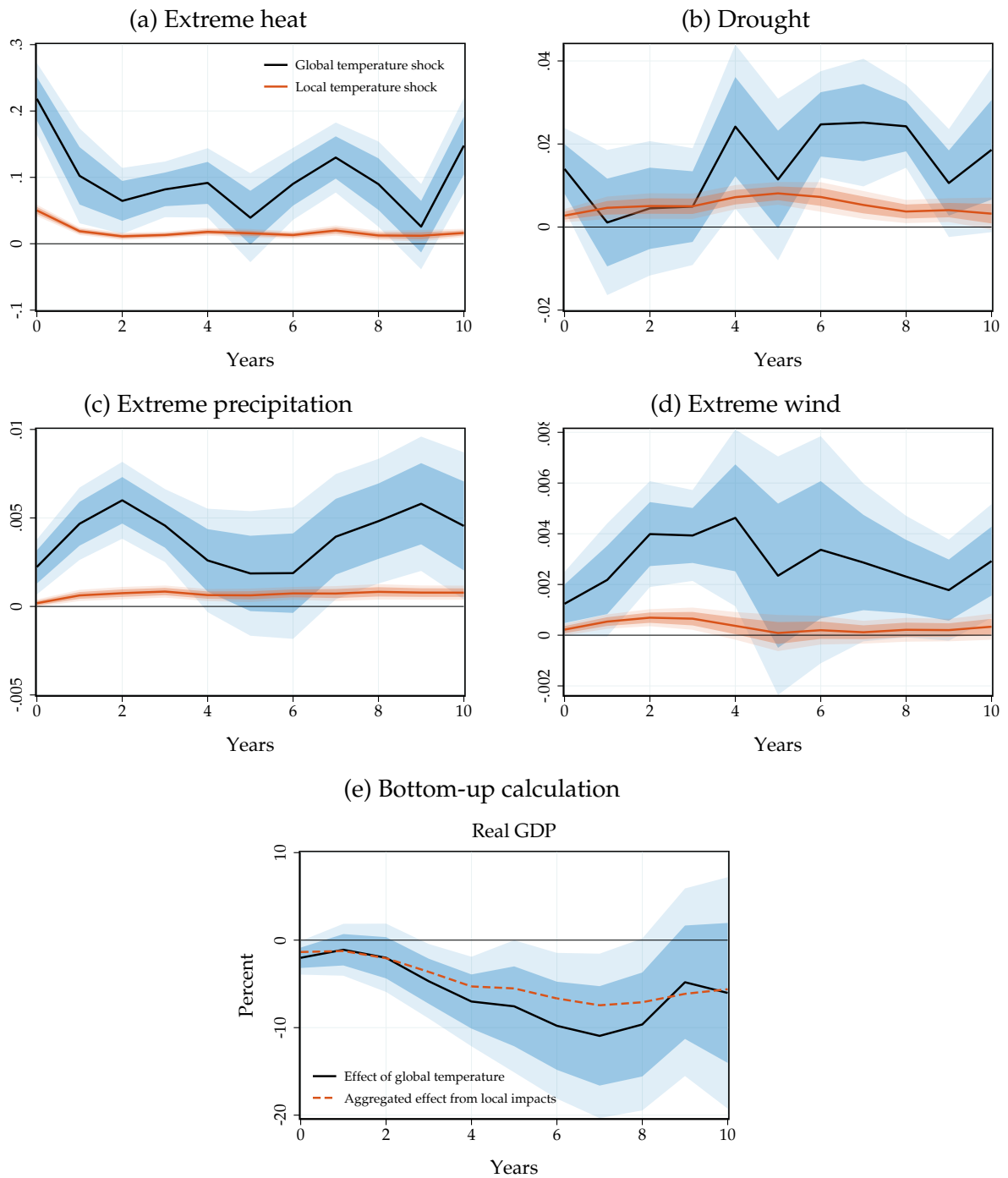
Notes: Reproduces Figures 3 and 4 for a global temperature shock measured as a one-step ahead forecast error.

Figure A.17: Panel Results Based on One-Step Ahead Forecast Error I



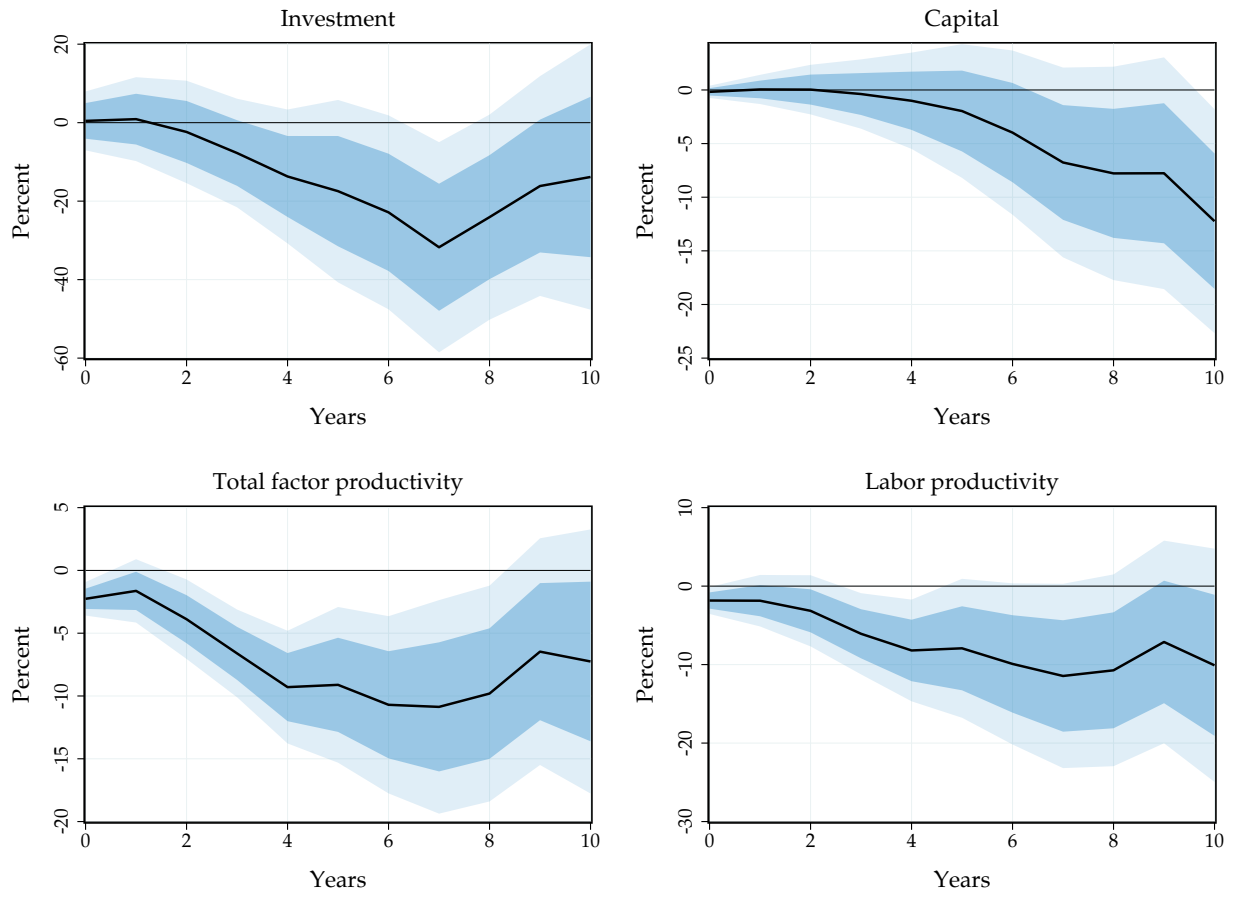
Notes: Reproduces Figures 5, 7 and 10 for global, local and external temperature shocks measured as a one-step ahead forecast errors.

Figure A.18: Panel Results Based on One-Step Ahead Forecast Error II



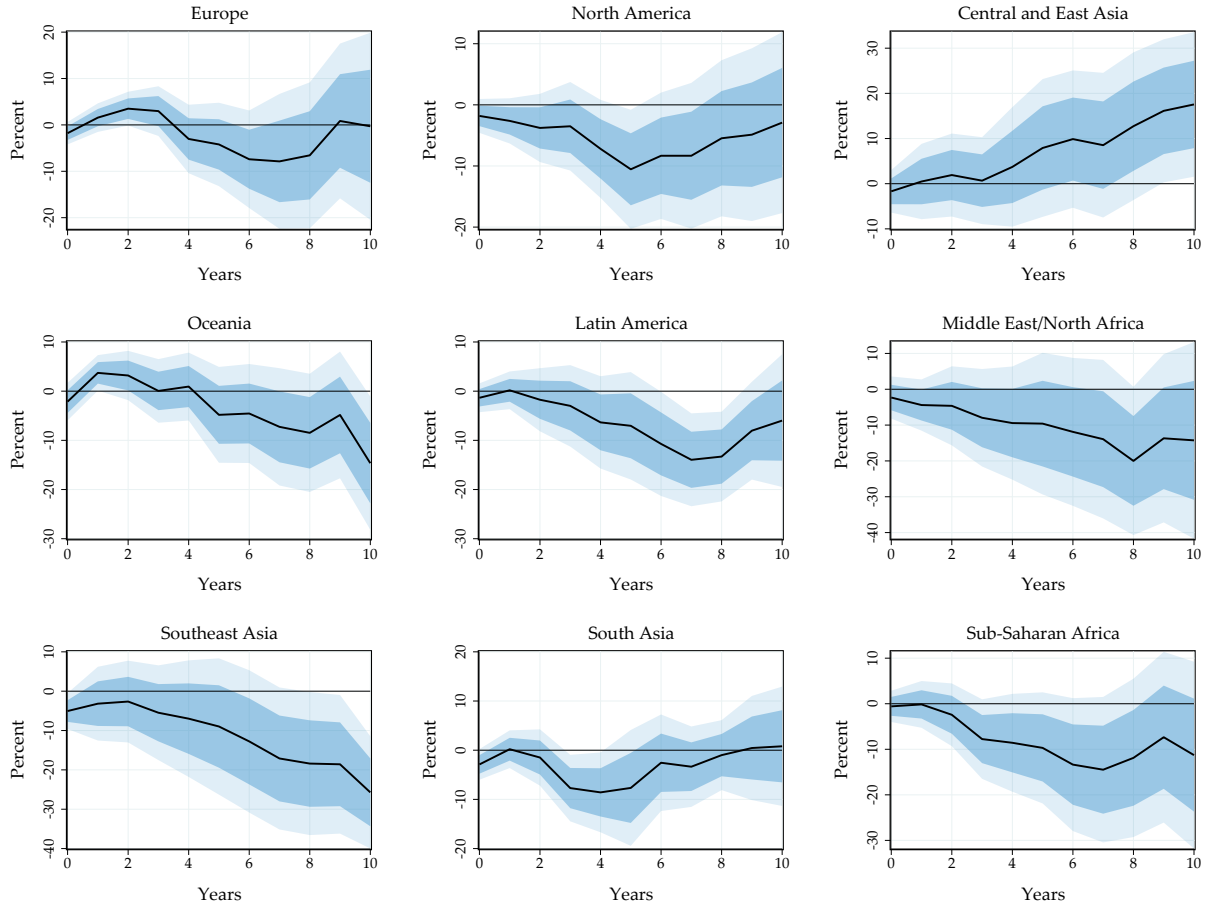
Notes: Reproduces Figures 8 and 9 for global, local, and external temperature shocks measured as a one-step ahead forecast errors.

Figure A.19: Panel Results Based on One-Step Ahead Forecast Error III



Notes: Reproduces Figure 11 for a global temperature shock measured as a one-step ahead forecast error.

Figure A.20: Panel Results Based on One-Step Ahead Forecast Error IV



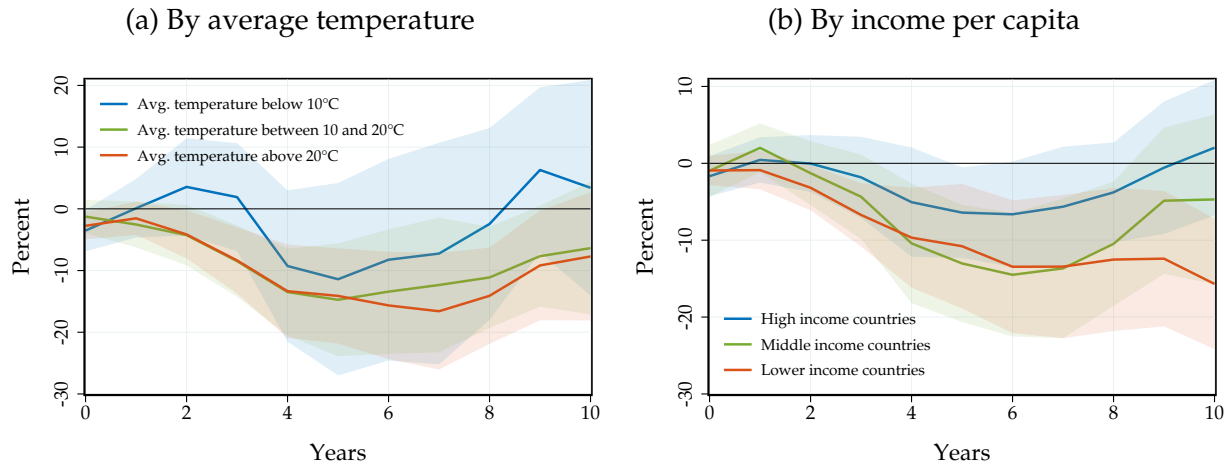
Notes: Reproduces Figure 12 for a global temperature shock measured as a one-step ahead forecast error.

A.13 Regional Impacts

We study how the impact of global temperature varies by average temperature and income. To this end, we bin countries into different groups based on temperature and income data. Specifically, we bin countries into three temperature and income groups, based on data from 1957-1959 to ensure that group characteristics are not influenced by the effects of the global temperature shocks.

Figure A.21 displays our results. Panel (a) shows the effects to a global temperature shock for cold countries (average temperature below 10°C), temperate climate countries (average temperature between 10°C and 20°C) and hot countries (average temperature above 20°C). Hot countries display the strongest adverse effects of temperature shocks.

Figure A.21: Heterogeneous Effects of Global Temperature Shocks



Notes: Impulse responses of real GDP per capita to a global temperature shock for different groups of countries. We estimate these responses based on (3), with our expanded set of controls, conditioning on the different groups. In Panel (a), we group countries by their average temperature in 1957-1959. In Panel (b), we group countries by their per capita income (in PPP terms) in 1957-1959. Solid line: point estimate. Dark and light shaded areas: 90% confidence bands.

This result is *qualitatively* consistent with previous evidence on local temperature shocks (Dell et al., 2012; Burke et al., 2015; Nath, 2022). *Quantitatively*, global temperature shocks have larger effects across all countries: they are more uniformly detrimental than local temperature shocks. Temperate countries also display a response that is economically large. Only colder countries display a somewhat smaller effect that is also not statistically significant.

Figure A.21(b) shows the responses by income per capita. We consider effects on poorer countries (real GDP per capita below 3,000 USD), middle income countries (real GDP per capita between 3,000 and 8,000 USD), and high income countries (real GDP per capita above 8,000 USD). Relative to the evidence based on local temperature, we find again more uniformly detrimental impacts: real GDP per capita falls across all income groups. Poor countries experience the most significant and persistent decline. Middle-income countries also see a considerable decrease in output. Only high-income countries are relatively more insulated, with a somewhat smaller and less enduring impact.

B Model

Our solution to the neoclassical growth model is entirely standard and we present it for completeness.

B.1 Equilibrium

The resource constraint is:

$$\dot{K}_t = Z_t K_t^\alpha - C_t - \Delta_t K_t.$$

Firm behavior and market clearing implies $r_t + \Delta_t = \alpha Z_t K_t^{\alpha-1}$ and $w_t = (1 - \alpha) K_t^\alpha$. The Euler equation is:

$$\dot{C}_t = \gamma^{-1} (\alpha Z_t K_t^{\alpha-1} - \Delta_t - \rho) C_t.$$

In steady-state,

$$\begin{aligned} r = \alpha Z K^{\alpha-1} &= \rho + \Delta \implies K = \left(\frac{\alpha Z}{\rho + \Delta} \right)^{\frac{1}{1-\alpha}} \\ C &= Z K^\alpha - \Delta K. \end{aligned}$$

B.2 Linearization

We denote steady-state variables without time subscripts. We denote deviations from steady-state with hats. We linearize the resource constraint:

$$\begin{aligned} \frac{d\hat{K}_t}{dt} &= (\alpha Z K^{\alpha-1} - \Delta) \hat{K}_t - \hat{C}_t + \hat{Z}_t K^\alpha - \hat{\Delta}_t K \\ &= \rho \hat{K}_t - \hat{C}_t + Y \hat{z}_t - K \hat{\Delta}_t. \end{aligned}$$

where we denoted $\hat{z}_t = \hat{Z}_t / Z$. Next, we linearize the Euler equation:

$$\begin{aligned} \frac{d\hat{C}_t}{dt} &= \frac{C}{\gamma} \left(-\alpha(1 - \alpha) Z K^{\alpha-2} \hat{K}_t + \alpha K^{\alpha-1} \hat{Z}_t - \hat{\Delta}_t \right) \\ &= \frac{C}{\gamma} \left(-\frac{(1 - \alpha)r}{K} \hat{K}_t + r \hat{z}_t - \hat{\Delta}_t \right). \end{aligned}$$

We define:

$$X_t = \begin{pmatrix} \hat{K}_t \\ \hat{C}_t \end{pmatrix}, \quad s_t = \begin{pmatrix} \hat{z}_t \\ \hat{\Delta}_t \end{pmatrix}.$$

We can summarize the linearized resource constraint and Euler equation as:

$$\dot{X}_t = AX_t + S_t,$$

where:

$$A = \begin{pmatrix} \rho & -1 \\ -\frac{(1-\alpha)rC}{\gamma K} & 0 \end{pmatrix}, \quad S_t = Bs_t, \quad B = \begin{pmatrix} Y & -K \\ \frac{rC}{\gamma} & -\frac{C}{\gamma} \end{pmatrix}.$$

We have an initial condition \hat{K}_0 , and a terminal condition $\hat{C}_t \rightarrow 0$. We now apply standard Blanchard-Kahn arguments. Let $A = M^{-1}DM$, with D diagonal. For determinacy we require that parameters are such that D has a positive eigenvalue in the top left position, and a negative eigenvalue in the bottom right position. We denote by $\mathcal{X}_t = MX_t$, so that

$$\dot{\mathcal{X}}_t = D\mathcal{X}_t + MS_t.$$

We then solve explicitly for \mathcal{X}_t :

$$\mathcal{X}_t = e^{tD} \left[\mathcal{X}_0 + \int_0^t e^{-sD} (MS_s) ds \right].$$

Hence, long-run stability requires the top entry of the bracket to be zero as time grows. That is:

$$0 = \mathcal{X}_{0,1} + \int_0^\infty e^{-sD_1} (MS_s)_1 ds.$$

Therefore,

$$M_{1\bullet} X_0 = - \int_0^\infty e^{-sD_1} M_{1\bullet} S_s ds.$$

We can thus solve for initial consumption:

$$\widehat{C}_0 = -\frac{1}{M_{12}} \left[M_{11} \widehat{K}_0 + \int_0^\infty e^{-sD_1} M_{1\bullet} S_s ds \right].$$

We denote $\varepsilon_K = -\frac{M_{11}}{M_{12}}$, $\varepsilon_S = -\frac{1}{M_{12}} M_{1\bullet}$ and $\varepsilon_{S,s} = e^{-sD_1} \varepsilon_S$. We can write more compactly:

$$\widehat{C}_0 = \varepsilon_K \widehat{K}_0 + \int_0^\infty \varepsilon_{S,s} S_s ds.$$

Of course, this condition must hold at all times:

$$\widehat{C}_t = \varepsilon_K \widehat{K}_t + \int_0^\infty \varepsilon_{S,s} S_{t+s} ds.$$

B.3 Model Inversion: Proof of Proposition 1

We substitute the solution for linearized consumption into the law of motion of capital:

$$\frac{d\widehat{K}_t}{dt} = (L_{11} - \varepsilon_K) \widehat{K}_t + S_{1t} - \int_0^\infty \varepsilon_{S,s} S_{t+s} ds.$$

Denote $\kappa = -(L_{11} - \varepsilon_K)$ and $\mathcal{S}_t = S_{1t} - \int_0^\infty \varepsilon_{S,s} S_{t+s} ds$ so that:

$$\frac{d\widehat{K}_t}{dt} = -\kappa \widehat{K}_t + \mathcal{S}_t.$$

Assuming we start in steady-state, we obtain:

$$\widehat{K}_t = e^{-\kappa t} \int_0^t e^{\kappa s} \mathcal{S}_s ds.$$

In percentage deviations:

$$\frac{\widehat{K}_t}{K} = \frac{e^{-\kappa t}}{K} \int_0^t e^{\kappa s} \mathcal{S}_s ds.$$

We can directly back out productivity shocks from the production function given movements in output and capital:

$$\frac{\widehat{Y}_t}{Y} = \widehat{z}_t + \alpha \frac{\widehat{K}_t}{K}.$$

We then use the capital accumulation equation to recover capital depreciation shocks. To do so, we express:

$$\begin{aligned}
\int_0^t e^{\kappa s} \mathcal{S}_s ds &= \int_0^t e^{\kappa s} \left(S_{1s} - \int_0^\infty \varepsilon_{S,r} S_{s+r} dr \right) ds \\
&= \int_0^t e^{\kappa s} S_{1s} ds - \int_0^\infty \int_0^\infty \mathbb{1}[s \leq t] \varepsilon_{S,r} S_{s+r} e^{\kappa s} ds dr \\
&= \int_0^t e^{\kappa s} S_{1s} ds - \int_0^\infty \int_0^\infty \mathbb{1}[s \leq t] \varepsilon_S S_{s+r} e^{\kappa s - D_1 r} ds dr.
\end{aligned}$$

Changing variables to $\tau = s + r$ over r , we obtain

$$\begin{aligned}
\int_0^t e^{\kappa s} \mathcal{S}_s ds &= \int_0^t e^{\kappa s} S_{1s} ds - \varepsilon_S \int_0^\infty \int_0^\infty \mathbb{1}[s \leq t, s \leq \tau] S_\tau e^{\kappa s - D_1(\tau-s)} ds d\tau \\
&= \int_0^t e^{\kappa s} S_{1s} ds - \varepsilon_S \int_{\tau=0}^\infty e^{-D_1 \tau} S_\tau \int_{s=0}^{\min\{t, \tau\}} e^{(D_1 + \kappa)s} ds d\tau \\
&\equiv \int_0^t e^{\kappa s} S_{1s} ds - \varepsilon_S \int_{\tau=0}^\infty J_{t,\tau} S_\tau d\tau,
\end{aligned}$$

where we defined:

$$J_{t,\tau} = e^{-D_1 \tau} \int_{s=0}^{\min\{t, \tau\}} e^{(D_1 + \kappa)s} ds = e^{-D_1 \tau} \frac{e^{(D_1 + \kappa) \min\{t, \tau\}} - 1}{D_1 + \kappa}.$$

Having estimated the productivity shocks, we can express:

$$S_t = \bar{S}_t + \hat{\Delta}_t \bar{S}_\Delta \quad \bar{S}_t \equiv \hat{z}_t \left(\frac{Y}{rC} \right) \quad S_\Delta \equiv \begin{pmatrix} -K \\ -\frac{C}{\gamma} \end{pmatrix}.$$

Then, we write

$$\int_0^t e^{\kappa s} \mathcal{S}_s ds = \int_0^t e^{\kappa s} \bar{S}_{1s} ds - \varepsilon_S \int_{\tau=0}^\infty J_{t,\tau} \bar{S}_\tau d\tau + \bar{S}_{\Delta,1} \int_0^t e^{\kappa s} \hat{\Delta}_s ds - (\varepsilon_S \bar{S}_\Delta) \int_0^\infty J_{t,s} \hat{\Delta}_s ds.$$

Hence, we have obtained that:

$$\frac{\hat{K}_t}{K} = \mathcal{K}_t(\hat{z}) + \mathcal{J}_{t,\bullet} \hat{\Delta}_\bullet,$$

where

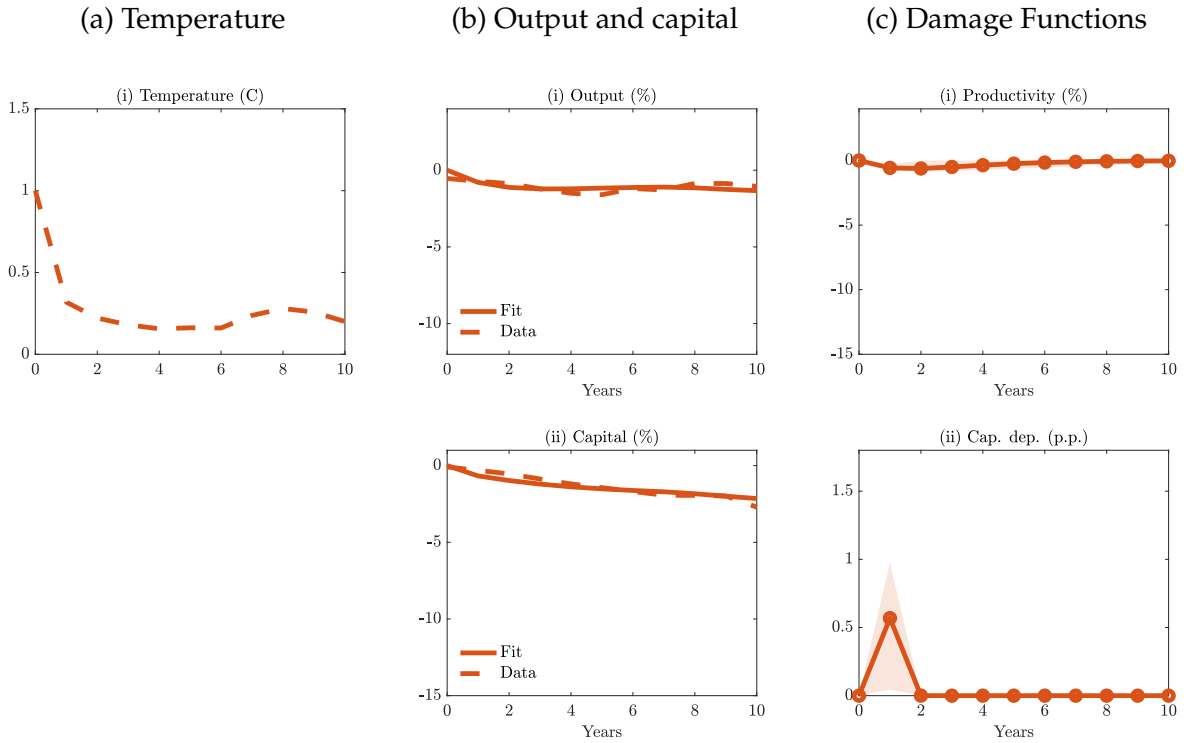
$$\begin{aligned}\mathcal{K}_t(\widehat{z}) &= \frac{e^{-\kappa t}}{K} \left[\int_0^t e^{\kappa s} \overline{S}_{1s} ds - \varepsilon_S \int_0^\infty J_{t,s} \overline{S}_s ds \right] \\ \mathcal{J}_{t,s} &= \frac{e^{-\kappa t}}{K} \left[\overline{S}_{\Delta,1} \mathbb{1}[s \leq t] e^{\kappa s} ds - (\varepsilon_S \overline{S}_\Delta) J_{t,s} ds \right].\end{aligned}$$

These equations conclude the proof of Proposition 1.

B.4 Estimation

Figure B.1 displays the productivity and capital depreciation effects of local temperature shocks, discussed in the main text.

Figure B.1: Productivity and Capital Depreciation after Local Temperature Shocks



Notes: Estimation results from matching the model impulse responses to the empirical responses to local temperature shocks. Column (a): underlying temperature path. Column (b): output and capital responses to this internally persistent temperature path. Dashed lines: data. Solid lines: model fit. Column (c): implied productivity and capital depreciation shocks, together with 68% confidence intervals (shaded area) based on 1,000 bootstrap draws from the empirical output, capital and temperature IRFs.

An alternative estimation strategy is to construct the impulse response function to a one-time transitory temperature shock with linear combinations of the impulse response function to the observed, persistent temperature shock *before* matching the model to the data. The interpretation of this approach is that households are surprised by elevated temperature each period after a global temperature shock.

We follow Sims (1986) to obtain the impulse response to one-time transitory temperature shocks. It is equivalent to using a recursive approach. Indeed, denote by \tilde{y}_t the unknown impulse response function of output to a transitory temperature shock. In discrete data and under linearity: $\hat{y}_t = \sum_{s=0}^t \hat{T}_{t-s} \tilde{y}_s$. We then obtain $\tilde{y}_t = (\hat{y}_t - \sum_{s=0}^{t-1} \hat{T}_{t-s} \tilde{y}_s) / \hat{T}_0$ recursively.

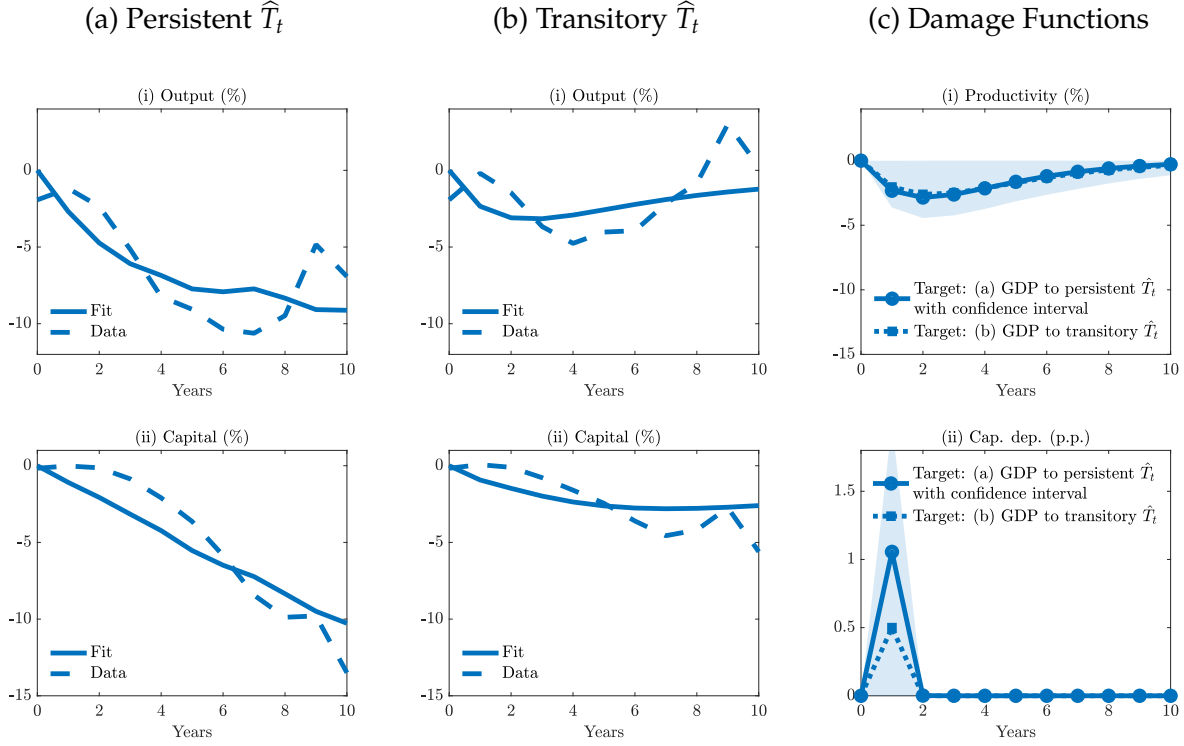
With the deconvoluted impulse response functions of output and capital to a one-time unit transitory temperature shock at hand, we use Proposition 1 and obtain the corresponding shocks \hat{z}_t , $\hat{\Delta}_t$. We then identify $\zeta_s = \hat{z}_s$ and $\delta_s = \hat{\Delta}_s / \Delta_0$.

Figure B.2 shows our estimation results. The panels in column (a) display the output (i) and capital (ii) responses to internally persistent temperature shocks, in the model (in which households are surprised by elevated temperature) and in the data. By construction, these responses account for the persistent increase in global temperature levels in response to global temperature shocks as estimated in the data (see Figure 8). The dashed lines are the impulse responses as estimated in Section 3. The solid lines show the corresponding responses in the estimated model. Our model closely tracks the empirical responses, even under the alternative treatment of expectations.

The dashed lines in column (b) show the deconvoluted responses of output and capital that we use for estimation under this alternative treatment of expectations. These correspond to a one-time transitory global temperature shock of 1°C. As expected, the output and capital responses are smaller, given the considerable degree of internal persistence of the estimated global temperature shock. However, they remain sizeable and peak at around -5%, respectively. The solid lines show again the model fit under our constrained functional form.

Finally, the panels in column (c) compare the estimated structural damage functions, ζ_s and δ_s under our baseline treatment of expectations in the main text (solid line) and under the alternative assumption that households are surprised every period (dotted line). Panel (c)(i) confirms our argument that estimated productivity shocks are independent from our treatment of expectations—or, equivalently, whether we deconvolute the data

Figure B.2: Productivity and Capital Depreciation after Global Temperature Shocks

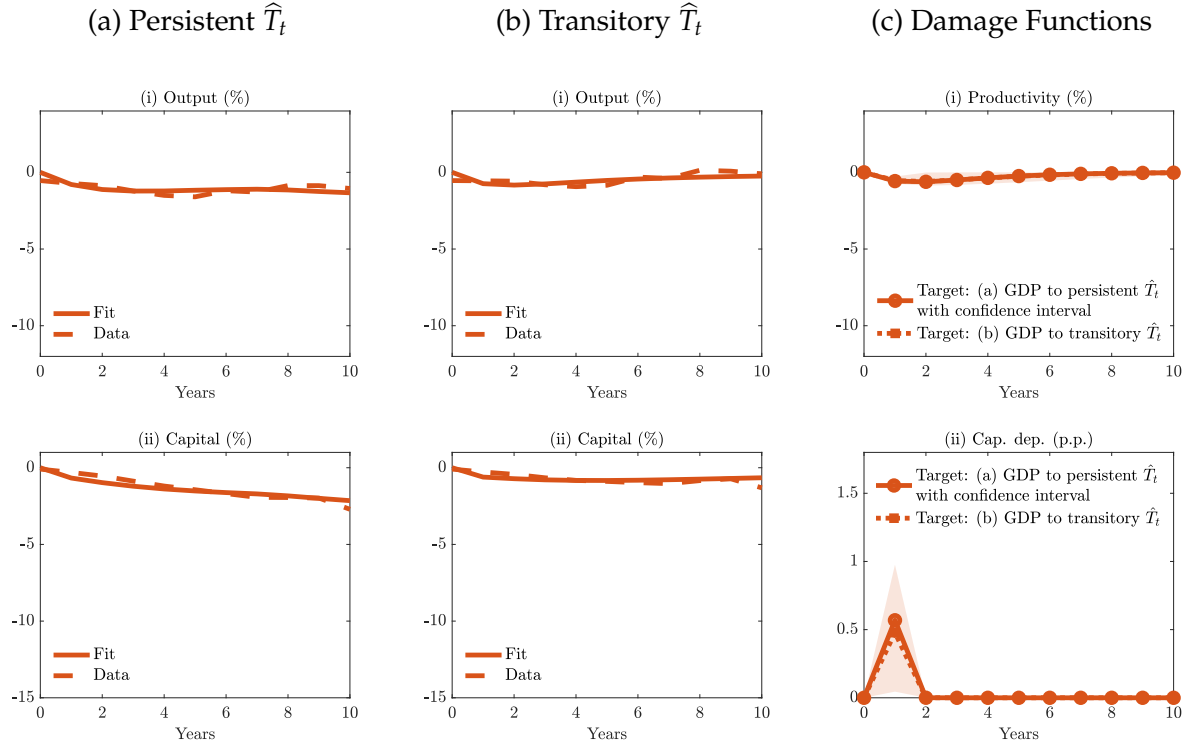


Notes: Estimation results from matching the model impulse responses to the empirical responses to global temperature shocks. The four left panels show the output and capital responses in the data and the model. Column (a) shows the responses to persistent temperature shocks. Column (b) shows the responses to transitory temperature shocks used in the estimation. Column (c) plots the implied productivity and capital depreciation shocks, together with 68% confidence intervals (shaded area) for the transitory case based on 1,000 bootstrap draws from the empirical output, capital and temperature IRFs.

before estimation or not. We obtain the same structural damage functions for productivity in both cases. Panel (c)(ii) indicates that expectations affect the estimation of the capital depreciation shocks in practice. We infer smaller capital depreciation shocks when we assume that households are surprised: in that case, households do not foresee future capital depreciation shocks that increase the marginal product of capital, and hence invest less than under rational expectations. The model then requires smaller capital depreciation shocks to rationalize the same decline in capital in the data.

Figure B.3 displays the productivity and capital depreciation effects of local temperature shocks under the baseline assumption of rational expectations. The productivity effect of local temperature shocks is five times smaller than under global temperature shocks. The impact response of capital depreciation is somewhat larger but vanishes immediately, so that the cumulated impact is substantially lower than under global shocks.

Figure B.3: Productivity and Capital Depreciation after Local Temperature Shocks



Notes: Estimation results from matching the model impulse responses to the empirical responses to local temperature shocks. The four left panels show the output and capital responses in the data and the model. Column (a) shows the responses to persistent temperature shocks. Column (b) shows the responses to transitory temperature shocks used in the estimation. Column (c) plots the implied productivity and capital depreciation shocks, together with 68% confidence intervals (shaded area) for the transitory case based on 1,000 bootstrap draws from the output, capital and temperature IRFs.

We conclude that global temperature shocks have much larger effects on economic fundamentals.

References Appendix

- Albright, Anna Lea, Cristian Proistosescu, and Peter Huybers** (2021). “Origins of a Relatively Tight Lower Bound on Anthropogenic Aerosol Radiative Forcing from Bayesian Analysis of Historical Observations”. *Journal of Climate* 34, 8777–8792.
- Azar, Christian, Jorge García Martín, Daniel JA. Johansson, and Thomas Sterner** (2023). “The Social Cost of Methane”. *Climatic Change* 176.
- Bansal, Ravi and Marcelo Ochoa** (2011). “Temperature, Aggregate Risk, and Expected Returns”. *NBER Working Paper Series* 17575.
- Berkeley Earth** (2023). *Data Overview*. <https://berkeleyearth.org/data/>. (Visited on 08/09/2023).
- Burke, Marshall, Solomon M. Hsiang, and Edward Miguel** (2015). “Global non-linear effect of temperature on economic production”. *Nature* 527.7577, pp. 235–239.
- Center for International Earth Science Information Network (CIESIN), Columbia University** (2018). *Gridded Population of the World, Version 4.11 (GPWv4): Population Count*. NASA Socioeconomic Data and Applications Center (SEDAC). <https://sedac.ciesin.columbia.edu/data/set/gpw-v4-population-count-rev11>. (Visited on 09/12/2023).
- Dell, Melissa, Benjamin F. Jones, and Benjamin A. Olken** (2012). “Temperature shocks and economic growth: Evidence from the last half century”. *American Economic Journal: Macroeconomics* 4.3, pp. 66–95.
- Dietz, Simon, Frederick van der Ploeg, Armon Rezai, and Frank Venmans** (2021). “Are Economists Getting Climate Dynamics Right and Does It Matter?” *Journal of the Association of Environmental and Resource Economists* 8.5, pp. 895–921.
- Feenstra, Robert C., Robert Inklaar, and Marcel P. Timmer** (Oct. 2015). “The Next Generation of the Penn World Table”. *American Economic Review* 105.10, pp. 3150–3182.
- Hamilton, James D.** (2018). “Why you should never use the Hodrick-Prescott filter”. *Review of Economics and Statistics* 100.5, pp. 831–843.
- Jordà, Òscar, Moritz Schularick, and Alan M. Taylor** (Jan. 2017). “Macrofinancial History and the New Business Cycle Facts”. *NBER Macroeconomics Annual* 31. Publisher: The University of Chicago Press, pp. 213–263.
- Lange, Stefan, Matthias Mengel, Simon Treu, and Matthias Büchner** (2023). *ISIMIP3a atmospheric climate input data (v1.2)*. ISIMIP Repository. <https://doi.org/10.48364/ISIMIP.982724.2>. (Visited on 12/04/2023).
- Lenssen, Nathan J. L., Gavin A. Schmidt, James E. Hansen, Matthew J. Menne, Avraham Persin, Reto Ruedy, and Daniel Zyss** (2019). “Improvements in the GISTEMP Uncertainty Model”. *Journal of Geophysical Research: Atmospheres* 124.12, pp. 6307–6326.

- Matsuura, Kenji and National Center for Atmospheric Research Staff** (2023). *The Climate Data Guide: Global (land) precipitation and temperature: Willmott & Matsuura, University of Delaware*. <https://climatedataguide.ucar.edu/climate-data/global-land-precipitation-and-temperature-willmott-matsuura-university-delaware>. (Visited on 08/09/2023).
- NASA Earth Observatory** (Jan. 2020). *World of Change: Global Temperatures*. <https://earthobservatory.nasa.gov/world-of-change/global-temperatures>. (Visited on 08/08/2023).
- NASA Goddard Institute for Space Studies** (2023). *GISS Surface Temperature Analysis (GISTEMP v4)*. <https://data.giss.nasa.gov/gistemp/>. (Visited on 08/08/2023).
- Nath, Ishan** (2022). “Climate Change, The Food Problem, and the Challenge of Adaptation through Sectoral Reallocation”. *Working Paper*.
- Nath, Ishan B., Valerie A. Ramey, and Peter J. Klenow** (2023). “How Much Will Global Warming Cool Global Growth?” *Mimeo*.
- NOAA National Centers for Environmental Information** (2023a). *Climate at a Glance: Global Time Series*. *Online Resource*. (Visited on 08/01/2023).
- (2023b). *Global Surface Temperature Anomalies: Mean Temperature Estimates*. <https://www.ncei.noaa.gov/access/monitoring/global-temperature-anomalies/mean>. (Visited on 08/01/2023).
- Ramey, Valerie A.** (2016). “Macroeconomic shocks and their propagation”. *Handbook of Macroeconomics* 2, pp. 71–162.
- Rohde, Robert A. and Zeke Hausfather** (Dec. 2020). “The Berkeley Earth Land/Ocean Temperature Record”. *Earth System Science Data* 12.4, pp. 3469–3479.
- Sheffield, Justin, Gopi Goteti, and Eric F. Wood** (July 2006). “Development of a 50-Year High-Resolution Global Dataset of Meteorological Forcings for Land Surface Modeling”. *Journal of Climate* 19.13. Publisher: American Meteorological Society Section: Journal of Climate, pp. 3088–3111.
- Sims, Christopher A.** (1986). “Are forecasting models usable for policy analysis?” *Quarterly Review* 10.Winter, pp. 2–16.